DOWNREGULATION OF THE CYTOSOLIC IRON-SULFUR ASSEMBLY PATHWAY IN CANCER BY AN E3 UBIQUITIN LIGASE

APPROVED BY SUPERVISORY COMMITTEE

Ryan Potts, Ph.D.

Benjamin Tu, Ph.D.

John Minna, M.D.

Yi Liu, Ph.D.

DEDICATION

To my parents John and Gui Weon, whose support, through undertaking this endeavor, I have come to realize is truly unconditional.

DOWNREGULATION OF THE CYTOSOLIC IRON-SULFUR ASSEMBLY PATHWAY IN CANCER BY AN E3 UBIQUITIN LIGASE

by

JENNY LINDA WEON

DISSERTATION

Presented to the Faculty of the Graduate School of Biomedical Sciences

The University of Texas Southwestern Medical Center at Dallas

In Partial Fulfillment of the Requirements

For the Degree of

DOCTOR OF PHILOSOPHY

The University of Texas Southwestern Medical Center at Dallas

Dallas, Texas

May 2019

ACKNOWLEDGEMENTS

I would like to first thank my mentor, Ryan Potts, for his unwavering energy and support over my PhD training. I still remember and am very thankful for his careful guidance when I first started, since I had only brief experiences in research prior to joining, in ensuring that I valued the understanding of not only why I am doing my experiments but also why I am doing each step of a protocol. As I progressed through my PhD training and grew scientifically, I am thankful for his flexible mentorship style and willingness to listen to my ideas and letting me come up with my own next steps. Lastly, but certainly not least, I am grateful for his faith in my abilities at times when I questioned it. I feel that I have come a long way in understanding, evaluating, and approaching science through his mentorship.

I would also like to thank John Minna and Suzie Hight for being the initial inspirations to additionally pursue a PhD after a summer in the Minna lab when I was a medical student. Through the experience of working with them and seeing the potential of research to advance medicine, I reached a turning point when I realized I did not want to leave the lab to go back to second year medical school classes. Many thanks additionally to both John Minna and Mike Peyton for helping me acquire numerous lung cancer lines for my project over the years.

I would also like to thank my committee members Benjamin Tu, John Minna, and Yi Liu for committing their time and effort to help me (despite their busy schedules and being on the committees of countless other students, I am sure) by listening when I needed an open ear and offering advice, proposing experiments, and writing letters of support, as I progressed through my training.

My graduate school experience would not have been the same without all the past and present members of the Potts lab for the conversations and companionship throughout the years of my PhD. My experience in this lab has been greatly enhanced by the humor and willingness to help of all my lab members, whatever the cause.

I would like to give thanks to Andrew Zinn, for allowing me to join the MD/PhD program despite joining two years after I started medical school, and for his assistance in the transition and support throughout graduate school.

Lastly, I would like to thank my former mentor Marc Lewis, for his faith in my abilities, without whose support I may not have considered continuing to pursue science many years later.

DOWNREGULATION OF THE CYTOSOLIC IRON-SULFUR ASSEMBLY PATHWAY IN CANCER BY AN E3 UBIQUITIN LIGASE

Publication No. 1

Jenny Linda Weon, Ph.D.

The University of Texas Southwestern Medical Center at Dallas, 2019

Supervising Professor: Ryan Potts, Ph.D.

Iron-sulfur (Fe-S) clusters are considered to be one of the oldest cofactors utilized by proteins and are essential for life from bacteria to mammals. Multiple processes in the cell require Fe-S cofactors, such as electron transfer in mitochondrial respiration, enzymatic reactions, and as structural components in DNA repair enzymes. We describe here the first post-translational mechanism to regulate Fe-S assembly and delivery through the ubiquitination and degradation of a key cytosolic iron-sulfur cluster assembly (CIA) pathway component by a MAGE-RING ligase (MRL). The MAGE protein family consists of ~40 members in humans that function in complex with E3 ubiquitin ligases to enhance ubiquitination activity, alter E3

subcellular localization, and/or specify E3 targets. Using biochemical and cellular approaches we have discovered that the MAGE-F1-NSE1 ligase disrupts Fe-S cluster delivery through ubiquitination and degradation of the CIA pathway protein MMS19. MMS19 is a substrate specifying, late-acting component of the CIA pathway that facilitates Fe-S transfer from the multi-component cascade of assembly proteins to specific recipient apoproteins. Notably, many MMS19 targets are enzymes involved in DNA repair. We found that MAGE-F1 directs the E3 ligase NSE1 to target MMS19 for ubiquitination and degradation. Knockdown of MAGE-F1 stabilized MMS19 and overexpression of MAGE-F1 decreased MMS19 levels without affecting MMS19 mRNA levels. We further confirmed MAGE-F1 inhibits Fe-S incorporation into known MMS19-dependent Fe-S proteins, such as FANCJ, POLD1, RTEL1, XPD, and DPYD, but not MMS19-independent Fe-S proteins, such as PPAT. Loss of Fe-S incorporation leads to decreased DNA repair capacity of cells, exemplified by decreased homologous recombination rates and altered sensitivity to DNA damaging agents. Importantly, numerous cancer types harbor copy-number amplification of MAGE-F1, including lung squamous carcinoma and head and neck squamous carcinoma. Consistent with MAGE-F1 inhibitory activity on Fe-S incorporation into key DNA repair enzymes, MAGE-F1-amplified tumors bear a significantly greater mutational burden than non-MAGE-F1-amplified cancers and the expression of MAGE-F1-NSE1 correlates with poor patient prognosis. In summary, we provide the first evidence for post-translational regulatory control of Fe-S cluster assembly and a novel mechanism by which a broad spectrum of DNA repair enzymes can be regulated and lead to genomic instability in cancer.

TABLE OF CONTENTS

PRIOR PUBLICATIONS

Pineda, C.T., S. Ramanathan, K. Fon Tacer, J.L. Weon, M.B. Potts, Y.H. Ou, M.A. White, and P.R. Potts, Degradation of AMPK by a cancer-specific ubiquitin ligase. Cell, 2015. 160(4): p. 715-28.

Weon, J.L. and P.R. Potts, The MAGE protein family and cancer. Curr Opin Cell Biol, 2015. 37: p. 1-8.

LIST OF FIGURES

LIST OF TABLES

LIST OF DEFINITIONS

CIA – Cytosolic iron sulfur cluster assembly machinery

CS – Cockayne syndrome

Fe-S cluster – Iron sulfur cluster

ISC – Mitochondrial iron sulfur cluster assembly machinery

KO – Knock out

MAGE – Melanoma antigen gene

MHD – MAGE homology domain

MMS – Methylmethanesulfonate

TCGA – The Cancer Genome Atlas

TTP - Trichothiodystrophy

WT – Wild type

XP – Xeroderma pigmentosum

UV – Ultraviolet light

CHAPTER ONE

MAGE FAMILY OF PROTEINS

Introduction

The Melanoma Antigen Gene (MAGE) family has garnered growing interest as biomarkers in cancer and targets of immunotherapies because a subset of these >40 human proteins are classified as cancer-testis antigens (CTAs), which have restricted expression to the testis (and occasionally ovary and placenta) and are aberrantly re-expressed in cancer where they can be immunogenic (reviewed in (Simpson et al. 2005)). Collectively, MAGEs have been found to be broadly expressed in many tumor types, including colon (Mori et al. 1996), melanoma (Brasseur et al. 1995; Barrow et al. 2006), brain (Scarcella et al. 1999), lung (Tajima et al. 2003; Gure et al. 2005; Kim et al. 2012), prostate (Karpf et al. 2009), and breast (Otte et al. 2001; Ayyoub et al. 2014), among others. For many years, the focus on MAGE CTAs was centered on their potential for cancer immunotherapy. However, this approach has had little success and met recent challenges. Detailed functional studies of these proteins have started to emerge and suggest that their expression in cancer is not simply due to non-specific, progressive promoter demethylation due to global genomic instability in cancer. MAGE genes are associated with hallmarks of aggressive cancers, including worse clinical prognosis, increased tumor growth, metastases, and enrichment in stem cell-like populations. Importantly, functional studies have shown that some MAGE CTAs can have non-overlapping oncogenic driver activity. Thus, MAGE CTAs may provide a novel means to develop cancer-specific therapeutics to treat a broad range of cancers.

MAGE Family of Proteins

MAGE genes are conserved in all eukaryotes and have rapidly expanded in gene number in mammals (Figure 1-1). Members of the human MAGE family can be divided into two categories based on tissue expression pattern: Type I MAGEs are considered CTAs and in humans include the MAGE-A, -B, and -C subfamily members which are clustered on the X-chromosome (reviewed in (Barker and Salehi 2002; Simpson et al. 2005)). Type II MAGEs (MAGE-D, -E, -F, -G, -H, -L subfamilies and Necdin) are expressed throughout many tissues in the body and are not restricted to the X chromosome (reviewed in (Barker and Salehi 2002)). Both type I and type II MAGEs contain a MAGE homology domain (MHD) that is approximately 170 amino acids (Figure 1-2 A), which on average is 46% conserved amongst all human MAGEs (Doyle et al. 2010). Structural studies have revealed that the MHD consists of tandem winged helix motifs (Figure 1-2 B through D) (Doyle et al. 2010). Our lab has shown that a defining biochemical function of MAGEs is their ability to bind to specific E3 RING ubiquitin ligases through their MHDs (Table 1-1), which may alter the relative orientation of the two winged helix motifs (compare Figure 1-2 B and C with D) (Doyle et al. 2010). Importantly, we and others have determined that MAGEs can regulate the ubiquitination of proteins through modulating the activity of their cognate E3 ligase. This includes, enhancing general ligase activity, binding to and specifying novel substrates for ubiquitination by the E3 ligase complex, and altering the subcellular localization of E3 ligases to dictate substrates (Figure 1-2 E) (Doyle et al. 2010; Hao et al. 2013; Pineda et al. 2015). Thus, aberrant expression of MAGEs in tumor cells can lead to alterations in cellular processes and signaling pathways through ubiquitination and potentially other activities to contribute to tumorigenesis.

MAGEs are associated with poor clinical prognosis

Extensive studies of MAGE expression in various cancers (Table 1-2) have shown their predictive association with poor clinical outcomes. For example, MAGE-A3 and -A9 expression is significantly correlated with decreased survival in non-small cell lung cancers (Gure et al. 2005; Zhang et al. 2015) and MAGE-A3, -A6, and -C2 expression in breast cancers is significantly associated with estrogen receptor-negative or progesterone receptor-negative status, higher grade tumors, and correlated with worse outcome (Ayyoub et al. 2014; Yang et al. 2014). In ovarian cancers, MAGE-A1, -A9, and -A10 expression are associated with worse prognosis (Daudi et al. 2014; Xu et al. 2015). MAGEs are also associated with increased rates of recurrence after therapy. In gastric carcinoma, MAGE-A1-6 expression in peritoneal washes after cancer resection correlated with a significant decreased disease-free survival rate (Jeon, Kim, and Chae 2014), and in hepatocellular carcinoma MAGE-A9 expression was significantly correlated with decreased disease-free survival, advanced tumor grade, metastasis, portal vein invasion, and overall survival (Gu et al. 2014).

MAGE CTAs have oncogenic activity

MAGEs are not only associated with poor clinical prognosis, but recent reports suggest they function as drivers of tumorigenesis. Upon expression, multiple cancer types become addicted to MAGEs for viability, such as MAGE-As or MAGE-Cs in breast (Pineda et al. 2015), lung (Pineda et al. 2015), colon (Pineda et al. 2015), mast cells (Yang, O'Herrin, Wu, Reagan-Shaw, Ma, Nihal, et al. 2007), multiple myeloma (Atanackovic et al. 2010), and melanoma (Yang, O'Herrin, Wu, Reagan-Shaw, Ma, Bhat, et al. 2007). MAGE-A3 and -C2 expression in cancer

lines has been shown to increase invasive potential *in vitro* (Liu et al. 2008; Yang et al. 2014). Furthermore, MAGE-A3 and -A6 promote the transformation of fibroblasts and increased soft agar growth of cancer cells (Pineda et al. 2015). More impressively, MAGE-A6 promotes anchorage-independent growth of normal diploid colonic epithelial cells (Pineda et al. 2015). In addition, MAGEs enhance tumor formation *in vivo*. Orthotopic xenografts of MAGE-A3 overexpressing human thyroid carcinoma cells exhibited increased tumor growth and metastases to the lung (Liu et al. 2008), and MAGE-C knockdown delayed tumor formation of metastatic melanoma *in vivo* (Bhatia et al. 2013). Furthermore, MAGE-B knockdown suppressed the growth of melanoma cells in a syngeneic mouse tumor model (Yang, O'Herrin, Wu, Reagan-Shaw, Ma, Bhat, et al. 2007). These studies suggest that MAGE CTAs may have oncogenic activity and additional rigorous studies in genetically engineered models of cancer in mice are warranted. Additionally, the contribution and activities of specific MAGEs (including many MAGE-B genes) needs further investigation.

Mechanism in cancer development and progression

Although mechanistic studies of MAGEs are limited, there is a growing body of evidence for their interactions with other proteins, especially E3 ubiquitin ligases. The MHDs of MAGE-A2, -A3, -A6, and -C2 can bind to the coiled-coil domain of the TRIM28/KAP1 ubiquitin ligase (Yang, O'Herrin, Wu, Reagan-Shaw, Ma, Bhat, et al. 2007; Doyle et al. 2010). MAGE-C2 increases phosphorylation of TRIM28/KAP1 and improves DNA repair after double-stranded breaks, possibly by enhancing complex formation between TRIM28/KAP1 and ATM (Bhatia et al. 2013). Our lab and others have shown that MAGE binding can enhance TRIM28/KAP1's

ubiquitin ligase activity against p53, resulting in its degradation in a proteasome-dependent manner (Doyle et al. 2010; Nardiello et al. 2011). In the presence of wild-type p53, knockdown of MAGE-A genes appears to increase p53 recruitment to target promoters (Marcar et al. 2010) and increase mRNA levels of p53 transcriptional targets (Nardiello et al. 2011; Marcar et al. 2010). Others have also suggested that MAGE-A binds to p53 DNA-binding domain directly which may prevent its transcriptional activity (Marcar et al. 2010; Monte et al. 2006). Additionally, MAGE-As and -C2 may downregulate p53 activity through preventing its acetylation (Yang, O'Herrin, Wu, Reagan-Shaw, Ma, Bhat, et al. 2007) at promyelocytic leukemia (PML) nuclear bodies by recruiting HDAC3 (Monte et al. 2006) and blocking p300-mediated PML acetylation (Peche et al. 2012).

However, the relevance of MAGE-As in cancer is not limited in scope to modulating p53 function. Expression of MAGE-A3 or -A6 does not correlate with p53 mutation status in multiple tumor types (Pineda et al. 2015). Most recently, our lab has determined the MAGE-A3-TRIM28 and MAGE-A6-TRIM28 ligase complexes can ubiquitinate the alpha catalytic subunit (PRKAA1) of the tumor suppressor AMPK that functions as the master cellular energy sensor and regulator (Hardie, Ross, and Hawley 2012; Pineda et al. 2015; Hardie 2015). This event leads to AMPK degradation and reduction of overall AMPK protein levels in tumors (Pineda et al. 2015). Furthermore, downregulation of AMPK by MAGE-A3 and -A6 led to significantly decreased autophagy levels and upregulation of mTOR signaling (Pineda et al. 2015), which may provide the optimal environment for early tumor formation and growth (Choi, Ryter, and Levine 2013; Wei et al. 2013; White 2012). Importantly, use of AMPK agonists significantly decreased MAGE-A6-mediated anchorage-independent growth *in vitro* (Pineda et al. 2015). Because

AMPK agonists (e.g. metformin) and mTOR inhibitors (e.g. everolimus) are already in use in the clinic (Kasznicki, Sliwinska, and Drzewoski 2014; Baselga et al. 2012), an immediate applicable point of these results may be to utilize MAGE-A3 and -A6 as a biomarkers for effective use of these drugs (Pineda et al. 2015).

MAGE-A11 is unique among the type I MAGEs in that it is known to be involved in the regulation of hormonal signals in prostate cancer (Karpf et al. 2009; Bai, He, and Wilson 2005). Binding of MAGE-A11 to the N-terminal FXXLF motif of the androgen receptor (AR) facilitates SRC/p160 co-activator binding (Bai, He, and Wilson 2005). Transcriptional activity of AR was also enhanced by epidermal growth factor (EGF)-mediated phosphorylation and ubiquitination of MAGE-A11 (Bai and Wilson 2008). In addition to modulating hormone signaling, MAGE-A11 may play a role in mediating survival of tumors in stressful conditions (such as when tumors outgrow their blood supply) by stabilizing HIF-1alpha levels, possibly by binding to and inhibiting PHD2, a prolyl 4-hydroxylase which modulates HIF-1alpha stability (Aprelikova et al. 2009).

MAGEs and cancer stem cells

In addition to their ability to function as oncogenes, MAGEs are enriched in the stem cell population of certain cancers. MAGE-A3 has much higher expression in a cancer stem cell-like side population in bladder cancer, which compared to the main population, exhibited more robust tumor growth *in vivo* (Yin et al. 2014). Additionally, MAGE-A2, -A3, -A4, -A6, -A12, and -B2 are highly enriched in the stem cell-like side population of multiple cancer cell lines (Yamada et al. 2013). Furthermore, analysis across the maturation stages of B-cells demonstrated that

MAGE-C1 is expressed with high frequency in CD34+ stem cells and early to immature B-cells (CD10+ or CD19+) (Wienand and Shires 2015), suggesting that MAGE-C1 may be intimately related to the initiating cell population in this disease. Consistently, MAGE-C1 correlates with decreased time to relapse after allogeneic stem cell transplant (Atanackovic et al. 2009) and decreased overall survival (Atanackovic et al. 2009; Andrade et al. 2008). Whether MAGEs contribute to maintenance of cancer stem cells within tumors will need to be examined.

Transcriptional regulation of MAGEs in cancer

Determining the regulatory processes controlling the aberrant re-expression of MAGEs in cancer may provide insight into potential drug targets for MAGE-expressing tumors. The use of demethylating agents such as 5-aza-2-deoxycytidine (5DC) can induce expression of MAGE-A1 in cell lines derived from malignant tumors (Weber et al. 1994; De Smet et al. 1999), and this effect can be augmented through the use of trichostatin A, an HDAC inhibitor (Schwarzenbach et al. 2014; Wischnewski, Pantel, and Schwarzenbach 2006). This suggests that type I MAGEs are not normally expressed in somatic cells due to methylation of CpG islands in their promoter regions. Mechanisms proposed for the demethylation of type I MAGE promoters include the deregulation of KIT tyrosine kinase activity (Yang, Wu, et al. 2007) and the FGFR2-IIIb that was found to be a putative upstream regulator of MAGE-A3/6 expression (Kondo et al. 2007). Fibronectin knockdown also led to increased MAGE-A3 expression (Liu et al. 2008). Fibronectin signaling through integrin receptors, FGFR2 signaling, and the c-KIT pathway all involve the PI3K/Akt (Khwaja et al. 1997; Hadari et al. 2001; Linnekin 1999) and Ras pathways

(Schlaepfer et al. 1994; Kouhara et al. 1997; Linnekin 1999), suggesting that these pathways may be the key to understanding how type I MAGEs are turned on in cancer cells.

In addition to CpG promoter demethylation, several studies have implicated additional transcriptional regulation of MAGEs in cancer. In one study, 5DC was not able to induce MAGE-A1 in several normal diploid cell lines (Weber et al. 1994), indicating that there may be more involved in the regulation of these CTAs than simply CpG demethylation. However, 5DC was able to induce MAGE-A1, -A2, -B1, and -B4 expression in normal XY karyotype human dermal fibroblasts (Vatolin et al. 2005). Brother of the Regulator of Imprinted Sites (BORIS) is a CTA and transcription factor that was found to induce the expression of MAGE CTAs in normal human dermal fibroblasts and cancer lines (Vatolin et al. 2005; Schwarzenbach et al. 2014). In addition, the Ets-1 and Sp1 transcription factors may potentially play a role in promoting expression of MAGE CTAs, but MAGE promoter demethylation is a prerequisite (De Smet et al. 1995; Wischnewski et al. 2007). The relevance of these factors in the regulation of MAGE expression is intriguing and should be further defined in the context of cancer progression.

MAGE-based therapy: from immunotherapies to direct targeting

The relatively restricted expression of MAGEs and their antigenicity has spurred research into utilizing them as targets for immunotherapies. In the largest therapeutic trial in lung cancer, MAGRIT (MAGE-A3 as Adjuvant Non-Small Cell Lung Cancer Immunotherapy), recombinant MAGE-A3 protein was injected in approximately 2,700 patients after lung cancer tumor resection (Tyagi and Mirakhur 2009). Although the MAGE-A3 vaccine was well-tolerated by patients, the phase III clinical trial failed to demonstrate an increase in disease-free survival

versus placebo (Ruiz, Hunis, and Raez 2014). Additionally, there have been unexpected deaths in anti-MAGE T-cell-based therapies due to cross-reactivity to unrelated proteins and to certain MAGEs found at low levels in normal brain (Linette et al. 2013; Morgan et al. 2013). These examples demonstrate the critical need to further pursue rigorous, detailed studies of MAGE expression across normal tissues and suggest that mechanistic studies of the MAGE proteins may offer valuable, alternative approaches to targeting a wide spectrum of cancers. For example, targeting MAGE-E3 ligase interactions, inhibiting MAGE-A11 binding to the androgen receptor in prostate cancers, and disrupting MAGE-A3/6 interaction with AMPKα1 or using AMPK agonists or mTOR inhibitors in MAGE-A positive cancers are all potential new routes to target the activity of MAGEs.

Conclusions

MAGEs are expressed in a wide-variety of cancers, but the transcriptional programs controlling their aberrant expression are unclear. MAGEs can drive tumor progression through various mechanisms, which ultimately result in more aggressive, metastatic tumors that have greater chance of recurrence. They are attractive targets of cancer therapy and more mechanistic studies of MAGE function in cancer will facilitate the development of targeted therapy across multiple types of cancers. Further study of MAGEs may facilitate determining their physiological function in the testis and may elucidate the role of a conserved gametogenic program in the context of cancer.

MAGE F1 AND POTENTIAL CLUES TO ITS FUNCTION

MAGE-F1

Human MAGE-F1 was discovered as the fourth type II MAGE in 2001, after the discoveries of MAGE-D1, -D2, and NECDIN (Stone et al. 2001). The gene is located on chromosome 3q separate from all other protein-coding MAGEs (which are located on either chromosomes 15 or the X chromosome) and is encoded by a single exon, which translates to a 307 amino acid protein. The MAGE homology domain in MAGE-F1 is composed of amino acids 83-253.

The gene was discovered while screening a cDNA library generated from stage III and IV serous ovarian tumors for genes that were immunogenic to serum from ovarian cancer patients (SEREX) (Stone et al. 2001). Whereas it was determined to be non-immunogenic, it was chosen out of interest in sequence homology to other known MAGE proteins (Stone et al. 2001). It was found to be expressed in all human tissues tested (Stone et al. 2001). An exclusive characteristic of MAGE-F1 compared to other MAGEs is a region of 6-7 GGA repeats (Stone et al. 2001), which encode a series of glutamates and is present near the center of the MAGE homology domain ~11 residues away from the dileucine motif (L87 L88) that is conserved across MAGEs and is required for E3 RING ligase binding (Doyle et al. 2010).

Curiously, MAGE-F1 may have been lost (nonsense mutation) and gained (restoration of full length gene) multiple times over the evolution of different species (Figure 1-3) Notably, it is a pseudogene in both mouse and rat due to an early stop codon.

There are no other studies solely devoted to MAGE-F1 in the literature. The few accounts of MAGE-F1 studies include a paper published by our lab in 2010 that found in an *in vitro*

screen of multiple MAGEs and E3 ligases that in vitro translated MYC-MAGE-F1 can bind to recombinant GST-NSE1 E3 ligase (Doyle et al. 2010). Prior to those results, another lab in 2008 demonstrated that a pulldown of FLAG-MAGE-F1 from cells does not bind endogenous NSE1 (Taylor et al. 2008). One other paper published in 2014 showed that FLAG-MAGE-F1 binds MYC-NSE1 in cells (Gur et al. 2014). In addition, the same paper found that MAGE-F1 bound the SUMO ligase PIAS1, as did MAGE-A1, MAGE-D1, MAGE-L2, and Necdin (Gur et al. 2014), but did not follow up on MAGE-F1 in either aspect, instead focusing on how Necdin promotes the degradation of PIAS1 and also inhibits its SUMOylation activity.

MAGE-G1, NSE1, and the SMC5/6 complex

MAGE-G1 is the MAGE family member that is closest in sequence similarity to MAGE-F1. Their MAGE homology domains are ~60% similar at the amino acid level (Doyle et al. 2010). MAGE-G1 binds the E3 ligase NSE1 in the structural maintenance of chromosomes (SMC) 5/6 complex, which also includes NSE4, SMC5, SMC6, and NSE2 in humans (Taylor et al. 2008). The SMC5/6 complex has roles in resolution of stalled replication forks (Irmisch et al. 2009), repair of double stranded DNA breaks by promoting homologous recombination between sister chromatids (De Piccoli et al. 2006), facilitating stable replication of ribosomal DNA, and maintenance of telomeres (Murray and Carr 2008; Potts 2009). MAGE-G1 binds NSE1 through its MAGE homology domain and conversely, NSE1 binds MAGE-G1 via its first winged-helix domain (WH1) (Doyle et al. 2010). The MAGE homology domain of MAGEs consists of two domains, winged-helix-A and winged-helix-B (Doyle et al. 2010). There is a conserved dileucine motif in the winged-helix-A domain of MAGEs, and a mutation of the dileucine motif of

MAGE-G1 (L96A L97A) is sufficient to disrupt binding to NSE1 but does not affect binding to NSE4a (Doyle et al. 2010).

It is thought that the SMC5/6 complex, similar to its fellow structural maintenance of chromosomes family members cohesin (SMC1/3) and condensin (SMC2/4), encircles DNA with its associated non-SMC proteins to perform its actions (Kanno, Berta, and Sjogren 2015; Uhlmann 2016).The SMC5 and SMC6 proteins are coiled-coil structures that each fold upon themselves such that they bring together their N- and C-termini ends, which is the structure that is dubbed the “head” of the protein (Palecek et al. 2006). The heads of SMC5 and SMC6 contain ATP-binding cassette (ABC) family ATPase domains which bind ATP and stabilize the interaction between the two proteins, with additional stabilization provided by the kleisin protein NSE4 (Uhlmann 2016). The interaction between the two proteins are also stabilized by interactions at the end opposite the heads (termed the “hinge”) (Uhlmann 2016). In vitro, NSE4 was found to bind via its C-terminal half to the heads of SMC5 and SMC6. Full-length MAGE-G1 likewise was found to bind to the heads of SMC5 and SMC6; however, MAGE-G1 binding to SMC5 was less dependent on a portion of the globular C-termini end of SMC5 (amino acids 1011-1065), suggesting that NSE4 and MAGE-G1 may bind SMC5 differentially (Palecek et al. 2006). It has not yet been elucidated as to which portion of MAGE-G1 binds SMC5 and SMC6.

Despite identification of NSE1 as an E3 ligase in the SMC5/6 complex, no direct ubiquitination target for the MAGE-G1-NSE1 complex has been reported, although the ubiquitination of NSE1, SMC5, and SMC6 have been observed in cells (Taylor et al. 2008). The E3 ligase NSE1 has a C-terminal RING domain (Pebernard et al. 2008), a domain which binds E2 enzymes and is necessary for ubiquitination activity (Plechanovova et al. 2012). Experiments

in fission yeast with deletion of the RING domain of NSE1 demonstrated sensitivity to MMS, HU, and UV, providing evidence that the RING domain, is necessary for DNA repair (Pebernard et al. 2008). In addition, fission yeast with deletion of the RING domain of NSE1 exhibited decrease NSE4 foci formation in the nucleus after DNA damage with MMS (Pebernard et al. 2008), though MMS addition to human cells did not exhibit a dramatic change in SMC5 or SMC6 ubiquitination, suggesting the ubiquitination of other proteins may be important for DNA damage response (Taylor et al. 2008). Although the aforementioned paper was not able to demonstrate E3 ligase ubiquitination activity for NSE1 and suggested instead that the RING domain is necessary for the trimeric interaction between NSE1, NSE3, and NSE4 (Pebernard et al. 2008), further experiments in our lab demonstrated that NSE1 does indeed have E3 ubiquitination activity in vitro, which is enhanced in the presence of MAGE-G1 (Doyle et al. 2010).

Intriguingly, gel filtration of the SMC5/6 complex members demonstrated that there is a subset of the MAGE-G1-NSE1 complex that fractionates separately from the SMC5/6 complex and a smaller subset of NSE1 that appears to also fractionate separately from MAGE-G1 (Taylor et al. 2008). Additionally, knockdown of any component of the SMC5/6 complex destabilizes all other members of the complex (Taylor et al. 2008), but our lab has observed that efficient knockdown of MAGE-G1 does not completely eliminate the levels of NSE1, suggesting there may be a pool of NSE1 that does not bind the SMC5/6 complex or MAGE-G1 (unpublished data by Melissa Brulotte).

Conclusions

MAGE-F1 is a yet functionally uncharacterized MAGE protein that is expressed throughout the human body and has been found to have unique properties including a stretch of glutamate residues in its MAGE homology domain and evidence for dynamic changes in its presence or absence in different species. Its potential binding partner NSE1 is a member of the SMC5/6 complex that binds to MAGE-F1's closest family member, MAGE-G1, which has important roles in recombination. Clarifying the interplay of this relationship will set the stage for new insights into the possible cause for MAGE family member expansion, which started rapidly in placental mammals, and potentially help determine the degree to which MAGEs have overlapping roles or possibly function as modular proteins to confer new targets for E3 RING ligases.

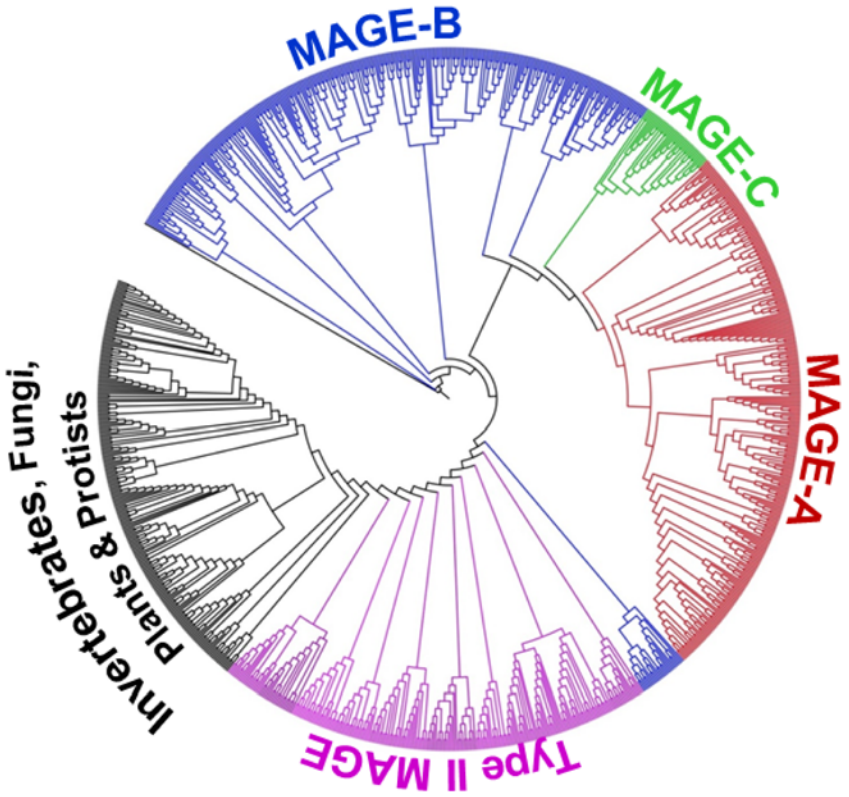

Figure 1-1. The MAGE protein family
Phylogenetic tree of eukaryotic MAGEs. Note, all non-mammalian MAGEs cluster together (black). Mammalian MAGEs have dramatically expanded in number and cluster into type II (pink) MAGEs that are anatomically broadly expressed and type I (MAGE-A, MAGE-B, and MAGE-C subfamilies) that are primarily restricted to expression in testis, ovary, and placenta.
(Weon and Potts, 2015)

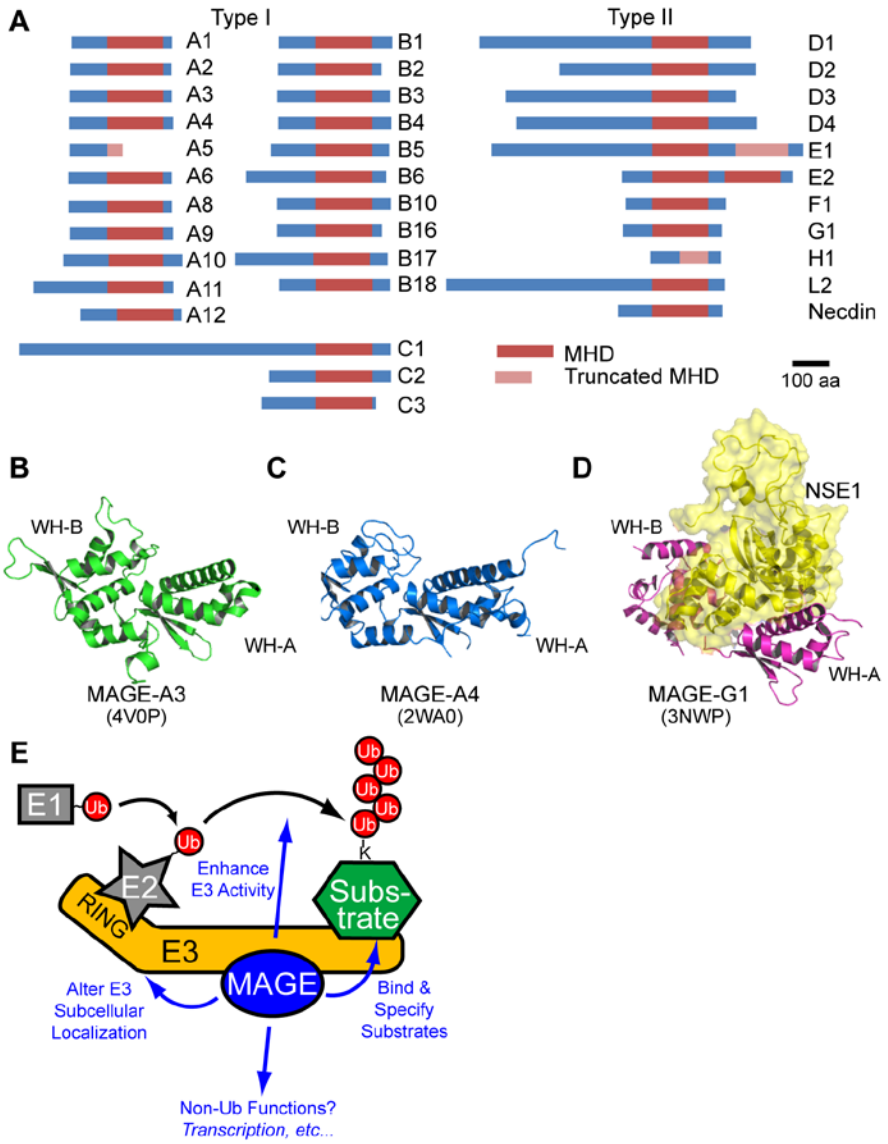

Figure 1-2. MAGE proteins structure and function
(A) List of human MAGE proteins and their known common domain, the MAGE homology domain (MHD). Note that a few MAGEs have truncated MHDs. MAGEs that are likely pseudogenes are not listed. (B–D) Crystal structures of MAGE-A3 (B), MAGE-A4 (C), and MAGE-G1 in complex with the NSE1 E3 ubiquitin ligase (D) are shown. The two winged-helix motifs (WH-A and WH-B) that form the MHD are noted. Note the change in the relative orientation of WH-A and WH-B motifs in MAGE-A3/-A4 compared to MAGE-G1 bound to NSE1. (E) Summary of known biochemical and cellular functions of MAGEs.
(Weon and Potts, 2015)

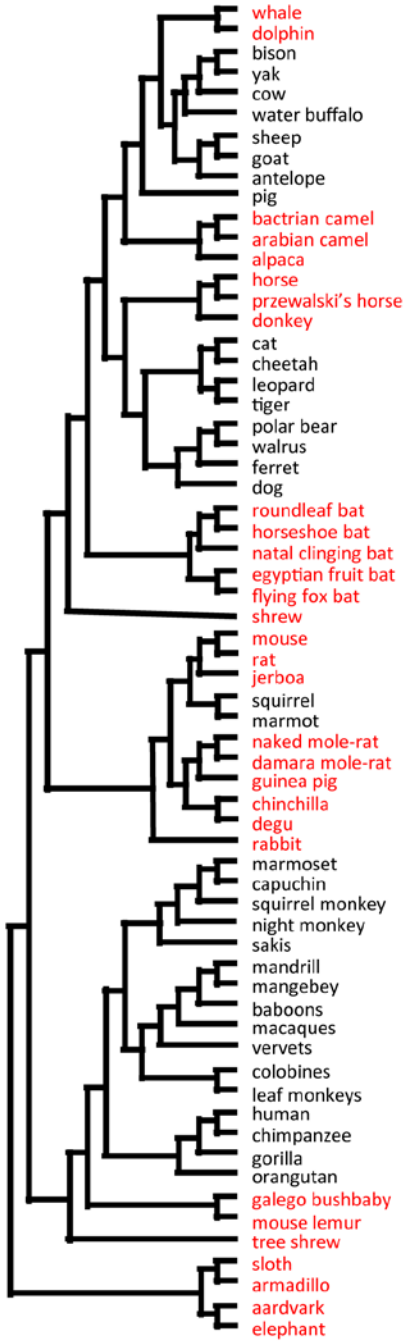

Figure 1-3. The evolution of the MAGE-F1 gene
Phylogenetic tree of sequenced vertebrates. Species with wild-type MAGE-F1 are denoted in black and species with nonsense mutations in MAGE-F1 are highlighted in red. (Figure courtesy of Ryan Potts)

Table 1-1.

Summary of high confidence interactions between MAGEs and E3 ubiquitin ligases.

MAGE	E3 Ubiquitin Ligase	Target
MAGE-A1	TRIM31 (Kozakova et al. 2015)	Unknown
MAGE-A2	MDM2 (Marcar et al. 2015)	Inhibit MDM2-mediated ubiquitination of MDM4 (Marcar et al. 2015)
MAGE-A2, -A3,-A6, -C2 MAGE-A3	TRIM28/KAP1 (Yang, O'Herrin, Wu, Reagan-Shaw, Ma, Bhat, et al. 2007; Doyle et al. 2010)	Ubiquitination and degradation of p53 (Doyle et al. 2010)
	TRIM28/KAP1 (Yang, O'Herrin, Wu, Reagan-Shaw, Ma, Bhat, et al. 2007; Doyle et al. 2010)	Ubiquitination and degradation of KZNFs containing A+B box KRAB domains (Xiao, Suh, and Longley 2014)
MAGE-A3, -A6	TRIM28/KAP1 (Doyle et al. 2010; Yang, O'Herrin, Wu, Reagan-Shaw, Ma, Bhat, et al. 2007)	Recruit AMPK alpha subunit for ubiquitination and degradation (Pineda et al. 2015)
MAGE-A4	TRIM69 (Rual et al. 2005)	Unknown
MAGE-B18	LNX1 (Doyle et al. 2010)	Unknown
MAGE-D1	Praja1 (Sasaki et al. 2002)	MAGE-D1 is ubiquitinated (Sasaki et al. 2002; Teuber et al. 2013) and modulates Dlx5 transcription factor activity (Sasaki et al. 2002)
MAGE-D1	Unknown	Ubiquitination of the serotonin transporter SERT (Mouri et al. 2012)
MAGE-D1	XIAP (Kendall et al. 2005; Jordan et al. 2001)	Unknown
MAGE-G1	NSE1 (Doyle et al. 2010; Taylor et al. 2008)	Unknown
MAGE-L2	TRIM27 (Hao et al. 2013)	K63-ubiquitination of WASH for proper actin assembly and endosomal protein recycling (Hao et al. 2013)
Necdin	Unknown	Ubiquitination and degradation of PIAS1 (Gur et al. 2014)

Table 1-2.

Summary of select cancer subtypes with percent MAGE-positive patient tumors.

Cancer Type	MAGE Gene	Percent	References
Lung, non-small cell	MAGE-A1	27-46%	(Gure et al. 2005; Kim et al. 2012; Tajima et al. 2003)
	MAGE-A3	38-55%	(Kim et al. 2012; Tajima et al. 2003; Gure et al. 2005)
	MAGE-A4	19-35%	(Tajima et al. 2003)
	MAGE-A6	26%	(Kim et al. 2012; Tajima et al. 2003; Gure et al. 2005)
	MAGE-A10	14-27%	(Gure et al. 2005; Jungbluth et al. 2002)
	MAGE-C1	19%-27%	(Barrow et al. 2006; Brasseur et al. 1995)
Melanoma	MAGE-A1, primary tumor	16-20%	(Barrow et al. 2006; Brasseur et al. 1995)
	MAGE-A1, metastases	48-51%	(Curioni-Fontecedro et al. 2011)
	MAGE-C1, primary tumor	24%	(Curioni-Fontecedro et al. 2011)
	MAGE-C1, metastases	40%	(Curioni-Fontecedro et al. 2011)
	MAGE-C2, primary tumor	33%	(Curioni-Fontecedro et al. 2011)
	MAGE-C2, metastases	40%	(Curioni-Fontecedro et al. 2011)
Breast	MAGE-A1	6%	(Otte et al. 2001)
	MAGE-A2	19%	(Otte et al. 2001)
	MAGE-A3/6	10-15%	(Otte et al. 2001; Ayyoub et al. 2014)
	MAGE-A4	13%	(Otte et al. 2001)
	MAGE-A9	45%	(Hou et al. 2014)
	MAGE-A11	67%	(Hou et al. 2014)
	MAGE-A12	9%	(Otte et al. 2001)
	MAGE-C1	14%	(Chen et al. 2011)
	MAGE-C2	8%	(Chen et al. 2011)
Ovarian	MAGE-A1	15%-53%	(Daudi et al. 2014; Zhang et al. 2010)
	MAGE-A3	36%-37%	(Daudi et al. 2014; Zhang et al. 2010)
	MAGE-A4	47%	
	MAGE-A9	52%	

	MAGE-A10	37%	(Daudi et al. 2014)
	MAGE-C1	16%	(Daudi et al. 2014) (Xu et al. 2015) (Daudi et al. 2014)
Colon	MAGE-A1	12%-30%	(Mori et al. 1996; Li et al. 2005)
	MAGE-A2	28%	
	MAGE-A3	20-27%	(Mori et al. 1996)
	MAGE-A4	22%	(Mori et al. 1996; Li et al. 2005) (Li et al. 2005)
Multiple myeloma	MAGE-A1	<10-26%	(Nardiello et al. 2011; Andrade et al. 2008)
	MAGE-A2	36%	
	MAGE-A3/6	37-41%	(Andrade et al. 2008)
	MAGE-A3/6, after relapse	77%	(Nardiello et al. 2011; Andrade et al. 2008)
	MAGE-A12	20%	
	MAGE-C1	77%	(Nardiello et al. 2011)
	MAGE-C2	50-59%	(Andrade et al. 2008) (Nardiello et al. 2011; Andrade et al. 2008) (Nardiello et al. 2011)

CHAPTER TWO

IRON SULFUR CLUSTER ASSEMBLY PATHWAY

Introduction

Iron and sulfur-containing inorganic clusters (Fe-S clusters) are considered to be one of the oldest cofactors used by proteins and they are utilized by living organisms in all three kingdoms of life. Proteins that utilize these clusters include those involved in essential processes, such as in mitochondrial respiration (Stehling, Sheftel, and Lill 2009; Sheftel et al. 2009), translation of mRNA (Paul et al. 2015), and repair of DNA lesions (Stehling et al. 2012; Gari et al. 2012). Therefore it is not surprising that many proteins involved in the assembly and incorporation of these Fe-S clusters into target proteins are required for viability (Lill and Muhlenhoff 2005). Iron sulfur clusters are most commonly found in [2Fe-2S] or [4Fe-4S] forms in eukaryotes (Rouault and Tong 2008) and are typically coordinated to cysteine residues in proteins (Rouault and Tong 2008).

Many mitochondrial, cytosolic, and nuclear proteins require Fe-S clusters for enzymatic (Lloyd et al. 1999), electron transfer (Johnson et al. 2005), and as structural components for stability (Stehling et al. 2012; Seki et al. 2013). Examples of mitochondrial proteins that require iron-sulfur clusters include those involved in heme synthesis (ferrochelatase), respiration (respiratory complexes I-III), and the citric acid cycle (aconitase), as well as those involved in the generation of other cofactors required in the cell, such as lipoate or biotin (Lill et al. 2015). Examples of cytosolic proteins that require iron-sulfur clusters include those involved in iron regulation (IRP1), synthesis of amino acids (glutamate dehydrogenase, sulfite reductase), production of ribosomes (Rli1), and again the synthesis of other cofactors such as molybdenum

(MOCS1A) (Lill and Muhlenhoff 2005). Examples of nuclear proteins that require iron sulfur clusters include proteins involved in nucleotide excision repair (XPD), homologous recombination (FANCJ), telomere maintenance (RTEL1), and lagging strand synthesis (POLD1) (Netz et al. 2014). Although there is not a conserved motif amongst Fe-S cluster-containing proteins (Fuss et al. 2015), the list of identified iron-sulfur proteins continues to grow through utilizing techniques such as native biomass analysis, electron paramagnetic resonance, and Mossbauer spectroscopy (Fuss et al. 2015).

The basic recipe for an Fe-S cluster calls for the following: 1) sulfur from L-cysteine, 2) ferrous iron, and 3) electron transfer (Paul and Lill 2015). Although Fe-S clusters can spontaneously form on an iron sulfur apoprotein *in vitro* with these components (Malkin and Rabinowitz 1966), free iron in the cell is toxic due to its ability to generate free radicals upon interaction with products of aerobic respiration (H_2O_2, $O2^{\bullet -}$) and can damage proteins and nucleic acids (Lemire, Harrison, and Turner 2013; Floyd and Carney 1992); thus the production of Fe-S clusters in vivo must be highly monitored and regulated. The machinery dedicated to the generation of Fe-S clusters consists of two main pathways, the mitochondrial iron sulfur clustery assembly machinery (ISC) and the cytosolic iron sulfur cluster assembly machinery (CIA). The ISC is responsible for the generation of Fe-S clusters for mitochondrial proteins, and both the ISC and CIA are required for the generation of Fe-S clusters for cytoplasmic and nuclear proteins (Paul and Lill 2015).

The mitochondrial iron sulfur cluster assembly pathway

The genesis of all Fe-S clusters in the cell begins in the mitochondria via the action of the mitochondrial iron sulfur cluster assembly machinery (ISC), which consist of 17 proteins in organisms from yeast to humans (Paul and Lill 2015). The evidence for the mechanistic details of the ISC machinery has been extensively studied in yeast and has been corroborated in humans. The mammalian ISC machinery will be described here, as it is more relevant to this study. Iron is first transported into the mitochondria by mitochondrial iron transporters mitoferrin-1 and -2 (MFRN1 and MFRN2) (Paradkar et al. 2009). Iron stores in the mitochondria are then possibly mobilized by frataxin (FXN), which is thought to be a potential iron donor in the generation of iron-sulfur clusters (Paul and Lill 2015). In the mitochondria, the cysteine desulfurase complex NFS1-ISD11 extracts sulfur from L-cysteine, which forms a persulfide on NFS1 at cysteine 383 before being transferred to the scaffold protein ISCU on cysteine 104 (Parent et al. 2015). Frataxin has been found to stimulate this reaction by either promoting the desulfuration step or promoting the transfer of the resulting persulfide to the scaffold protein ISCU (Bridwell-Rabb et al. 2014; Bencze et al. 2006; Parent et al. 2015) and may also provide the source of iron (Stemmler et al. 2010), though the source of iron is still under debate. Additionally, electron transfer from the NADPH-ferredoxin reductase-ferredoxin chain is required and is theorized to reduce sulfur to the S^{2-} state that is present in Fe-S clusters (Paul and Lill 2015; Lill 2009). These components generate a [2Fe-2S] cluster on the scaffold protein ISCU (Paul and Lill 2015). The [2Fe-2S] cluster is then released from ISCU via the binding of chaperones HSCB and mortalin and transferred to GLRX5 (Ciesielski et al. 2012; Uzarska et al. 2013; Stehling and Lill 2013; Paul and Lill 2015). The cluster may then be delivered to [2Fe-2S] mitochondrial proteins (Lill et

al. 2015). Other mitochondrial proteins require [4Fe-4S] clusters, so IBA57 and ISCA serve to then reductively combine 2 [2Fe-2S] clusters to one [4Fe-4S] (Paul and Lill 2015). The [4Fe-4S] is then targeted to recipient apoproteins through the actions of NFU1 and IND1 (Paul and Lill 2015).

A number of human diseases are associated with defects in the mitochondrial iron sulfur cluster machinery. Deficiencies in frataxin (FXN) expression due to intronic expansion of a trinucleotide GAA sequence in the gene cause Friedriech's ataxia, an autosomal recessive disease characterized by motor defects and defects in mitochondrial iron sulfur cluster assembly leading to abnormal mitochondrial overload (Campuzano et al. 1996; Rotig et al. 1997; Rouault and Tong 2008). A homozygous mutation in GLRX5 (c.294A>G) that leads to a splicing defect in the first intron of GLRX5 reduces expression of the gene and was determined to be the cause of sideroblastic anemia in a patient (Camaschella et al. 2007; Ye and Rouault 2010). A mutation in ISCU (G7044C) found in several patients of Swedish descent is ineffectively spliced and the resulting low expression of this gene results mitochondrial overload in the muscle and exercise intolerance due to myopathy (Mochel et al. 2008; Olsson et al. 2008; Haller et al. 1991; Ye and Rouault 2010). Interestingly, a commonality that can be seen amongst depletion of many different mitochondrial iron sulfur cluster assembly pathway members and in these diseases is the result in increased mitochondrial iron load and decreased cytosolic iron levels (Rouault and Tong 2008), suggesting that deregulation of the mitochondrial iron sulfur cluster machinery perturbs overall cellular iron homeostasis.

The cytosolic iron sulfur cluster assembly pathway

The cytosolic iron sulfur cluster assembly machinery (CIA) members are not structurally homologous to mitochondrial ISC members, but similarly acts upon the principle of an initial electron transfer (reductive) reaction upon an iron sulfur cluster-holding scaffold protein, then eventual transfer to targeting proteins which have different specificities for downstream apoproteins (Lill 2009). The mammalian cytosolic iron sulfur cluster pathway begins with the mitochondrial ABCB7-mediated export of a yet unknown sulfur-containing compound (X-S) that requires the core mitochondrial ISC machinery, which includes all the steps up to the transient binding of the [2Fe-2S] cluster to GLRX5 and prior to the formation of the [4Fe-4S] cluster by IBA57 and ISCA (Paul and Lill 2015). The putative X-S has been theorized to be a GSH-coordinated Fe-S cluster (Qi et al. 2012) or alternatively, GSSSG (Schaedler et al. 2014). The X-S compound is then thought to interact with a scaffolding complex composed of a heterotetrameric complex composed of NTPases, two NBP35 and two CFD1 proteins and assist with the formation of [4Fe-4S] clusters (Lill et al. 2015). Two [4Fe-4S] clusters have been found to be tightly bound by the two N-termini of each NBP35, and two additional labile [4Fe-4S] compounds can be sandwiched between the interfaces of NBP35 and CFD1 (Paul and Lill 2015). The N-termini [4Fe-4S] of NBP35 must receive a reducing electron from NADPH that runs through NDOR1 and CIAPIN, and a yet unknown nucleotide must bind to the NBP35-CFD1 complex and may or may not be hydrolyzed for the maturation of the cluster (Lill et al. 2015). It is thought that the labile [4Fe-4S] sandwiched between each NBP35 and CFD1 are then assisted by the action of IOP1 (it itself harbors two [4Fe-4S] clusters, one of which is more labile than the other, but it remains to be proven if either of these clusters is then passed on to targets) and the

CIA targeting complex composed of different modules of CIA1, CIA2A, CIA2B, and MMS19 for assembly into target aproproteins (Lill et al. 2015). Whereas CIA1, CIA2B and MMS19 are thought to be involved in targeting a variety of the currently known downstream Fe-S protein targets, CIA2A is thought to be specific for the iron regulatory protein IRP1 (Paul and Lill 2015; Stehling et al. 2013), a protein that can bind to iron response elements in mRNA and can either stabilize their half-life (such as for transferrin, which will consequently increase iron uptake) or inhibit their translation (such as for ferritin, which will decrease storage of iron) (Rouault 2006). Incorporation of a [4Fe-4S] cluster into IRP1 converts it into the enzyme aconitase, which functions to converts citrate to isocitrate (Kennedy et al. 1992). CIA2A can also stabilize IRP2 (which does not have an Fe-S cluster) by direct binding, which similarly functions to increase iron uptake and mobilize iron stores in the cell (Rouault 2006). It is thought that IRP2 is actually the primary sensor for iron homoeostasis in the cell and that IRP1 mostly functions as cytosolic aconitase (Rouault 2006). In contrast to humans, yeast only possess one CIA2 protein; thus the presence of this extra CIA2 protein in humans is an intriguing factor that suggests more nuanced iron regulation (Lill et al. 2015).

The role of MMS19

MMS19 was originally discovered in yeast as a gene in which mutation conferred sensitivity to DNA alkylating agent methylmethanesulfonate (MMS) (Prakash and Prakash 1977) and caused elongated telomeres, methionine auxotrophy, in addition to susceptibility to DNA damage (Lauder et al. 1996; Stehling et al. 2012). MMS19 is a 113 kDa protein that functions at the end of the cytosolic iron sulfur cluster machinery in modular complexes with other Fe-S cluster

targeting members CIA1 and CIA2B and is responsible for binding to specific target proteins of interest and assisting the final step of incorporation (Paul and Lill 2015). Therefore, modulating MMS19 will alter the function of a subset of Fe-S cluster proteins. In particular, many MMS19-dependent Fe-S cluster proteins include those destined for the nucleus and are involved in DNA metabolism and repair (Table 2-1) (Stehling et al. 2012; Gari et al. 2012; van Wietmarschen et al. 2012; Seki et al. 2013).

MMS19 downstream targets

The functions of a subset of downstream MMS19-dependent targets will be covered briefly here since they are included in this study. MMS19 targets XPD, FANCJ, RTEL1, and DDX11, constitute four of the five members of the Rad3/XPD 5'-3' superfamily 2 DNA helicases (Fairman-Williams, Guenther, and Jankowsky 2010). The proteins in this family contain four conserved cysteines required for Fe-S cluster incorporation in their Fe-S domain (Fairman-Williams, Guenther, and Jankowsky 2010; Paul and Lill 2015) and also all contain an arch domain. The fifth protein, DDX12, has not yet been verified to be dependent on MMS19. FANCJ was originally discovered as a BRCA1-interacting protein (Cantor et al. 2001), therefore it is also known as Brca1-Associated C-terminal Helicase (BACH1). It was later elucidated that deficiencies in BACH1 in patients led to Fanconi anemia of complementation group J (FANCJ) (Litman et al. 2005). FANCJ is required for repair of DNA double stranded breaks, interstrand cross-links, and has also been more recently implicated in alleviating replicative stress associated with resolution of G-quadruplex (G4) nucleic acid structures (Brosh and Cantor 2014). An A349P mutation in FANCJ leads to Fanconi anemia and resides directly adjacent to the fourth

conserved cysteine, C350, that is required for [4Fe-4S] coordination. This mutant was found to bind DNA and possess ATPase activity like the wild-type protein but was unable to unwind G4 and forked duplex DNA, demonstrating a loss of its ability to function as a helicase (Wu et al. 2010). XPD is a member of the TFIIH complex (Schaeffer et al. 1994) that plays a role in transcription-coupled nucleotide excision repair, which is important for the removal of bulky lesions such as pyrimidine dimers formed after UV damage (Svejstrup 2002). Point mutations related to XPD have been implicated in a number of diseases, including xeroderma pigmentosum (XP), trichothiodystrophy (TTD), and Cockayne syndrome (CS), which are all characterized by sensitivity to UV light, although only xeroderma pigmentosum has been associated with cancer (Kraemer et al. 2007; Paul and Lill 2015). One the most frequently observed mutations in trichothiodystrophy patients is R112H, which is very close to C116, the first [4Fe-4S]-coordinating cysteine in XPD (Wu and Brosh 2012). Generating mutations in the 4Fe-4S cluster coordinating cysteines have been found to eliminate helicase activity and dramatically reduce ATPase activity (Fan et al. 2008). Regulator of telomere elongation helicase 1 (RTEL1) is important for telomere homeostasis and via its helicase activity can unwind triple-stranded DNA structures such as D-loops that are intermediates of homologous recombination and T-loops that exist at telomeres (Uringa et al. 2011). Mutations in this gene have been associated with a rare disease called Hoyeraal-Hreidarsson syndrome, in which telomeres are abnormally shortened (Le Guen et al. 2013). In addition to helicases, a number of polymerases have been shown to be dependent on Fe-S clusters, and polymerase delta (POLD1) is one key example that is regulated by MMS19. The B family of DNA polymerases, which includes polymerase delta, epsilon, and zeta are structurally related in that they possess an N-terminal catalytic domain and a C-terminal

domain that includes both zinc-coordinating and Fe-S coordinating cysteines (Fuss et al. 2015). POLD1 is required for lagging strand synthesis and is involved in nucleotide excision repair, base excision repair, and mismatch repair (Iyama and Wilson III, 2013).

Mechanism of MMS19 binding to target proteins

With such a broad repertoire of substrate proteins, some of which are in different families of proteins, how does MMS19 determine which proteins are its targets? One paper found that phosphorylation of DNA polymerase epsilon (POLE1) after DNA damage (ultraviolet irradiation, ionizing radiation) on S1940 by ATM is required for interaction with MMS19 (Moiseeva et al. 2016). In theory, the idea of MMS19 having specificity for binding to targets in conditions of DNA damage is palatable because when the genome is at stake it would make sense to generate more DNA repair enzymes and incorporate more essential [4Fe-4S] clusters into these targets. However, the necessity of a post-translational modification on other MMS19-target proteins is unclear, as many other papers validating the binding of MMS19 to target proteins were performed without addition of DNA damaging agents (Stehling et al. 2012; Gari et al. 2012; Seki et al. 2013; van Wietmarschen et al. 2012). Other studies have utilized domain mapping to determine the domains necessary for MMS19 binding to target proteins or vice versa. For mouse XPD, it has been determined that MMS19 binds to a stretch of residues that is C-terminal to the arch domain (van Wietmarschen et al. 2012). For human XPD, it has been determined that MMS19 binds to a small region within the arch domain, and mutant XPD with a deletion of this region (Δ277-286) fails to resist DNA damage and showed decreased survival compared to wild-type XPD when treated with UV (Vashisht et al. 2015).

Possible explanations for the requirement of iron sulfur clusters in DNA repair

It is puzzling why proteins that are required for DNA repair also harbor such potentially toxic cofactors. Fe-S clusters are easily susceptible to degradation by oxidative stress and are more stable in anerobic conditions (Imlay 2006). Oxidation of a [4Fe-4S] cluster by oxygen or hydrogen peroxide causes it to become unstable and undergo loss of one of the Fe, which can separately then undergo the fenton reaction and produce reactive oxygen species that are damaging to both DNA, protein, and lipid products (Imlay 2006; Lemire, Harrison, and Turner 2013). One theory as to why proteins have kept their Fe-S clusters over years of evolution is that Fe-S clusters can both accept or donate electrons and can be utilized to efficiently sense the presence of DNA damage over a large span by detecting changes in charge transfer (CT) over DNA (Fuss et al. 2015). Undamaged, double-stranded DNA is thought to be able to conduct charge over long distances, like a wire, through pi electron cloud stacking in the bases (Fuss et al. 2015). However, when there is a lesion in the DNA or if the DNA is single stranded, this charge transfer is abated (Fuss et al. 2015). It is thought that DNA repair proteins can utilize this charge transfer property of DNA to more easily and rapidly congregate around sites of damage. For example, if an Fe-S cluster-containing DNA repair enzyme was bound to DNA and a then second Fe-S cluster-containing enzyme bound DNA, the cluster of the second enzyme could reduce the first Fe-S cluster-containing enzyme and cause it to be more loosely associated with the DNA. Conversely, if there was a lesion in the DNA that would prevent charge transfer, then the second enzyme would not be able to reduce the first and both enzymes would be more likely to stay longer around the site of damage, potentially setting the stage for more accumulation of DNA repair enzymes.

Hints at post-translational mechanisms affecting iron sulfur cluster assembly

Changes in protein stability of mitochondrial or cytosolic Fe-S cluster assembly members have been suggested to regulate the pathway, but the specific mechanism by which these observations occur have not been elucidated. Yeast Isu (ISCU in humans), which is the scaffold protein that mitochondrial Fe-S clusters are built upon, was found to be stabilized both at the mRNA and protein levels upon deletion of the Ssq1 chaperone, partial loss-of-function Jac1 co-chaperone, Grx5, and Yfh1 (Andrew et al. 2008). All except Yfh1 lie upstream of Isu in the mitochondrial Fe-S cluster assembly pathway (Lill 2009). Pim1, a mitochondrial protease, degrades Isu when it is not bound to an Fe-S cluster or has a hydrophobic domain exposed due to lack of binding to its partners Nfs1 and Jac1 (Ciesielski et al. 2016). However, it is unclear under what circumstances yeast Isu may need to be actively regulated. A more targeted mechanism of ISCU regulation was described in drosophila, where dIscU was found to be phosphorylated at serine 20 by dMK2 (drosophila MAPK-activated protein kinase 2), which mediates p38-responses to stress pathways (Tian et al. 2014). dIscU knockout flies exhibited diminished survival in the face of oxidative stress from paraquat or H_2O_2 treatment (Tian et al. 2014). Rescue of dIscU knockout flies with phosphorylation mutants did not affect mitochondrial or cytosolic aconitase activity, but the S20A mutant was found to increase complex I activity, whereas the S20E mutant diminished complex I activity, suggesting that phosphorylation of dIscU may alter the production of Fe-S clusters for specific pathways during cellular stress (Tian et al. 2014). In addition, knockdown of human MK2 diminished phosphorylation of human ISCU2, suggesting that this stress-response pathway may also be conserved in mammals (Tian et al. 2014).

Possible mechanisms of post-translational regulation of cytosolic iron-sulfur cluster assembly members has been even less characterized than that of the mitochondrial components and at its current state, only describes the necessity of the proteasome without any possible hints at what proteins target these members for degradation. In yeast, MMS19 has been found to be destabilized under low iron conditions. Depletion of iron using a membrane-imperable ferrous iron (Fe^{2+}) chelator bathophenanthroline disulfonate (BPS) cause robust decrease in MMS19 protein levels within 11 hours, which could be rescued by the addition of a proteasome inhibitor MG132 (Lev et al. 2013). It has not yet been elucidated what machinery targets MMS19 for degradation in this context. In humans, the cytosolic iron-sulfur cluster assembly member MIP18 (also known as CIA2B) has been shown to be stabilized via binding to its cognate partner, MMS19, but the details of which protein ubiquitinates MIP18/CIA2B for degradation and the conditions in which this may be regulated has not been explored (Odermatt and Gari 2017).

Thus far, post-translational mechanisms by which to control aspects of the iron sulfur cluster machinery has been hinted at, but not fully elucidated. In particular, mechanisms of regulating the cytosolic iron sulfur cluster assembly have only hinted at possible involvement of the proteasome machinery, and thus determining which proteins may be responsible for post-translational modification and regulation of MMS19 or MIP18 may lend further insights into ways the machinery could be dysregulated or manipulated for therapeutic use.

MMS19 and iron in cancer

It was previously shown that knockdown of MMS19 causes an increase in protein levels of iron regulatory protein 2 (IRP2) by an unknown mechanism, leading to an increase of transferrin receptor (TFR1) on the surface of cells (Stehling et al. 2013). The transferrin receptor functions to bind ferric iron (Fe^{3+})-bound transferrin and is then internalized for cellular iron uptake (Aisen 2004). Interestingly, the role of iron as a cancer-promoting agent has been observed in multiple cancer types, including lung, colon, liver, breast, among others (Torti and Torti 2013). These cancers exhibit dysregulation of iron metabolism, including increased iron uptake and reduction of iron storage in ferritin, leading to higher levels of overall labile iron (Torti and Torti 2013). Increased iron availability due to these two events is thought to help initiate tumor development by causing damage via the production of reactive oxygen species (Fenton reaction) and also promote tumor growth by way of the necessity of iron for processes such as DNA replication and amino acid biosynthesis (Torti and Torti 2013). Many cancers, including lung cancers, have been shown to express higher levels of TFR1 (Torti and Torti 2013). In addition, IRP2-overexpression has been shown to robustly promote tumor growth over control in H1299 lung cancer mouse xenografts (Maffettone et al. 2010).

Conclusions

The concerted efforts of the mitochondrial and cytosolic iron sulfur cluster assembly machineries allow for the careful assembly of Fe-S clusters in the cell, which are critical components of multiple essential processes such as respiration, translation, and DNA metabolism. MMS19 serves as a critical gateway between the assembly and incorporation of Fe-S clusters into specific

target proteins, many of which are DNA repair enzymes and thus is necessary for genomic stability. Thus, it is no surprise that the machinery for the assembly of Fe-S clusters is present in all three kingdoms of life and is has conserved components throughout evolution. In addition to its direct role in Fe-S cluster targeting in the cytosolic iron sulfur cluster pathway, MMS19 has been shown to regulate iron uptake in cells via repression of the IRP2-transferrin receptor axis. It is possible that dysregulation of this pathway may be relevant in tumorigenesis, as multiple cancer types have been shown to harness larger free labile iron pools for growth by increasing iron uptake.

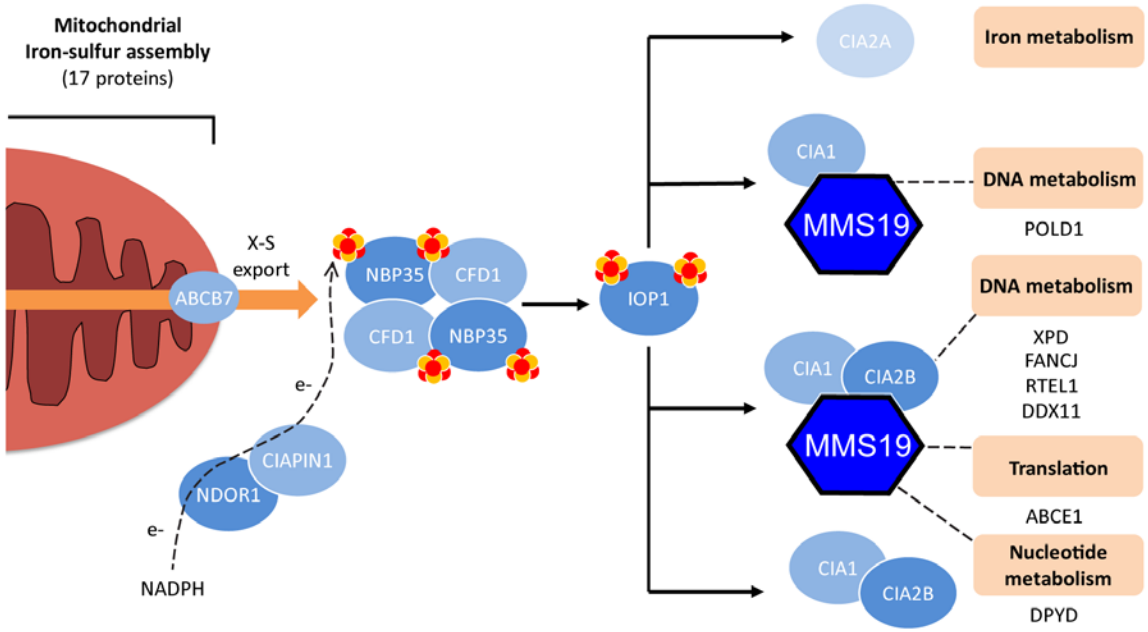

Figure 2-1. The cytosolic iron sulfur cluster assembly (CIA) pathway
The mitochondria is required for the generation of all iron sulfur clusters in the cell, including those within the mitochondria and those destined for incorporation into proteins in the cytoplasm and nucleus. Mitochondrial ABCB7 facilitates export of an unidentified but critical sulfur-containing compound (X-S) and the production of cytosolic iron sulfur clusters begins with the assembly of 4Fe-4S clusters on the heterotetrameric scaffolding complex NBP35-CFD1. The generation of cytosolic iron clusters requires an electron donor through the NADPH-NDOR1-CIAPIN1 chain. With the assistance of IOP1 and the iron sulfur cluster targeting complexes that directly bind specific apoproteins (composed of different modular components of CIA1, CIA2A, CIA2B, and MMS19), the iron sulfur clusters are incorporated into targets to generate holoenzymes. Select proteins that require MMS19 for iron-sulfur cluster assembly are highlighted at the end of the pathway. Of note, MMS19 is required for many enzymes that are involved in DNA metabolism. (Figure adapted from Paul and Lill, 2015)

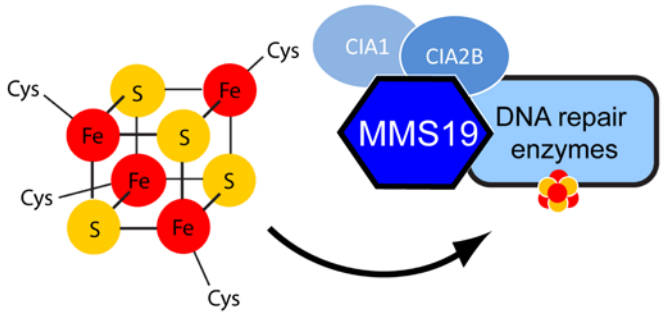

Figure 2-2. The MMS19-CIA1-CIA2B targeting complex
The MMS19-CIA1-CIA2B targeting complex is one of the modular complexes in the cytosolic iron sulfur clustery machinery that binds target apoproteins, including many DNA repair enzymes. The complex directly binds the apoprotein of interest and facilitates [4Fe-4S] transfer from upstream CIA components NBP35-CFD1 in a manner that requires IOP1. The targeting complex members themselves do not harbor iron sulfur clusters.

Table 2-1.

List of human MMS19 targets and their functions

Gene	Full name	Function	Evidence
FANCJ	Fanconi anemia group J protein	Homologous recombination	Binds MMS19 (van Wietmarschen et al. 2012) Destabilized by MMS19 knockdown (Seki et al. 2013; Gari et al. 2012)
XPD	Xeroderma pigmentosum group D	Nucleotide excision repair	Binds MMS19 (van Wietmarschen et al. 2012) Destabilized by MMS19 knockdown (Seki et al. 2013; Gari et al. 2012)
RTEL1	Regulator of telomere elongation helicase 1	Telomere maintenance	Binds MMS19 (Gari et al. 2012) Destabilized by MMS19 knockdown (Seki et al. 2013)
DDX11	DEAD/H-Box Helicase 11	rDNA metabolism	Destabilized by MMS19 knockdown (Seki et al. 2013)
POLD1	DNA polymerase delta 1, catalytic subunit	DNA lagging strand synthesis	Binds MMS19 (Stehling et al. 2012) Destabilized by MMS19 knockdown (Seki et al. 2013)
DPYD	Dihydropyrimidine dehydrogenase	Pyrimidine catabolism	MMS19 depletion leads to decreased enzymatic activity (Stehling et al. 2012)
DNA2	DNA2-like helicase	Double stranded break repair	Binds MMS19 (van Wietmarschen et al. 2012; Gari et al. 2012)
POLE1	DNA polymerase epsilon, catalytic subunit	DNA leading strand synthesis	Binds MMS19 (Seki et al. 2013)
PRIM2	Primase (DNA) subunit 2	Synthesis of RNA primers	Binds MMS19 (Seki et al. 2013; Gari et al. 2012)
MPG	DNA-3-methyladenine glycosylase	Base excision repair	Binds MMS19 (van Wietmarschen et al. 2012)
MUTYH	MutY DNA glycosylase	Base excision repair	Binds MMS19 (van Wietmarschen et al. 2012)

CHAPTER THREE

Methodology

Cell Culture

HEK293, HEK293/A658, HeLa Tet-ON (Clontech), and HeLa-Cas9 stable cells were grown in DMEM supplemented with 10% FBS, 2 mM L-glutamine, and 100 units/mL penicillin, 100 mg/mL streptomycin, and 0.25 mg/mL amphotericin B. HeLa-Cas9 stable cells were a gift from Dr. Ezra Burstein (UT Southwestern). HCC95, H520, Calu-3, H1648, H2126, HCC193, H358, and H2228 cells were grown in RPMI supplemented with 5% heat inactivated serum. siRNA transfections were performed using Lipofectamine RNAiMAX (Invitrogen) and plasmid transfections were performed using Effectene (Qiagen) according to the manufacturer's instructions.

Antibodies, siRNAs, and CRISPR/Cas9 knockouts

Antibodies used in this paper are as follows: anti-actin (Abcam #ab6276), anti-DPYD (Santa Cruz Biotechnology #sc-50521), anti-FANCJ (Bethyl Laboratories #A300-561A), anti-FLAG (Sigma-Aldrich #F3165-1MG), anti-GAPDH (Cell Signaling Technology #2118S), anti-HA (Roche #11666606001), anti-IOP1 (Sigma-Aldrich #SAB4502760-100UG), anti-IRP2 (Santa Cruz Biotechnology #sc-33682), anti-MMS19 (Proteintech #16015-1-AP), anti-MYC (Roche #9E10), anti-POLD1 (Santa Cruz Biotechnology #sc-17776), anti-RTEL1 (Santa Cruz Biotechnology #sc-85900), anti-SMC5 (Bethyl Laboratories #A300-236A), anti-SMC6 (Bethyl

Laboratories #A300-237A), and anti-XPD (Abcam #ab47186). Rabbit polyclonal antibodies were generated against MAGE-F1 (first 59 amino acids from N-terminus) and NSE1 (full length protein) (Cocalico Biologicals, Inc).

siRNAs used in this paper are as follows: siControl: 5'-ACUACAUCGUGAUUCAAACUU-3', siFANCJ-1: 5'-AGUCAAGAGUCAUCGAAUA-3' (Zou et al. 2013), siFANCJ-2: 5'-UAACCCAAGUCGCUAUAUA-3' (Zou et al. 2013), siMAGE-F1 #1: 5'-GGUGCAACCCUCAAAGUAU-3', siMAGE-F1 #2: 5'-CGAAGAGGCUUAUUAUGGA-3', siMMS19-1: 5-' AGGCCCUAGUGCUCAGAUA-3', siMMS19-2: 5'-GACUCUGAAUGCUUGCUGU-3', siNSE1: 5'-GGAACUGAUUAUUGACUCA-3', siPOLD1-1: 5'-CGGGACCAGGGAGAAUUAAUA-3' (Hocke et al. 2016), siPOLD1-2: 5'-CAGUUGGAGAUUGACCAUUAU-3' (Hocke et al. 2016), siRTEL1-1: 5'-GCCUGUGUGUGGAGUAUGA-3' (Schertzer et al. 2015), siRTEL1-2: 5'-GACCAUCAGUGCUUACUAU-3' (Schertzer et al. 2015), siXPD-1, -2, and -3 were purchased from Sigma (Rosetta predictions: SASI_Hs01_00232954, SASI_Hs01_00232955, SASI_Hs01_00232956).

For generation of HeLa-Cas9 MAGE-F1 knockout cells, synthetic tracrRNA (Dharmacon #U-002000-20) and custom crRNAs targeting near the 3' and 5' ends of MAGE-F1 were purchased from Dharmacon (MAGE-F1 crRNA #1: 5'-CUCCCGGUCCCGCAGGCCGAGUUUUAGAGCUAUGCUGUUUUG-3'; MAGE-F1 crRNA #2: 5'-CUAGGGCCGGCAUCCACCUCGUUUUAGAGCUAUGCUGUUUUG-3'). Both

tracrRNA and custom crRNAs were resuspended in sterile Tris buffer pH 7.4 to 10 uM. HeLa-Cas9 MAGE-F1 knockout cells were generated by plating $1.2x10^6$ HeLa-Cas9 stable cells in 10 cm plates. 24 hours later, the tracrRNA and 2 crRNAs were transfected using Lipofectamine RNAiMAX. A 1:2 ratio of RNA:RNAiMAX was utilized, and tracrRNA and total crRNA were utilized in a 1:1 ratio (total 20 nM final concentration in 10 cm plate) and transfected as per manufacturer's instructions. Media was changed at 24 hours after transfection and expanded at 48 hours. Cells were then diluted to single cell density per 2 wells in 96-well plates. Clones were expanded and then tested for knockout by harvesting genomic DNA via Wizard Genomic DNA Purification Kit (Promega) as per manufacturer's instructions and PCR amplifying for MAGE-F1 utilizing two primers: MAGE-F1 forward 5'-AGCTCCCGCTGCCATTGCTCCTTGTAC-3' and MAGE-F1 reverse 5'-TCGCCCCACCCATATTACTTATGACTCAGG-3'. Loss of MAGE-F1 expression was also validated by qPCR.

RNA Preparation and quantitative reverse transcription PCR analysis (qRT-PCR)

RNA was extracted from cultured cells using RNAStat60 (TelTest) according to manufacturer's instructions and subsequently treated with DNAse I (Roche) and converted to cDNA utilizing reagents from High Capacity cDNA Reverse Transcription kit (Life Technologies). cDNA from cells were plated in triplicate in a 384-well plate and expression of genes of interest was measured using SYBR Green with the following primers: human MAGE-F1 forward: 5'-AGTACCGTGAGGCCCTAGC-3', human MAGE-F1 reverse: 5'-TCATACTGGCTTCAGCTCTGG -3', human MMS19 forward: 5'-AATCCAGCTTTTGTCACAGGTG-3', human MMS19 reverse: 5'-

AGTATCAGGTGTACCACTTCCTT-3', human 18s rRNA forward: 5'-ACCGCAGCT AGGAATAATGGA-3', human 18s rRNA reverse: 5'-GCCTCAGTTCCGAAAACCA-3'. Primer validation and analysis of qRT-PCR data was performed as previously surprised (Pineda et al., 2015).

Co-immunoprecipitation and immunoblotting

$4x10^5$ HeLa cells were plated in 6 cm dishes and transfected 24 hours later with Effectene (Qiagen) according to manufacturers' protocol. 16 hrs post-transfection, media was changed. 48 hrs post-transfection, cells were washed and scraped in cold PBS, spun down, and resuspended in NP-40 lysis buffer (50 mM Tris-HCl pH 7.7, 150 mM NaCl, 0.5% NP-40 (v/v), 1 mM dithiothreitol (DTT), 1X protease inhibitor cocktail) for 45 minutes on ice prior to spinning down insoluble material. Soluble lysate was incubated with respective antibodies conjugated to Protein A beads (Bio-Rad) for 2 hours at 4°C while rotating. Beads were then washed in NP-40 lysis buffer 3-5 times and eluted with 2X sodium dodecyl sulfate (SDS) sample buffer (7.3% SDS (w/v), 1% Tris base (w/v), 30% glycerol (v/v), 0.1% Bromophenol blue (w/v), 1.6% DTT (w/v)).

For immunoblotting, samples prepared in SDS sample buffer were resolved on SDS-PAGE gels and then transferred to nitrocellulose membranes prior to blocking in TBST with 5% milk (w/v) or 5% bovine serum albumin (w/v) and probing with primary (as indicated above) and secondary antibodies (donkey anti-rabbit IgG, GE Healthcare, NA934V; sheep anti-mouse IgG, GE Healthcare, NA931V). Protein signal was visualized after addition of ECL detection reagent (GE Healthcare, RPN2209; GE Healthcare, RPN2236) as per manufacturer's instructions.

Purification of recombinant proteins

His-NSE1 and His-MAGE-F1-NSE1 complex were purified from 6 liter LB cultures of BL21(DE3) or Rosetta 2(DE3) competent cells (EMD Millipore), respectively. Bacterial pellets were lysed in high salt lysis buffer (50 mM Tris-HCl pH 7.7, 500 mM NaCl, 100 µM $ZnCl_2$, 10 mM imidazole), sonicated, and spun down at $2x10^4$ RPM for 1 hour. Soluble lysate was filtered through a 0.45 µm filter and incubated with His Select Nickel Affinity Gel (Sigma, P6611) for 1 hour at 4°C rotating. Beads were then washed with high salt wash buffer (50 mM Tris-HCl pH 7.7, 500 mM NaCl, 100 µM $ZnCl_2$, 20 mM imidazole) and eluted with 2 different elution buffers (50 mM Tris-HCl pH 7.7, 500 mM NaCl, 100 µM $ZnCl_2$, 140 or 200 mM imidazole).

In vitro binding

30 µg of either His-NSE1 or His-MAGE-F1-NSE1 complex were incubated with 8.75 µl TALON Metal Affinity Resin (Clontech) in TBST buffer (25 mM Tris pH 8.0, 2.7 mM KCl, 137 mM NaCl, 0.05% Tween-20 (v/v), and 10 mM 2-mercaptoethanol) for 1 hour vibrating at room temperature. Beads were then blocked with 5% non-fat milk (w/v) powder in TBST for 1 hour vibrating at room temperature. MYC-MMS19 was in vitro translated using TNT SP6 Quick In Vitro Transcription/Translation Kit (Promega) and added to the recombinant proteins in 5% milk (w/v) in TBST buffer vibrating for 1 hour. Beads were washed four times with TBST buffer prior to addition of 2X SDS sample buffer to elute.

Denaturing His-ubiquitin pulldown

$4x10^5$ HeLa cells were plated in 6 cm dishes and transfected 24 hours later with Effectene according to manufacturers' protocol. 16 hrs post-transfection, media was changed. 48 hrs post-transfection, cells were washed and scraped in PBS, spun down, and resuspended in denaturing lysis buffer (6M guanidinium-HCl, 100 mM Na_2HPO_4-NaH_2PO_4, 10 mM Tris-HCl pH 8.0, 5 mM imidazole, 10 mM 2-mercaptoethanol) and rotated for four hours at room temperature. Beads were spun down and washed successively with the following buffers for 5 minutes each at room temperature: 1) denaturing lysis buffer without imidazole 2) buffer A pH 8.0 (8 M urea, 100 mM Na_2HPO_4-NaH_2PO_4, 10 mM Tris-HCl pH 8.0, 10 mM 2-mercaptoethanol) 3) buffer A pH 6.3 with 0.2% triton X-100 (v/v) (8M urea, 100 mM Na_2HPO_4-NaH_2PO_4, 10 mM Tris-HCl pH 6.3, 10 mM beta-mercaptoethanol, 0.2% triton X-100 (v/v)) 4) buffer A pH 6.3 with 0.1% triton X-100 (v/v) (8M urea, 100 mM Na_2HPO_4-NaH_2PO_4, 10 mM Tris-HCl pH 6.3, 10 mM beta-mercaptoethanol, 0.1% triton X-100 (v/v)). Beads were then incubated with elution buffer (200 mM imidazole, 150 mM Tris-HCl pH 6.7, 30% glycerol (v/v), 5% SDS (w/v), 720 mM 2-mercaptoethanol) for 20 minutes at room temperature.

Homologous recombination assay

HR assays were performed essentially as described previously (Porteus and Baltimore 2003; Potts, Porteus, and Yu 2006). Briefly, a 293 cell line (293/A658) expressing a *GFP* gene containing in-frame stop codons and a I-SceI recognition site (5'-TAGGATAACAGGGTAAT-3') at bp 327. The I-SceI/repair plasmid contained: an I-SceI expression cassette and a 2100 bp repair substrate that contains a truncated *GFP* gene (*truncGFP*) followed by an additional 1300

bp of 3'-homology to the mutated *GFP* genomic target. HR mas measured by transfecting 293/A658 cells with the I-SceI/repair plasmid and the indicated plasmids or siRNA oligonucleotides. Cells were grown for three days and the percentage of GFP-positive cells was measured by flow cytometry and normalized to transfection efficiency controls.

^{55}Fe incorporation assay

^{55}Fe incorporation assays were performed as described previously (Stehling et al. 2004; Teichmann and Stremmel 1990). Briefly, $3.5x10^5$ HeLa cells were plated in 6 cm dishes and transfected 24 hours later with Effectene according to manufacturer's protocol. 72 hours after transfection cells were labeled with 2 µCi/mL ^{55}Fe-NTA for 18 hours in DMEM supplemented with 3.75% FBS (v/v) and 150 µM ascorbate. ^{55}Fe-NTA was prepared by incubation of 16 µM $^{55}FeCl_3$ (Perkin Elmer) in 100 mM HCl, 63 µM nitrilotriacetic acid (NTA), and 20 mM HEPES pH to 6.0 with Tris followed by titration to pH 7.0 with 100 mM NaOH. After ^{55}Fe-NTA labeling, cells were washed in complete media, ice-cold PBS, and cell lysates were prepared in RIPA buffer (150 mM NaCl, 5 mM EDTA pH 8.0, 50 mM Tris-HCl pH8.0, 1% NP-40 (v/v), 0.5% sodium deoxycholate (w/v), 0.1% SDS (w/v), 1mM DTT, and 1X protease inhibitor cocktail (Roche)). Fe-S proteins were IPed by incubation of cell lysates with 5 µg antibody for 1 hour on ice followed by immunocomplex capture by addition of protein-A agarose beads (Bio-Rad) for 1 hour rotating at 4 °C. Beads were washed three times with RIPA buffer followed by scintillation counting. Data were normalized to protein lysate concentrations as determined by BCA analysis (Pierce).

Transferrin uptake assay

Transferrin uptake was performed as described previously (Stehling et al. 2008). Briefly, $3.5x10^5$ HeLa cells were plated in 6 cm dishes or $2x10^5$ HeLa-Cas9 cells were plated in 6-well dishes and transfected 24 hours later with Effectene according to manufacturers' protocol. 72 hours after transfection cells were washed once in PBS followed by incubation with 0.1 mg/mL FITC-Transferrin (Invitrogen) in PBS for 1 hour at 37 °C. Cells were then washed in PBS, cell lysates prepared in RIPA buffer, and FITC-Transferrin present in cell lysate was determined with a 96-well Enspire plate reader. Data were normalized to protein lysate concentrations as determined by BCA analysis (Pierce) and background signal from cells not treated with FITC-Transferrin.

Cell viability assays

Cells were reverse transfected with 20-35 nM siRNA and Lipofectamine RNAiMAX according to manufacterers' protocol and left to incubate for 72-120 hours prior to changing the media and adding MTT (Life Technologies) and incubating for 4 hours at 37 °C in the dark. Media was then removed and DMSO was added to each well to solubilize crystals for 20 minutes. Plates were read at 540 nm on an Enspire plate reader. For MMS treatment, HeLa-Cas9 cells were plated at low density in 6-well plates and 16 hours later MMS was added at specified concentrations diluted in media. After 11 days fresh media was added and MTT (Life Technologies) was added according to manufactores' instructions. Cells were incubated for 4 hours at 37°C in the dark, media was then removed and DMSO was added to each well to solubilize crystals for 20 minutes. Plates were read at 540 nm on Enspire plate reader. For UV

treatment, $5x10^5$ HeLa-Cas9 cells were plated in 6 cm plates. 16 hours later the cells were washed with PBS then directly irradiated using a Stratagene Stratalinker 2400 and immediately trypsinized and plated at low density in 6-well plates. Cells were then left to grow for 11 days and collected with MTT as described above.

Assessment of mRNA/copy-number analysis in human tumors and statistical analysis

mRNA levels (RNA-seq) and copy-number variation from tumors were determined by examining the cancer genome atlas (TCGA). Tumors were stratified into diploid, gain (low level amplification), and amplified (high level amplification) from normalized segmentation values by the GISTIC method. Correlation of patient survival to copy-number variation status was similarly analyzed from TCGA data and plotted as a Kaplan-Meier survival curve for head and neck squamous cell carcinoma. Mutational burden was determined by stratification of tumors into amplified and non-amplified and total number of de novo intragenic mutations and specific types of mutations (insertion, deletion, A:T>C:G, A:T>G:C, A:T>T:A, G:C>A:T, G:C>C:G, G:C>T:A) were determined from the TCGA datasets for lung and head and neck squamous cell carcinoma tumors. Results were analyzed for statistical significance using Chi-square ($\chi 2$), Pearson correlation (r), ANOVA, or student t-test as appropriate.

CHAPTER FOUR

THE MAGE-F1-NSE1 E3 LIGASE UBIQUITINATES MMS19 AND DEREGULATES CYTOSOLIC IRON SULFUR CLUSTER INCORPORATION

Introduction

Iron-sulfur (Fe-S) clusters are one of the most ancient inorganic cofactors utilized by proteins from bacteria to humans (Lill 2009). Generation of Fe-S, typically in the form of [2Fe2S] or [4Fe4S] (Rouault 2015), requires the coordinated activity of members of the mitochondrial iron sulfur cluster assembly (ISC) machinery for mitochondrial Fe-S proteins or both the ISC and the cytosolic iron-sulfur cluster assembly (CIA) machinery for cytoplasmic and nuclear Fe-S proteins (Netz et al. 2014). The CIA pathway, consisting of at least 9 components in humans (Paul and Lill 2015), serves as a conduit by which iron and sulfur-containing cofactors are generated from a precursor product of the mitochondria ISC and passed through a series of proteins to ultimately be incorporated into cytosolic or nuclear proteins that require the Fe-S cluster as a structural (Stehling et al. 2008; Stehling et al. 2012), enzymatic (Beinert 2000), or electron transfer component (Beinert, Holm, and Munck 1997). One of the critical end target binding adaptors for this process is MMS19, which binds a number of proteins including those important for DNA repair processes, such as FANCJ, POLD1, XPD, and RTEL1, amongst others. Characterization of the loss of MMS19 has been well documented in yeast and more recently in human cells as displaying greater susceptibility to DNA damaging agents (Seki et al. 2013; Stehling et al. 2012). Although new discoveries in the CIA pathway have focused on

identifying the core assembly proteins, binding modalities of members of the pathway, and the specific Fe-S proteins targeted, there remains a large gap in understanding how the CIA pathway is regulated and altered in disease.

Here we report that an E3 ubiquitin ligase in the MAGE-RING ligase (MRL) family controls flux through the CIA pathway through ubiquitination and degradation of MMS19. MRLs are a family of E3 ubiquitin ligases that consist of a complex between an E3 RING ligase and a modulatory MAGE protein, which can function to specify substrates for the ligase (Doyle et al. 2010; Pineda et al. 2015). There are >40 MAGE proteins in humans with all having a common MAGE homology domain (MHD) that mediates binding to distinct E3 ubiquitin ligases (Doyle et al. 2010; Pineda et al. 2015; Hao et al. 2013; Yang, O'Herrin, Wu, Reagan-Shaw, Ma, Bhat, et al. 2007; Kozakova et al. 2015). The specific cellular function of the majority MAGE proteins has not been elucidated, including MAGE-F1. In this study, we identify a function for the orphan MAGE-F1 in specifying MMS19 for ubiquitination and degradation by the NSE1 E3 ubiquitin ligase. This results in decreased Fe-S cluster assembly into MMS19 targets that functionally renders cells less competent to repair a spectrum of DNA damage. Interestingly, MAGE-F1 is copy-number amplified in several cancers resulting in increased tumor mutation burden suggesting downregulation of the CIA pathway may be important event in tumorigenesis.

Results

No known functions for MAGE-F1 have been reported. Thus we searched for MAGE-F1 interacting partners by performing a large-scale pulldown of FLAG-MAGE-F1 from HEK293 cells and identified a single E3 RING ubiquitin ligase, NSE1, which has previously been shown

to bind MAGE-F1 in screens from cells (Gur et al. 2014) and in vitro (Doyle et al. 2010). We confirmed that MAGE-F1 interacts with NSE1 by performing co-immunoprecipitation (co-IP) studies from cells (Figure 3-1 A). In addition, recombinant His-MAGE-F1 and untagged NSE1 co-purify in a stoichiometric stable complex from bacterial cultures and in vitro binding assays revealed that bacterially purified GST-NSE1 directly binds Myc-MAGE-F1 (Figure 3-1 B and C). A conserved di-leucine motif has been identified in the MHD of most MAGEs and is critical for interaction with their cognate E3 ligases (Doyle et al. 2010). Mutation of this motif in MAGE-F1 (L87-88A) abolished binding of MAGE-F1 to NSE1 (Figure 3-1 B). This along with further mapping of MAGE-F1-NSE1 interaction revealed that MAGE-F1 MHD interacts with the N-terminal portion of NSE1 (Figure 3-1 D). NSE1 has previously been shown to interact with a closely related MAGE protein, MAGE-G1 (Taylor et al. 2008). The MAGE-G1-NSE1 MRL incorporates into the SMC5/6 complex to facilitate homologous recombination (HR) between sister chromatids and telomeres (Potts 2009; Taylor et al. 2008; De Piccoli et al. 2006). Thus, we wondered if MAGE-F1 could simply replace MAGE-G1 in the SMC5/6 complex and function in a similar manner. However, MAGE-F1, unlike MAGE-G1, failed to interact with co-expressed or endogenous SMC5 or SMC6 (Figure 3-2 A through C). Whereas knockdown of MAGE-G1 results in impaired sister chromatid recombination and increased episomal recombination, knockdown of MAGE-F1 did not recapitulate these results (Figure 3-2 D and E). Additionally, it has been observed that a fraction of cellular NSE1 exist outside the SMC5/6 complex (Taylor et al. 2008). These results suggest that MAGE-F1 forms a complex with the NSE1 ubiquitin ligase, but does not integrate into and function as part of the SMC5/6 complex like MAGE-G1-NSE1.

Next we search for targets of the MAGE-F1-NSE1 ubiquitin ligase to provide insights into its cellular function. Analysis of the MAGE-F1 interactome revealed three high confidence substrates (MMS19, MAT2a, and PPM1G) that we confirmed to bind to (Figure 3-3 A and B) and be ubiquitinated by MAGE-F1-NSE1 (Figure 3-4 A through C). Of these three substrates, MAGE-F1-NSE1 bound to and ubiquitinated MMS19 most robustly (Figure 3-4 A). Using deletion fragments we determined that MAGE-F1-NSE1 mediated robust ubiquitination of the C-terminal portion of MMS19 (Figure 3-5 F). Expression of HA-NSE1 alone did not promote the ubiquitination of MYC-MMS19, suggesting that MAGE-F1 specifies ubiquitination of MMS19 by NSE1 (Figure 3-4 A). Consistent with this, MMS19 bound recombinant His-MAGE-F1-NSE1 complex in vitro, but not His-NSE1 alone (Figure 3-5 A). Ubiquitination of MMS19 by MAGE-F1-NSE1 resulted in its degradation as expression of MAGE-F1 reduced endogenous MMS19 protein levels (Figure 3-5 B) and knockdown of MAGE-F1 increased MMS19 protein levels (Figure 3-5 C) without affecting MMS19 mRNA levels (Figure 3-5 D). Consistent with these findings, MMS19 ubiquitination was inhibited by expression of a K48R ubiquitin (but not other KtoR ubiquitin mutants) that blocks generation of proteasome-targeting K48-linked ubiquitin chains (Figure 3-5 E). These results suggest that MAGE-F1 specifies MMS19 for ubiquitination by NSE1 leading to its degradation.

MMS19, in conjunction with CIA1 and CIA2, acts late in the CIA pathway to recruit Fe-S apoproteins to the CIA machinery (namely IOP1/Nar1) for incorporation of the Fe-S cluster to form functional Fe-S holoproteins (Stehling et al. 2012; Gari et al. 2012; Paul and Lill 2015; Seki et al. 2013). In order to directly determine if MAGE-F1-NSE1-mediated ubiquitination and degradation of MMS19 has an effect on CIA pathway flux and incorporation of Fe-S cluster into

downstream targets, we labeled cells with ^{55}Fe, IPed specific Fe-S proteins, and quantitated the amount of radioactivity present via scintillation counting as has been previously described (Teichmann and Stremmel 1990; Stehling et al. 2004). We found that expression of MAGE-F1 decreased Fe-S cluster incorporation into downstream MMS19-dependent targets POLD1, FANCJ, XPD, DPYD, and RTEL1, to a similar extent as MMS19 knockdown (Figure 3-6 A). Importantly, MAGE-F1 did not affect ^{55}Fe incorporation into a MMS19-independent Fe-S protein, PPAT (also known as GPAT) (Stehling et al. 2012) (Figure 3-6 A) suggesting MAGE-F1 specifically modulates the MMS19 arm of the CIA pathway. Changes in ^{55}Fe incorporation upon MAGE-F1 expression were not due to altered ^{55}Fe labeling or unequal IP of proteins (Figure 3-6 B and C). Consistent with MAGE-F1 affecting the MMS19 CIA pathway in conjunction with NSE1, knockdown of NSE1 abrogated the effects of MAGE-F1 expression on ^{55}Fe incorporation into FANCJ (Figure 3-6 D) and MAGE-F1 L87-88A that fails to bind NSE1 was incompetent to alter ^{55}Fe incorporation into FANCJ and XPD (Figure 3-6 E). In contrast to MAGE-F1, no significant changes were found with ^{55}Fe incorporation into targets upon expression of MAGE-G1, again suggesting distinct functions of MAGE-G1-NSE1 and MAGE-F1-NSE1 (Figure 3-6 F). Importantly, the diminished CIA pathway activity upon MAGE-F1 expression could be rescued by rescuing MMS19 protein levels (Figure 3-6 G). These effects of MAGE-F1 are not restricted to over-expression as knockout of MAGE-F1 increased levels of ^{55}Fe incorporation into FANCJ, POLD1, DPYD, and RTEL1 (Figure 3-6 H). It has previously been shown that knockdown of MMS19 destabilizes a number of downstream target proteins due to their reliance on the Fe-S cluster for stability (Stehling et al. 2012; Gari et al. 2012). Similar to these findings, MAGE-F1 expression decreased FANCJ levels and to a smaller extent decreased

XPD, POLD1, and DPYD (Figure 3-7 A). Rescuing MMS19 proteins levels in MAGE-F1 expressing cells rescued the levels of FANCJ (Figure 3-7 B).

Consistent with MAGE-F1-NSE1 abrogating MMS19 function, we also observed defects in iron homeostasis previously reported upon knockdown of MMS19 (Stehling et al. 2013). Specifically, knockdown of MMS19 by siRNAs or expression of MAGE-F1 in HeLa cells showed robust increases in uptake of FITC-labeled transferrin (Figure 3-8 A). In contrast, knockout of MAGE-F1 decreased transferrin uptake, which could be rescued by re-expression of MAGE-F1 (Figure 3-8 B). Similarly to MMS19 knockdown (Stehling et al. 2013), MAGE-F1 expression increased IRP2 protein levels that control transferrin uptake (Figure 3-8 C). These results suggest that MAGE-F1-NSE1 ubiquitination and degradation of MMS19 impairs MMS19 functions, including flux through the CIA pathway and regulation of iron homeostasis.

Because MAGE-F1-mediated degradation of MMS19 leads to decreased incorporation of ^{55}Fe into several DNA repair enzymes, we examined if this would lead to a functional effect on cellular DNA repair mechanisms. To test this hypothesis, we utilized a previously described HR assay (Porteus and Baltimore 2003; Potts, Porteus, and Yu 2006) in which a non-functional GFP containing in-frame stop codons can be repaired upon induction of a double-strand break by the I-SceI endonuclease and recombination with an episomal repair template (Figure 3-2 D). We found that dose-dependent expression of wild-type MAGE-F1, but not MAGE-F1 L87-88A that fails to bind NSE1, reduced HR rates (Figure 3-9 A and B). Similarly, knockdown of MMS19 in a dose-dependent manner also decreased rates of HR (Figure 3-9 C). Importantly, MAGE-F1-mediated decrease in HR was reversed by rescuing MMS19 protein levels (Figure 3-9 D). In order to determine what particular downstream MMS19 target may be mediating its effect on

HR, we measured HR rates in cells depleted of several MMS19 targets affecting DNA metabolism, including FANCJ, POLD1, RTEL1, and XPD (Figure 3-9 E). Consistent with previously reports demonstrating that FANCJ and POLD1 play important roles in HR (Litman et al. 2005; Maloisel, Fabre, and Gangloff 2008), knockdown of either, but not XPD or RTEL1, reduced HR rates similarly to MMS19 knockdown or MAGE-F1 expression (Figure 3-9 E). Previous studies have also shown that depletion of MMS19 results in increased sensitivity to DNA damaging agents (Stehling et al. 2012; Seki et al. 2013; Lauder et al. 1996). Consistent with MAGE-F1 inhibition of the MMS19 pathway, stable expression of MAGE-F1 reduced cellular viability upon exposure to MMS (Figure 3-10 A) and knockout of MAGE-F1 reduced sensitivity to both MMS and UV (Figure 3-10 B and C). These results suggest that downregulation of MMS19 CIA pathway by MAGE-F1-NSE1 reduces the DNA repair capacity of cells.

Given the importance of DNA repair mechanisms to maintain genomic stability and that genomic instability is a hallmark of cancers, we examined whether the MAGE-F1-NSE1 pathway may be altered in tumors. Remarkably, based on genomic analysis of TCGA (The Cancer Genome Atlas) tumors, several cancer types, including >40% of lung squamous cell carcinomas, have high amplification of MAGE-F1, but not other MAGEs (Figure 3-11 A and B). Copy-number amplification of MAGE-F1 correlated with increased mRNA levels (Pearson coefficient 0.773, Spearman coefficient 0.822) in multiple cancer types (Figure 3-11 C and D). Of note, amplification of MAGE-F1 does not happen in isolation and likely cooperates with other oncogenic drivers as it is co-amplified with other known oncogenes on chr 3q including PIK3CA, SOX2, and TP63 (Figure 3-11 E). Given our findings that MAGE-F1 specifies

downregulation of the MMS19 CIA pathway and reduces DNA repair capacity of cells, we examined whether tumors that harbor high amplification of MAGE-F1 exhibit greater genomic instability. Indeed, lung squamous cell carcinoma patient tumors with high levels of MAGE-F1 amplification and mRNA levels harbored a greater number of mutations per tumor, with a wide spectrum of mutations as would be consistent with modulation of a large number of DNA enzymes that function in multiple pathways (Figure 3-12 A through D). Importantly, high expression of other MAGEs, such as MAGE-A3, did not alter tumor mutation burden (Figure 3-12 E) and the effects of MAGE-F1 on mutational burden was not driven by difference in exposure to smoke-related carcinogens (Figure 3-12 F). We similarly found increased total mutational burden in MAGE-F1-amplified head and neck squamous cell carcinomas as compared to non-MAGE-F1-amplified cases (Figure 3-12 G through I). These results are likely clinical significant as MAGE-F1 amplification, NSE1 expression levels, and the combination all showed robust decreases in survival of head and neck squamous carcinoma patients (Figure 3-13 A-C). Given these findings, MAGE-F1 amplification could be a predictive biomarker for current therapeutics like immune checkpoint inhibitors that depend on neoantigens for activity (Van Allen et al. 2015; Rizvi et al. 2015). Furthermore, MAGE-F1 itself may be a therapeutic target, as MAGE-F1 upregulated cancer lines showed decreased viability upon MAGE-F1 knockdown (Figure 3-14).

Conclusions

In summary, we have found that the previously uncharacterized MAGE-F1 protein binds to the E3 RING ligase NSE1 and switches its role from protecting genomic integrity as a member of the SMC5/6 complex to inhibiting DNA repair by targeting MMS19, a member of the cytosolic iron sulfur cluster assembly machinery that is critical for the incorporation of Fe-S cluster cofactors into many DNA repair enzymes. To our knowledge, this is the first targeted post-translational mechanism of the CIA Fe-S pathway that has been described. This role, in combination with evidence for widespread MAGE-F1 amplification across many cancers, highlights an underappreciated role of the CIA pathway in tumorigenesis and overall genomic stability and opens up a new potential avenues to approach multiple tumor types.

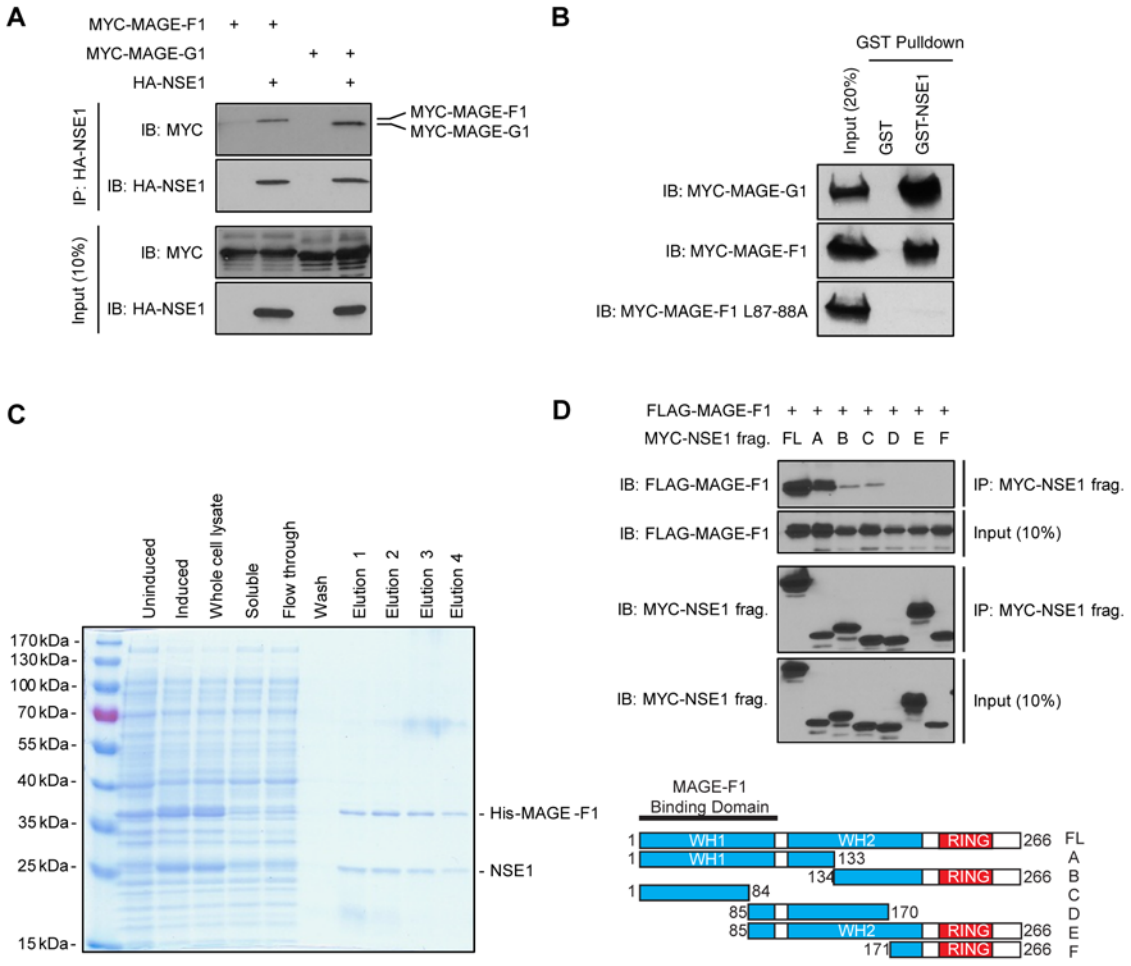

Figure 3-1. MAGE-F1 binds the E3 ligase NSE1
(A) Immunoprecipitation (IP) of HA-NSE1 shows it binds MYC-MAGE-F1, similar to MYC-MAGE-G1. **(B)** Pulldown of recombinant GST-NSE1 demonstrates binding to MYC-MAGE-F1, similar to MYC-MAGE-G1, but not the MYC-MAGE-F1 L87-88A dileucine mutant. **(C)** Purification of recombinant His-MAGE-F1 and untagged-NSE1 from bacteria demonstrate robust interaction between the two proteins. **(D)** Domain mapping of MYC-NSE1 shows that FLAG-MAGE-F1 binds NSE1 at its first winged helix domain (WH1).

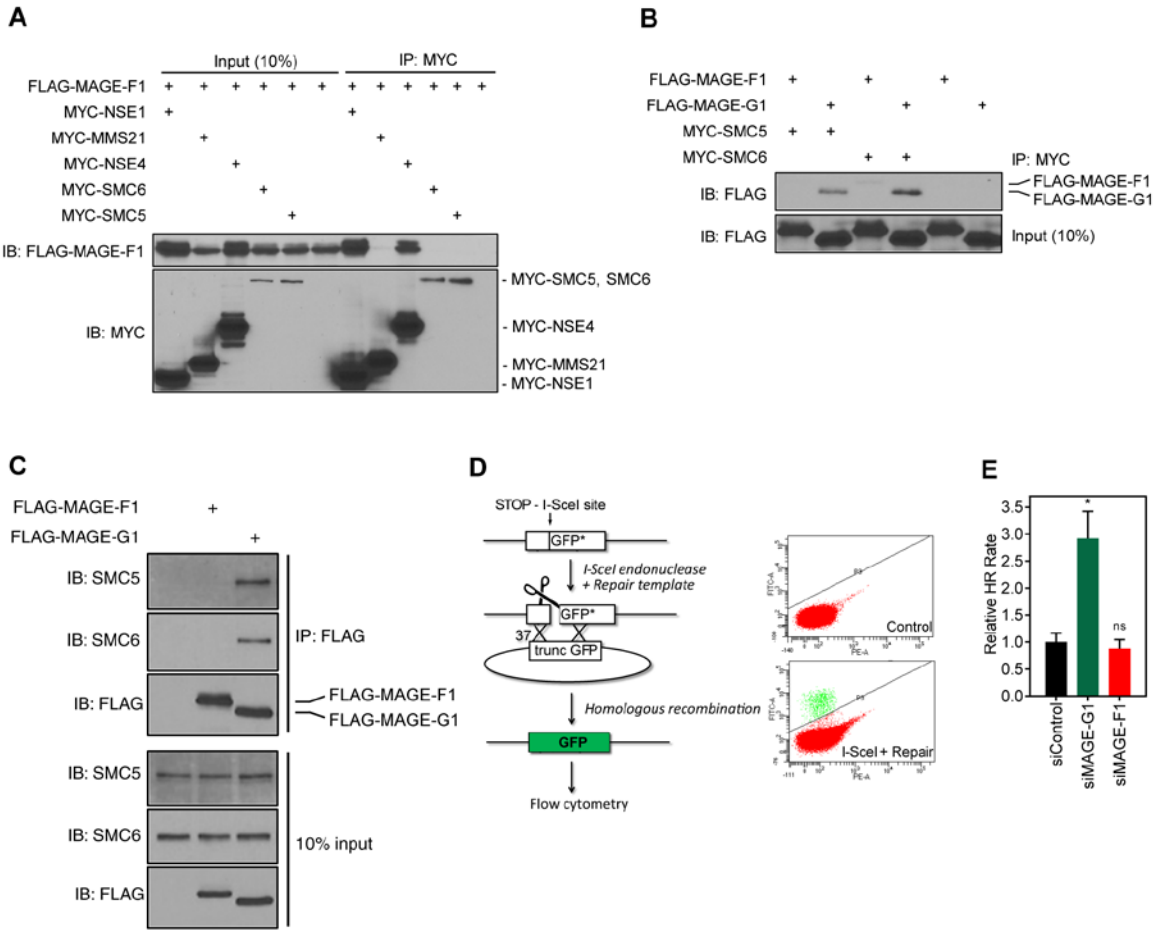

Figure 3-2. MAGE-F1 does not function as a member of the SMC5/6 complex
(A) Immunoprecipitation of MYC-tagged members of the SMC5/6 complex shows that FLAG-MAGE-F1 only significantly interacts with NSE1 and NSE4. **(B)** Pulldown of MYC-SMC5 or MYC-SMC6 demonstrates that FLAG-MAGE-F1 does not have the robust affinity for SMC5 or SMC6 as does FLAG-MAGE-G1. **(C)** Pulldown of FLAG-MAGE-F1 or FLAG-MAGE-G1 shows that endogenous SMC5 and SMC6 bind to MAGE-G1, but not MAGE-F1. **(D)** Diagram of the homologous recombination assay and representative FACS plots for control and I-SceI-transfected and repaired conditions. **(E)** Knockdown of MAGE-F1 does not exhibit changes in the homologous recombination assay as seen for MAGE-G1 and is comparable to control knockdown.

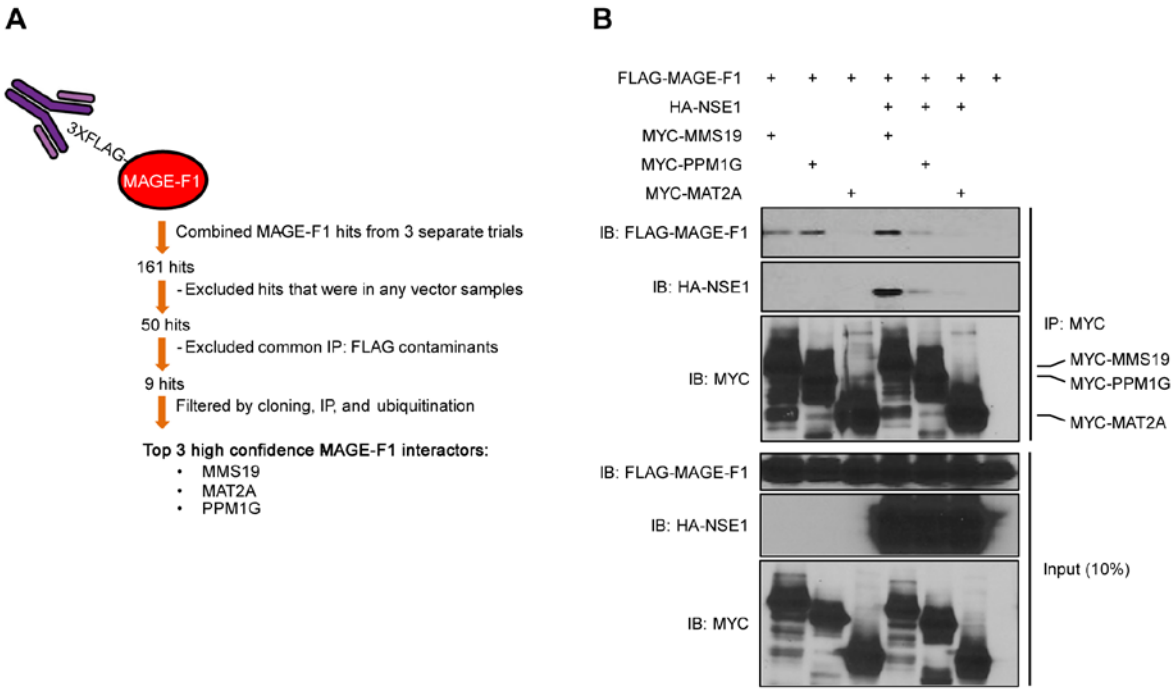

Figure 3-3. MAGE-F1 binds potential substrates from 3XFLAG-MAGE-F1 pulldown
(A) Schematic of filtering process used to deduce top 3 high confidence MAGE-F1 interactors from 3XFLAG-MAGE-F1 pulldown and LC/MS. **(B)** Immunoprecipitation of MYC-tagged top 3 high confidence MAGE-F1 interactors validated FLAG-MAGE-F1 and HA-NSE1 interaction with these potential substrates.

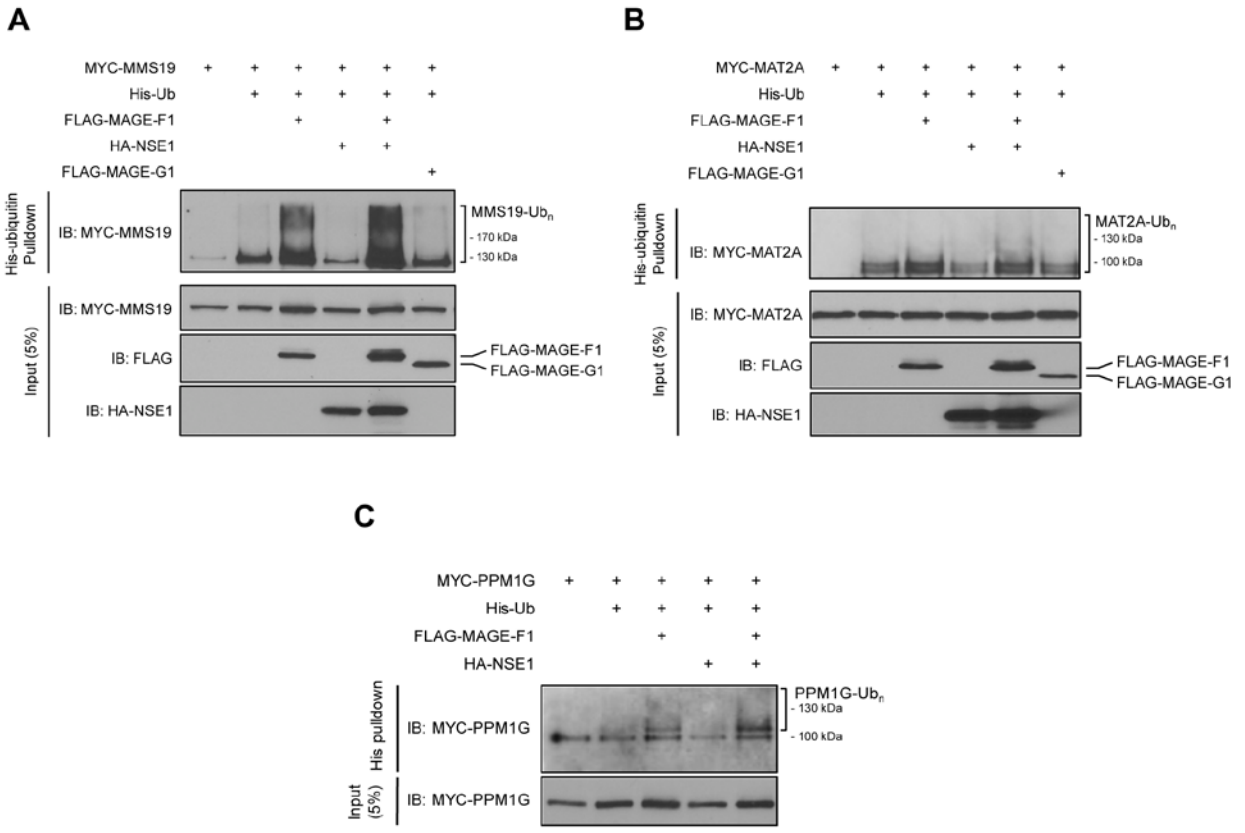

Figure 3-4. MAGE-F1 ubiquitinates MMS19 most robustly of all potential substrates **(A)** Denaturing His-ubiquitin pulldown from HeLa shows that addition of FLAG-MAGE-F1 robustly increases ubiquitination of MMS19, which is further augmented by co-expression with HA-NSE1. **(B)** Denaturing His-ubiquitin pulldown from HeLa cells demonstrates that expression of FLAG-MAGE-F1 and HA-NSE1 increases ubiquitination levels of MYC-MAT2A. **(C)** Denaturing His-ubiquitin pulldown from HeLa cells demonstrates that expression of FLAG-MAGE-F1 and HA-NSE1 increases ubiquitination levels of MYC-PPM1G.

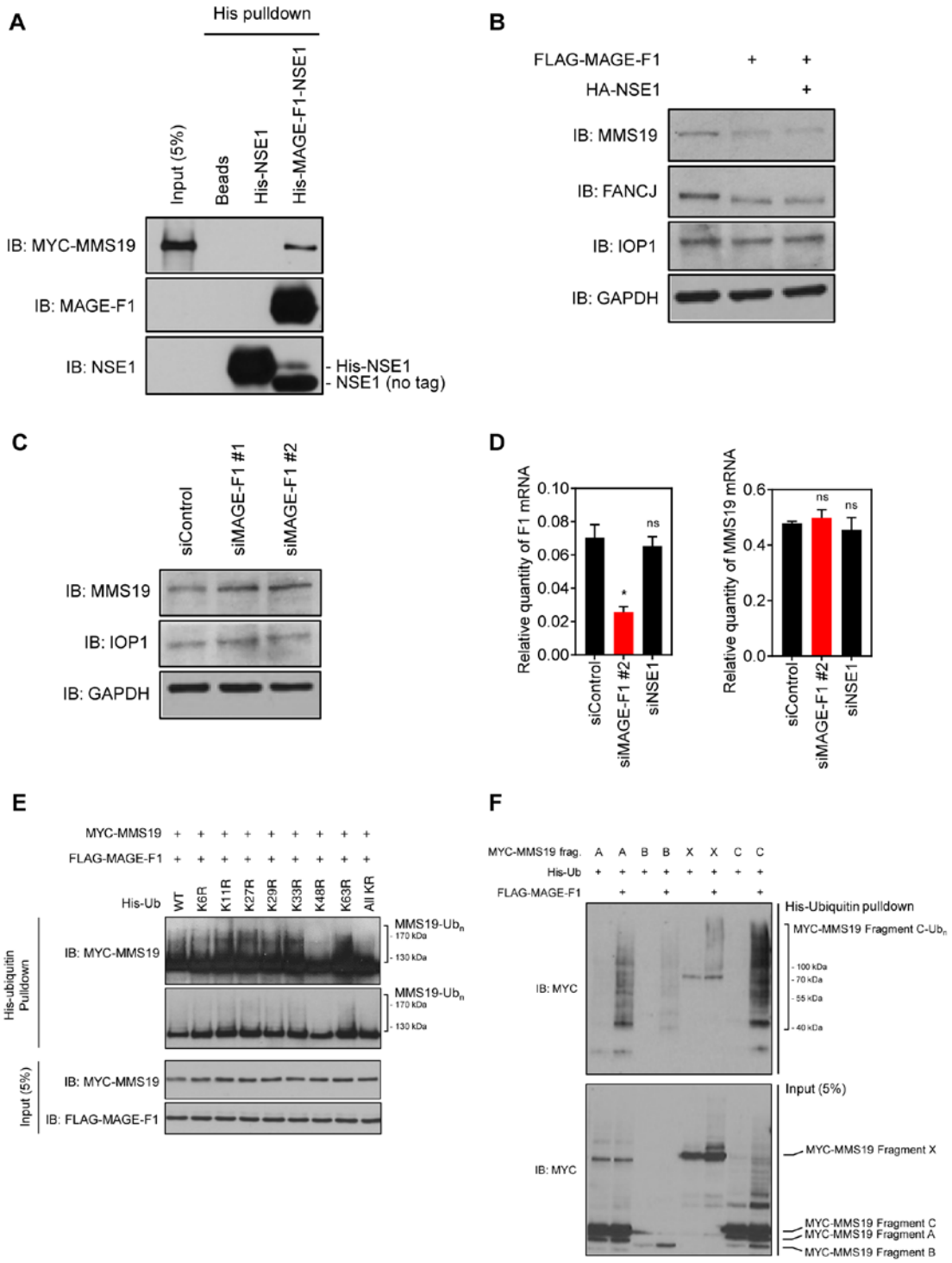

Figure 3-5. MAGE-F1 destabilizes MMS19
(A) Recombinant His-MAGE-F1-NSE1, but not His-NSE1, binds directly to MYC-MMS19 in vitro. **(B)** Expression of FLAG-MAGE-F1 alone or in conjunction with HA-NSE1 in HeLa cells decreases MMS19 protein levels. **(C)** Knock-down of endogenous MAGE-F1 with two different oligos stabilizes MMS19 protein levels. **(D)** Knockdown of MAGE-F1 or NSE1 does not affect MMS19 at the mRNA level. **(E)** Denaturing His-ubiquitin pulldown from HeLa with ubiquitin mutants after MG132 treatment shows robust reduction of MMS19 ubiquitination in the presence of MAGE-F1 with the K48R ubiquitin mutant. **(F)** Denaturing His-ubiquitin pulldown from HeLa cells demonstrates that expression of FLAG-MAGE-F1 robustly increases ubiquitination levels of the C-terminus of MMS19.

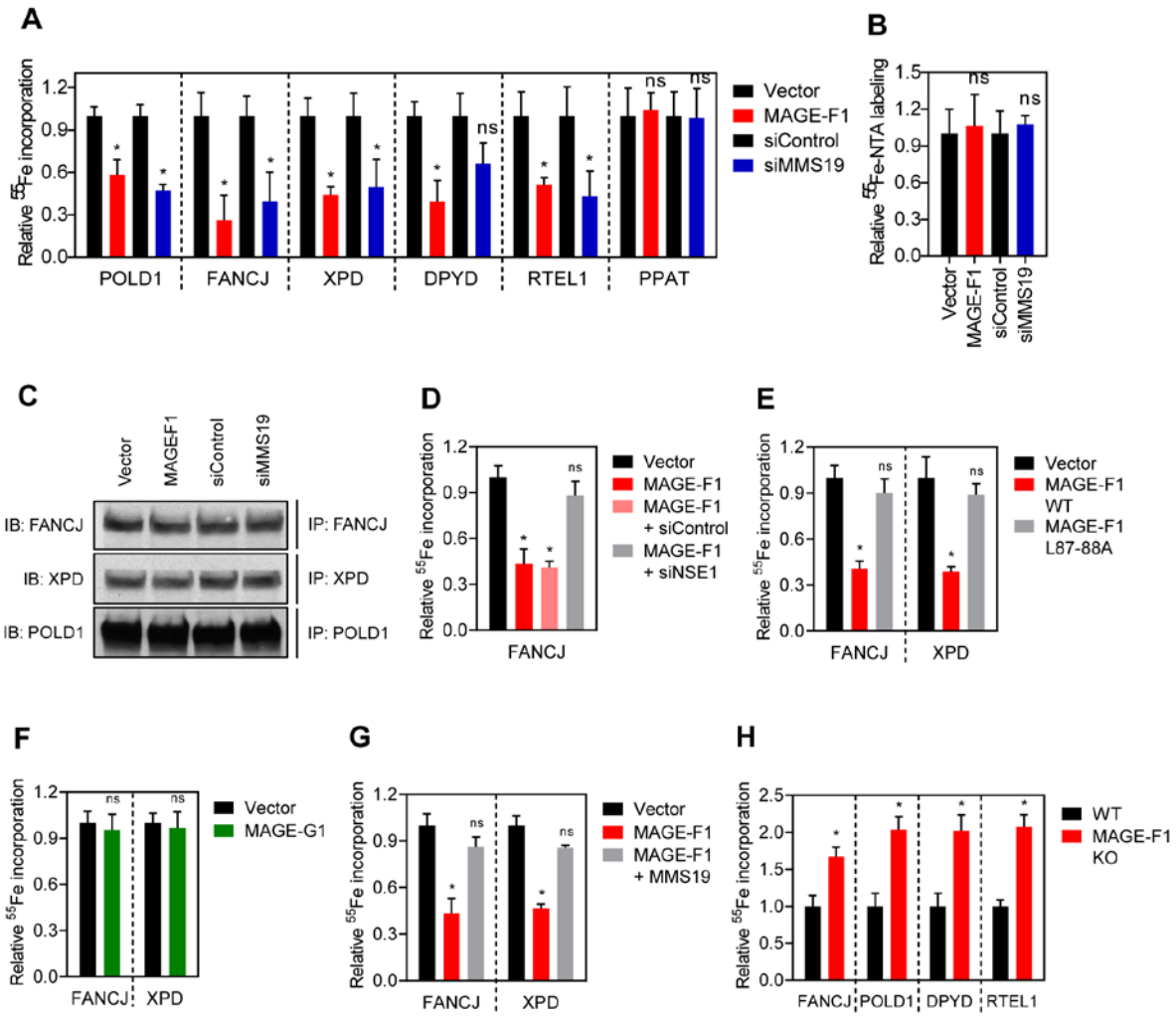

Figure 3-6. MAGE-F1 decreases iron incorporation into MMS19 targets
(A) Immunoprecipitation (IP) of endogenous MMS19 target proteins after 55Fe treatment demonstrates decreased incorporation of Fe either with MAGE-F1 over-expression or MMS19 knockdown, but not a non-MMS19 target protein (PPAT). **(B)** 55Fe uptake into MAGE-F1 over-expressing, MMS19 knockdown, or respective controls showed no significant variation between samples. **(C)** Pulldown of MMS19 target proteins from MAGE-F1 over-expressing, MMS19 knockdown, or respective controls showed no significant variation in immunoprecipitation saturation. **(D)** Knockdown of NSE1 abrogates MAGE-F1-mediated decrease of Fe incorporation into a target of MMS19. **(E)** MAGE-F1 dileucine mutant is incapable of altering Fe incorporation into MMS19 target proteins. **(F)** 55Fe incorporation into MMS19 targets in cells expressing untagged MAGE-G1 was not altered compared to control. **(G)** Over-expression of MMS19 in the context of MAGE-F1 rescues Fe incorporation into MMS19 target proteins. **(H)** HeLa-Cas9 MAGE-F1 knockout cells exhibit greater Fe incorporation into MMS19-dependent proteins than their wild type counterparts.
(Figure courtesy of Ryan Potts)

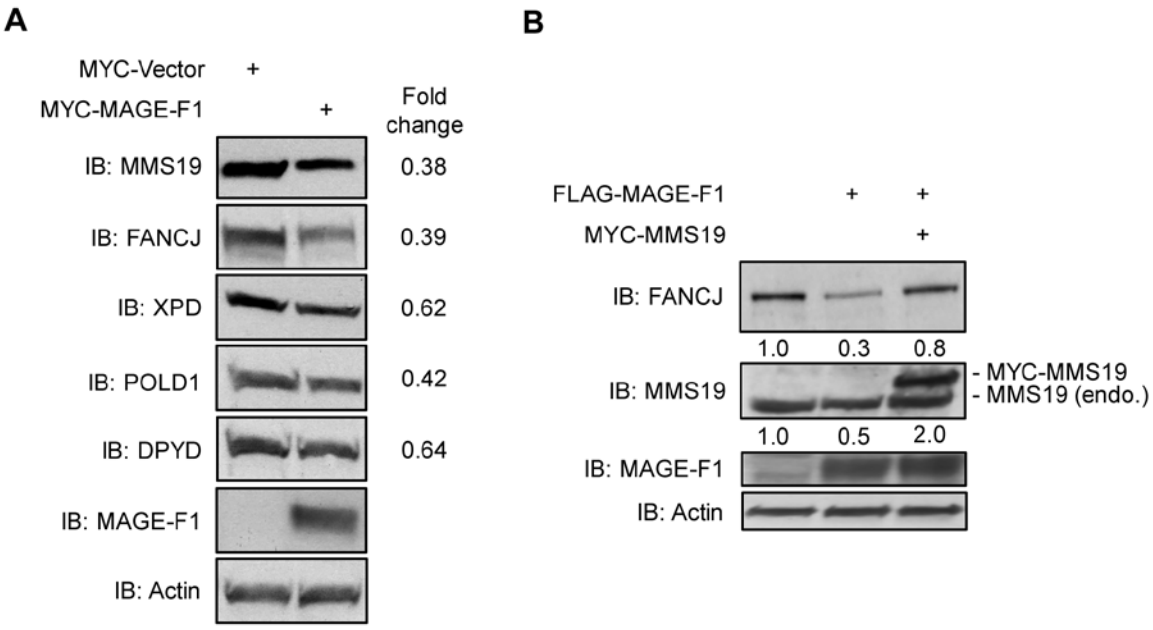

Figure 3-7. MAGE-F1 decreases the stability of MMS19-dependent iron sulfur proteins
(A) MYC-MAGE-F1 expression in HeLa cells causes decreased protein levels of MMS19 and downstream target proteins. **(B)** Over-expression of MMS19 in the context of MAGE-F1 rescues FANCJ protein levels. (Figure courtesy of Ryan Potts)

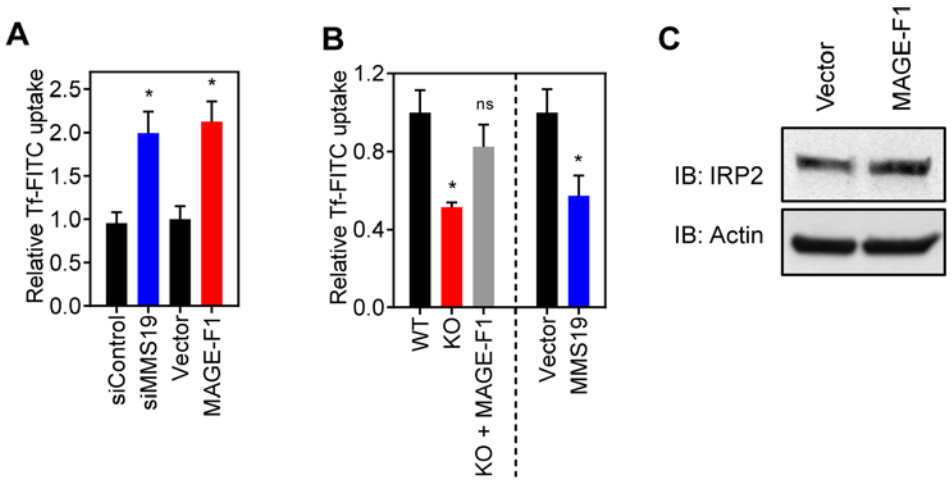

Figure 3-8. MAGE-F1 decreases the stability of MMS19-dependent iron sulfur proteins **(A)** Uptake of FITC-conjugated transferrin was increased in both MMS19 knockdown or MAGE-F1 over-expressing cells as compared to respective controls. **(B)** Uptake of FITC-conjugated transferrin was decreased in HeLa-Cas9 MAGE-F1 knockout cells as compared to its wild-type counterpart, which was rescued by expression of untagged-MAGE-F1. **(C)** IRP2 levels are increased in MAGE-F1-transfected cells as compared to vector cells.
(Figure courtesy of Ryan Potts)

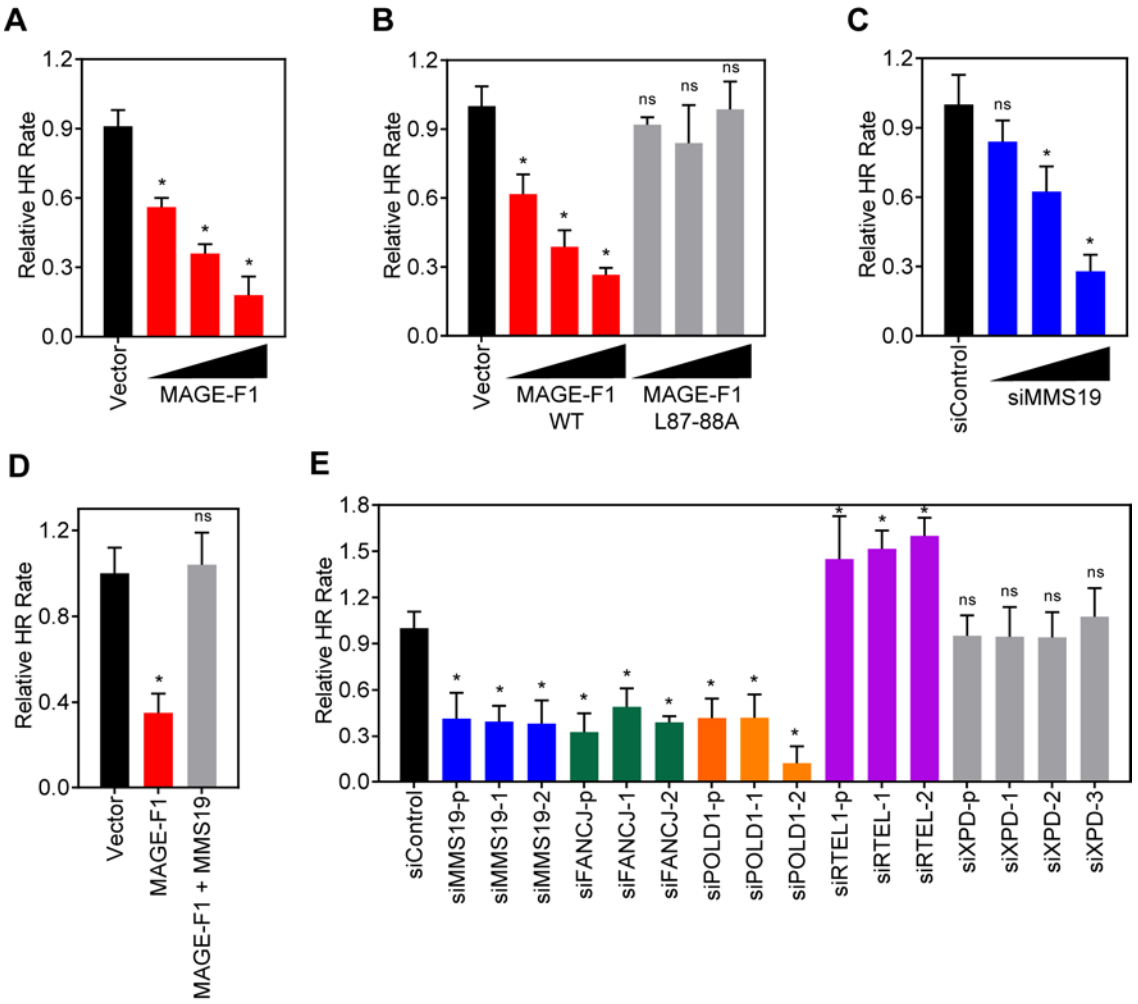

Figure 3-9. MAGE-F1 inhibits homologous recombination
(**A)** Increasing MAGE-F1 expression levels in 293/0 cells decreases rates of homologous recombination in a dose-dependent manner. **(B)** The dileucine mutant of MAGE-F1 is incapable of inhibiting homologous recombination. **(C)** Knockdown of MMS19 decreases rates of homologous recombination in a dose-dependent manner. **(D)** Over-expression of MMS19 in the context of MAGE-F1 rescues the MAGE-F1-mediated defect in homologous recombination. **(E)** Knockdown of downstream MMS19 targets show that FANCJ and POLD1 phenocopy and likely mediate the defect in homologous recombination seen with MMS19 knockdown. (Figure courtesy of Ryan Potts)

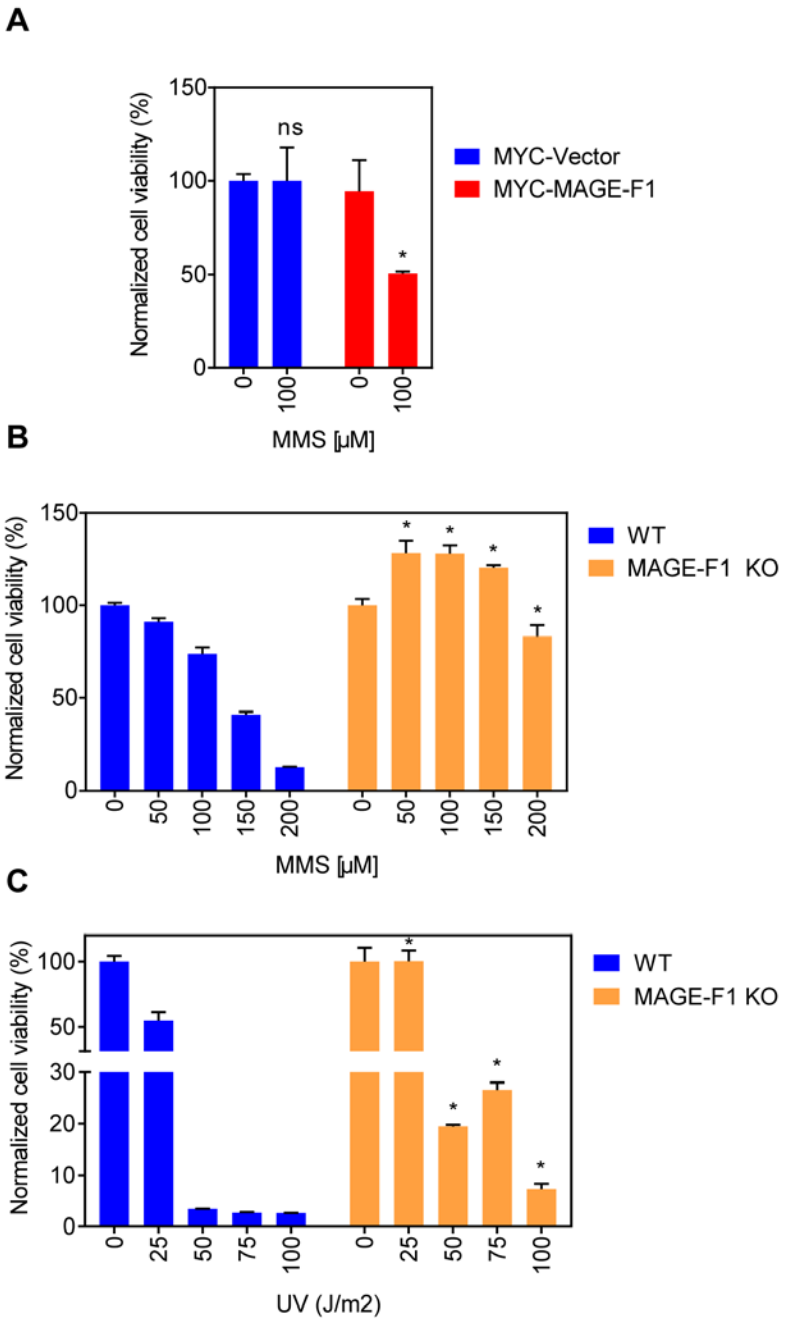

Figure 3-10. MAGE-F1 sensitizes cells to DNA damaging agents
(**A**) MYC-MAGE-F1-expressing HeLa-Cas9 cells exhibit increased sensitivity to DNA damage by MMS compared to MYC-vector cells. **(B)** HeLa-Cas9 MAGE-F1 knockout cells are less sensitive than HeLa-Cas9 WT cells to MMS. **(C)** HeLa-Cas9 MAGE-F1 knockout cells are less sensitive than HeLa-Cas9 WT cells to MMS.

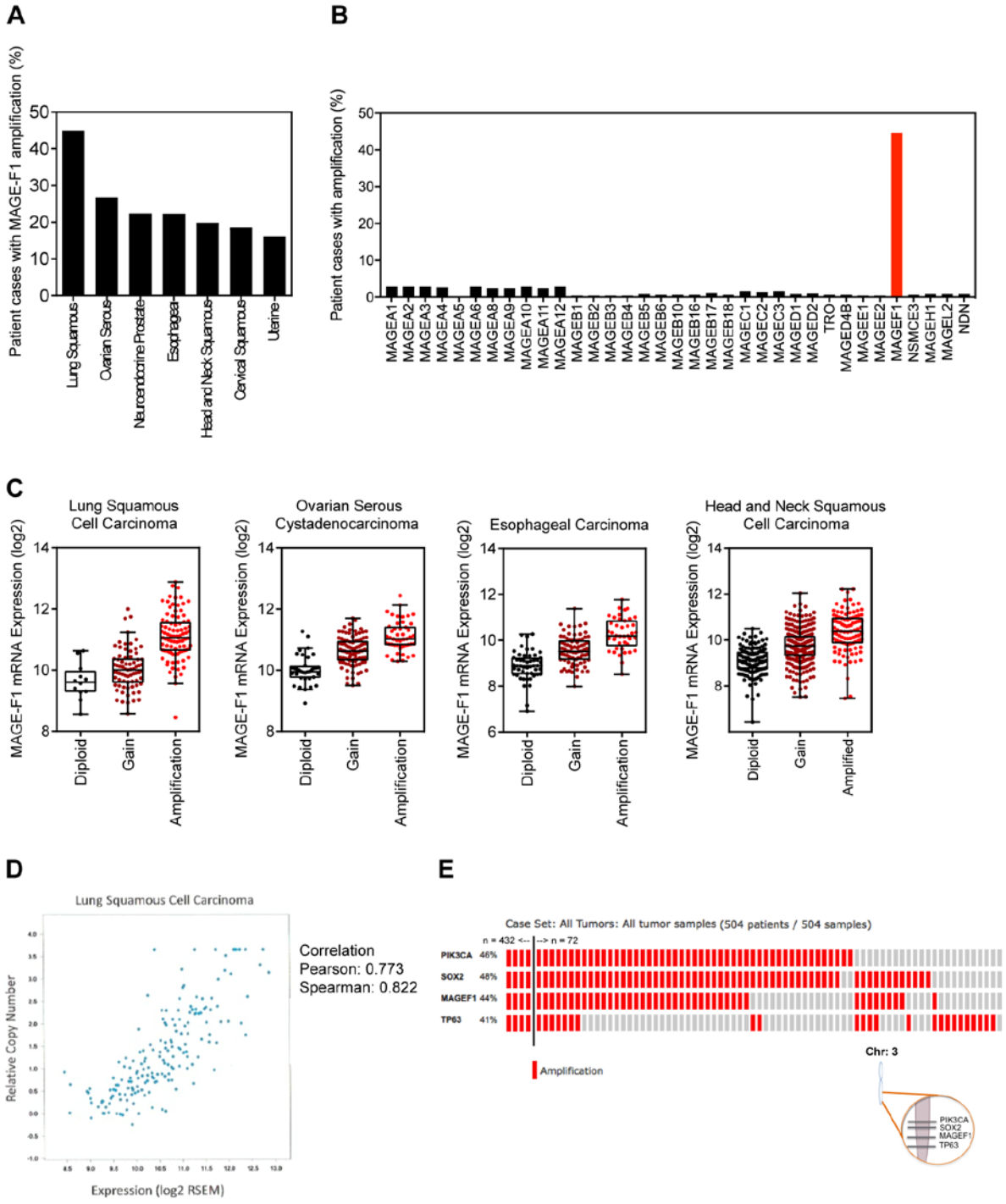

Figure 3-11. MAGE-F1 is amplified in multiple cancers and is associated with increased mRNA
(A) MAGE-F1 is highly amplified in multiple cancer types. **(B)** (A) MAGE-F1, but not other MAGEs, is highly amplified in lung squamous cell carcinoma. (C) Amplification of MAGE-F1 is associated with increased MAGE-F1 mRNA levels in multiple cancer types. **(D)** MAGE-F1 amplification levels correlate with MAGE-F1 mRNA levels. **(E)** The MAGE-F1 gene resides on commonly amplified segment of chromosome 3q which includes PIK3CA, SOX2, and TP63.

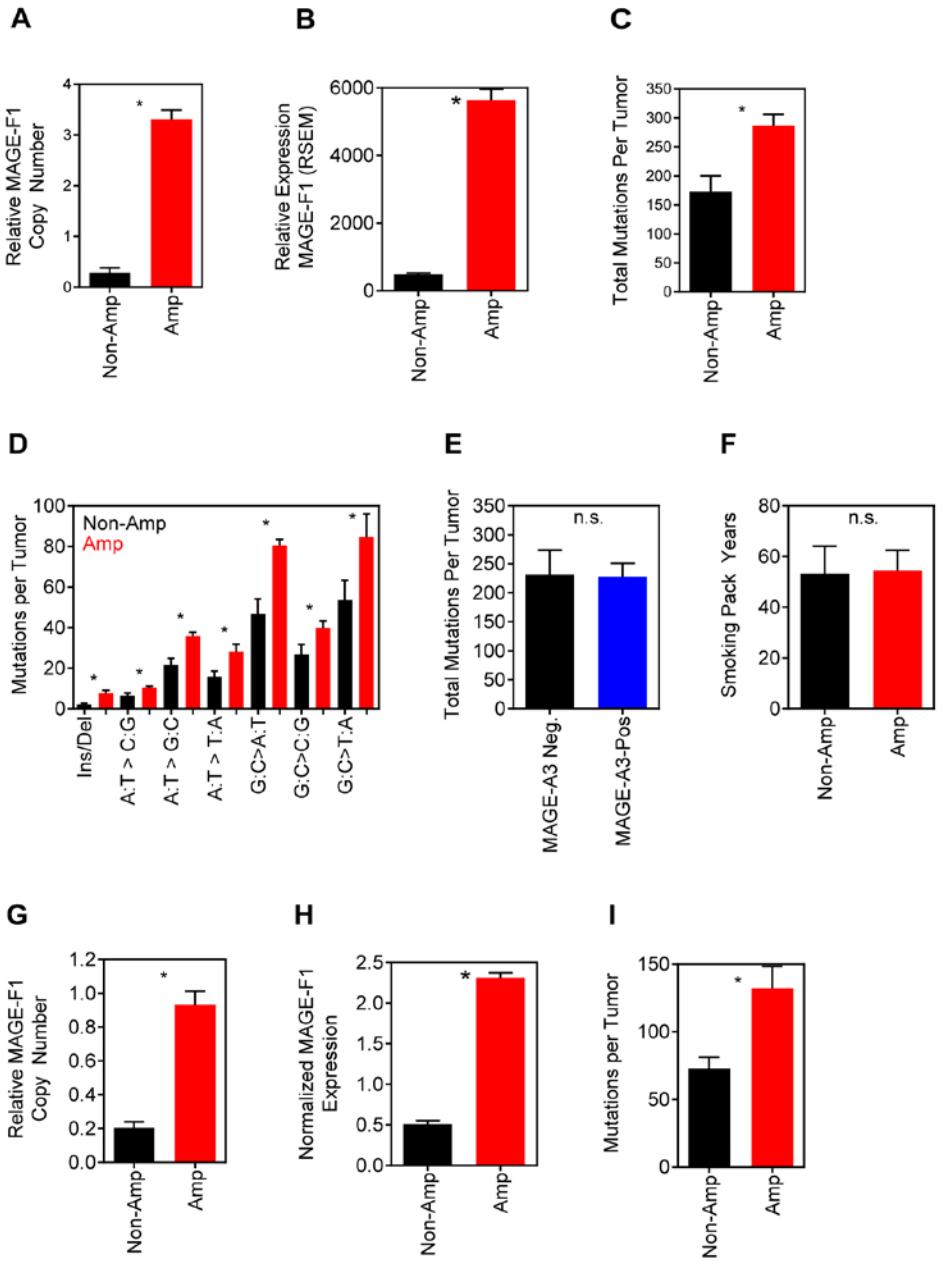

Figure 3-12. Amplification of MAGE-F1 is associated with increased mutational burden
(A) Significantly greater copy numbers of MAGE-F1 are observed in MAGE-F1 amplified lung squamous cell carcinoma cases. **(B)** MAGE-F1 mRNA expression is significantly higher in lung squamous cell carcinomas that harbor MAGE-F1 amplification compared to non-amplified cases. **(C)** Total mutation burden is higher in MAGE-F1 amplified lung squamous cell carcinomas than in cases without amplification. **(D)** A variety of mutational spectra are observed at higher frequencies in MAGE-F1 amplified lung squamous cell carcinomas. **(E)** Total mutations per tumor in lung squamous cell carcinoma are not significantly different between MAGE-A3 negative and MAGE-A3 positive cases. **(F)** Smoking pack years are not significantly different between MAGE-F1 amplified and non-amplified lung squamous cell carcinomas. **(G)** Significantly greater copy numbers of MAGE-F1 are observed in MAGE-F1 amplified head and neck squamous cell carcinoma cases. **(H)** MAGE-F1 mRNA expression is significantly higher in head and neck squamous cell carcinomas that harbor MAGE-F1 amplification compared to non-amplified cases. **(I)** Total mutation burden is higher in MAGE-F1 amplified head and neck squamous cell carcinomas than in cases without amplification.
(Figure courtesy of Ryan Potts)

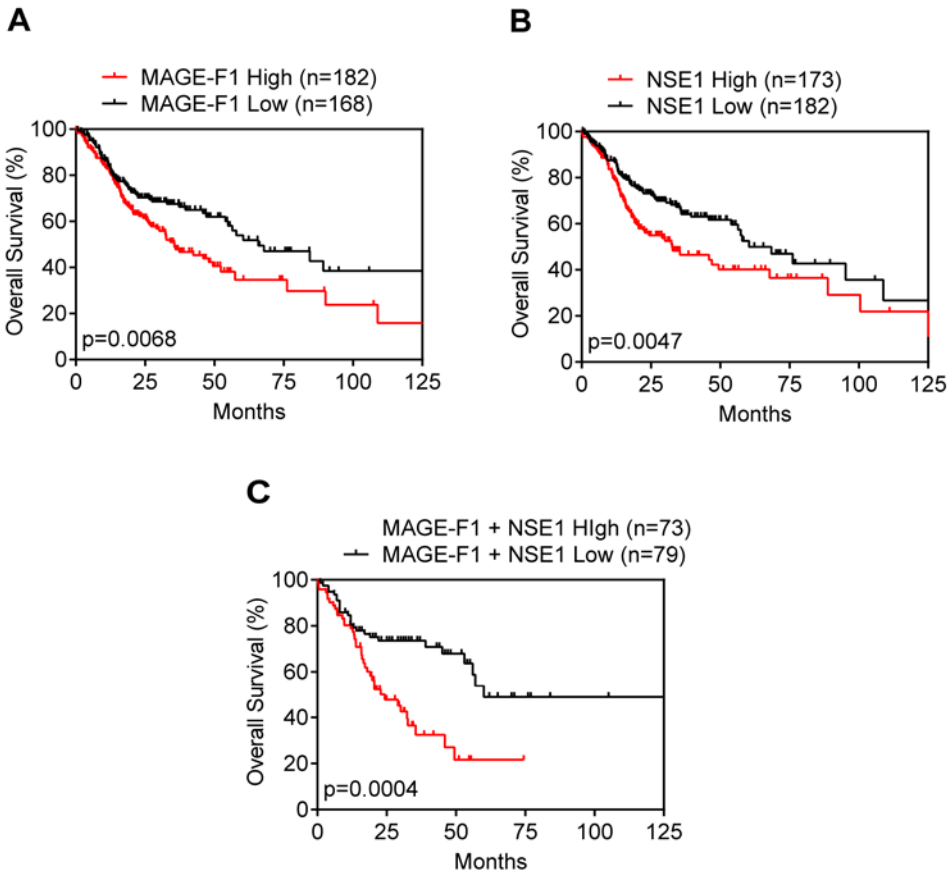

Figure 3-13. High MAGE-F1 and NSE1 levels are associated with worse prognosis
(A) Head and neck squamous cell carcinomas with high MAGE-F1 expression have significantly worse prognosis than those with low expression. **(B)** Head and neck squamous cell carcinomas with high NSE1 expression have significantly worse prognosis than those with low expression. **(C)** Head and neck squamous cell carcinomas with high expression of both MAGE-F1 and NSE1 exhibit significantly worse clinical prognosis than those with low expression of both genes.
(Figure courtesy of Ryan Potts)

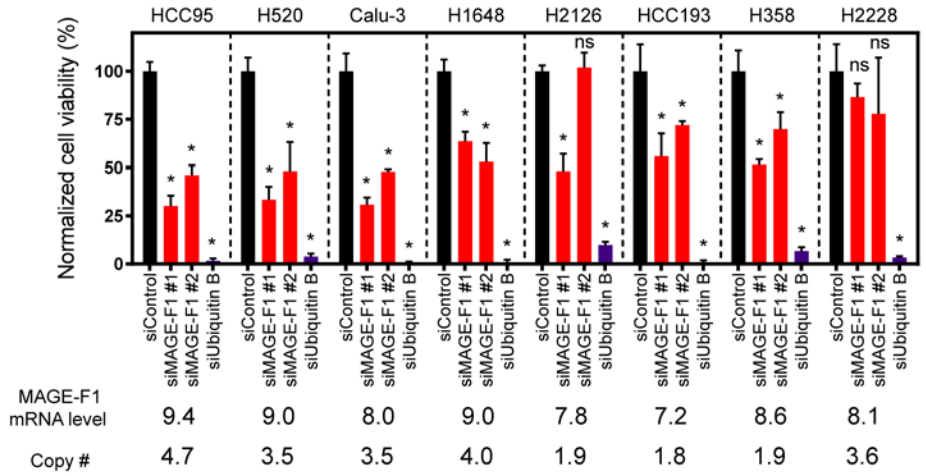

Figure 3-14. MAGE-F1-amplified lung cancer lines are sensitive to MAGE-F1 loss
Targeting MAGE-F1 via siRNA knockdown across a variety of lung cancer lines demonstrates MAGE-F1-dependent viability across lines. mRNA level represented as log2(signal) from Illumina-V3 microarray data.
(MAGE-F1 mRNA level and copy numbers courtesy of John Minna)

CHAPTER FIVE

DISCUSSION AND FUTURE DIRECTIONS

Mechanisms behind a MAGE-dependent switch for NSE1

Mechanistically, how may the binding of two different MAGEs switch the function of an E3 RING ligase? The obvious hypothesis is that although the MAGE homology domain is similar enough to bind to the same E3 ligase, the N- or C-terminus of the MAGE may differ enough to bind different substrates and expand the substrate repertoire for the ligase. However, in the case of MMS19, both MAGE-F1 and MAGE-G1 can bind to this target when over-expressed in cells (data not shown); however, only MAGE-F1 can promote the ubiquitination activity. How is this possible? One theory is that MAGE-G1 does not facilitate the ubiquitination of MMS19 due to steric reasons, as it is known that MAGE-G1 also binds to the heads of SMC5 and SMC6 (Palecek et al. 2006), whereas MAGE-F1 does not bind to either of these proteins (Figure 3-2 A through C). It would be interesting to deduce which part of MAGE-G1 binds to SMC5 and SMC6 through domain mapping and determine the differences between MAGE-G1 and MAGE-F1 at these regions.

Another explanation is that MAGE-F1 and MAGE-G1 are differentially localized in the cell and regulate different pools of NSE1. MMS19 has been found largely in the cytoplasmic pool of cells, as is consistent with its function the cytosolic iron sulfur cluster machinery (van Wietmarschen et al. 2012). Transfecting HeLa cells with N- and C-terminal-tagged construct of MAGE-F1 showed localization of the protein to unusual, small circular structures in the nucleus

(usually 2-3) (data not shown). However, it remains to be seen where endogenous MAGE-F1 localizes to. We have tried to generate an antibody against MAGE-F1, with success detecting over-expressed protein, but not endogenous protein.

Lastly, the binding of MAGE-F1 and MAGE-G1 may exert differential conformations on NSE1 that may promote different activities. The crystal structure of the MAGE homology domain bound to NSE1 has been solved (Doyle et al. 2010). It would be interesting to see whether a crystal structure of the MAGE homology domain of MAGE-F1 bound to NSE1 exhibits differences in the conformation of the ligase, as one obvious difference in MAGE-F1's MAGE homology domain compared to MAGE-G1 is the presence of a stretch of glutamate resides (Stone et al. 2001)

Details of the MAGE-F1 and MMS19 interaction

Targeting the interface between MAGE-F1-NSE1 and MMS19 may disrupt binding and promote increased DNA repair. In order to target this interface, however, it is necessary to determine how MAGE-F1 binds MMS19 and vice versa. Domain mapping of MAGE-F1 to MMS19, as well as the converse experiment, may be helpful to elucidate the specifics of binding.

Context of MAGE-F1 regulation of MMS19

MAGE-F1 amplification in cancers is one context in which high levels of MAGE-F1 may only be one of possible different contexts in which MAGE-F1 may be necessary to regulate MMS19 levels. Considering that MAGE-F1 is a ubiquitously expressed protein and the nature of inhibiting DNA damage at a basal level in all tissues may seem counter-intuitive, it is worthwhile

to consider why this is necessary or if there are also specific contexts in which this regulation may need to be perturbed in either direction.

Insufficient cellular iron content may be one setting in which it would be beneficial to decrease the production of MMS19, because if there is not enough iron for the production of Fe-S clusters, then it would be inefficient use of cellular machinery to use energy to keep producing robust amounts of cytosolic iron sulfur cluster assembly machinery. In the case of E. coli, when iron becomes limiting, the bacterium reduces the transcript levels of highly expressed Fe-S proteins (Imlay 2006). Experiments from yeast cells demonstrated that limiting available iron using the cell membrane-impermeable ferrous (Fe^{2+}) iron chelator bathophenanthroline disulfonate (BPS) caused a robust decrease in MMS19 protein levels after as little as 11 hours (Lev et al. 2013). This decrease in protein levels could be rescued by addition of a proteasome inhibitor, MG132, suggesting that MMS19 is post-translationally regulated in the context of low iron availability in yeast cells (Lev et al. 2013). However, treatment of human HEK293 cells with a ferric (Fe^{3+}) iron chelating agent, desferrioxamine (DFO), did not exhibit obvious changes in MMS19 protein levels after 18 hours (Gari et al. 2012). This experiment should be repeated with multiple time points and with additional verification for sufficient iron depletion to clarify if MMS19 is also regulated by low iron levels in humans.

In contrast, acute insults to DNA by carcinogens or the environment may necessitate the further stabilization of MMS19 levels with a decrease in MAGE-F1 to support the repair of widespread DNA damage. Indeed, MMS19 protein levels in cells have been shown to be increased after UV damage (Ito et al. 2010). It would be interesting to determine whether this increase in MMS19 is due to decreased degradation or if this is transcriptionally-mediated. If due

to degradation, then it would be interesting to determine whether MAGE-F1 would be transcriptionally or post-translationally regulated to decrease levels of this DNA repair-inhibiting protein after DNA damage with agents such as UV or MMS.

In contrast, one setting in which generation of DNA repair machinery components may be inhibited in favor of other effects of MMS19 downregulation (iron uptake) is when host defense against pathogens is necessary. Many infectious agents (bacteria, viruses) require iron to proliferate, and thus a key host-defense mechanism is to sequester iron away from pathogen access (Ganz and Nemeth 2015). The importance of this defense mechanism is highlighted by the high pathogen susceptibility of patients with hereditary hemochromatosis, characterized by systemic iron overload due to mutations in various genes required to regulate iron homeostasis, including TFR2 (Johnson and Wessling-Resnick 2012). In particular, these patients are susceptible to extracellular pathogens such as E. coli, V. vulnificus, and Y. enterocolitica (Johnson and Wessling-Resnick 2012). Normally upon infection, iron is sequestered by preventing cellular iron export, sequestration of plasma iron into proteins, and import of iron into cells (Ganz and Nemeth 2015). Import of iron into cells away from extracellular pathogens can occur in part through uptake of iron from transferrin through the transferrin receptor (Soares and Weiss 2015). Indeed, rats treated with lipopolysaccharide (LPS), an agent commonly used to illicit an immune response because it is a major component of Gram-negative bacteria (Alexander and Rietschel 2001), were found to have increased transferrin receptor mRNA and proteins levels in the lung by 4 hours (Upton et al. 2003). Therefore, in the setting of extracellular infection it may be beneficial for cells to upregulate the transferrin receptor via

downregulation of MMS19 through MAGE-F1-NSE1-mediated ubiquitination in lieu of DNA repair.

Alternatively, MAGE-F1 may also be involved in the regulation of the innate immune response to DNA damage. Not only do viruses cause activation of the innate immune response and production of cytokines via DNA double-stranded breaks and integration, but endogenous double-stranded DNA breaks also have been shown to activate immune responses. For example, damaging DNA through etoposide stimulates the production of IFN response genes, and germ cells from C. elegans have been shown to activate a conserved immune response pathway that involves ERK signaling after double-stranded breaks in DNA (Nakad and Schumacher 2016). It has also been shown that alterations in MUTYH, an Fe-S cluster-containing DNA glycosylase that has been shown to bind MMS19 (van Wietmarschen et al. 2012), are associated with the production of cytokines IL-1, IL-6, and IL-1B (Nakad and Schumacher 2016). This evidence then postulates a question: would uncorrected DNA damage via MAGE-F1-mediated loss of iron-sulfur cluster assembly lead to a sustained inflammatory response and better resistance to infections? Alternatively, could dysregulated, high levels of MAGE-F1 lead to chronic inflammation and disease? Examining the context and temporal regulation of MAGE-F1 would be crucial to answer these questions.

The iron sulfur cluster assembly pathway, MAGE-F1, and smoking-induced cancers

It should be noted that many of the cancers in which MAGE-F1 is amplified include those that are frequently associated with smoking: lung squamous cell carcinoma, esophageal carcinoma (Cook et al. 2010), and head and neck squamous cell carcinoma (Mashberg et al. 1993). Lesions

caused by smoking include bulky adduct formation on purines, such as 8-oxo-guanine, which must be repaired through nucleotide excision repair pathways after RNA polymerase stalls upon the bulky structure while transcribing (Pleasance, Stephens, et al. 2010). It has been observed that indeed, there are more unrepaired lesions on the non-transcribed strand of DNA in cancers caused by smoking, such as lung cancers with TP53 mutations (Pleasance, Cheetham, et al. 2010; Martincorena and Campbell 2015; Alexandrov et al. 2013). MMS19 was initially identified as a gene important for both nucleotide excision repair and transcription-coupled repair, which are now corroborated with the evidence for XPD (a critical component TFIIH, a complex required for transcription-coupled nucleotide excision repair) being a target of MMS19. It is possible, then, that MAGE-F1 is upregulated early in cancers, downregulates MMS19 and leads to the build up of mutations during cancer progression. It will be worthwhile to see whether MAGE-F1 is amplified and whether mRNA levels and protein levels may be increased early during in tumorigenesis.

Other possible modes of MAGE-F1-mediated MMS19 regulation

Although the focus of the aforementioned data was mostly restricted to regulation of MMS19 by MAGE-F1-NSE1 by ubiquitination and degradation, there still remains other additional mechanisms by which MAGE-F1 may modulate MMS19. The possibility remains open because the ubiquitination and degradation of MMS19 by MAGE-F1-NSE1 is not complete, meaning that as per western it appears that though MMS19 levels are decreased, there still remains an undegraded pool, yet the decreased Fe^{55} incorporation into MMS19 targets by MAGE-F1 recapitulates MMS19 knockdown, which is more complete. This could be explained by the

requirement of a threshold level of MMS19 needed to properly incorporate Fe-S clusters into target proteins, or there may be additional mechanisms by which MAGE-F1 may regulate MMS19. Another possible mechanism by which MAGE-F1-NSE1 may regulate iron-sulfur cluster assembly is by altering binding of MMS19 to its cognate CIA partners, such as CIA2A, CIA2B, or CIA. A reverse PCA screen in yeast, developed to identify genes that may alter the interaction of two target proteins, identified NSE1, NSE4, and NSE5, among others, as a regulator of MMS19 and CIA2 (yeast has only one CIA2 protein) (Lev et al. 2013). NSE4 was another member of the SMC5/6 complex that can also be found outside of the complex paired with MAGE-G1 and NSE1 (Taylor et al. 2008). Likewise, MAGE-F1 was also found to bind NSE4 (Figure 3-2 A). NSE5 is a member of the SMC5/6 complex that is specific to yeast (Uhlmann 2016).

MAGE-F1-NSE1 ubiquitination of MMS19 may alter the binding of MMS19 to its CIA partners and could also affect MMS19 targeting of substrates. For example, MAGE-F1 enhances ubiquitination particularly at the C-terminus of MMS19, which includes the HEAT repeat domain. This domain is known to mediate protein-protein interactions and a HEAT repeat domain deletion mutant of MMS19 was shown to be unable to promote affects in both transcription and nucleotide excision repair (Hatfield et al. 2006). In addition, immunoprecipitation of MMS19 with a deletion of the HEAT repeat domain showed that NARFL (IOP1), XPD, MUTYH were no longer able to bind to MMS19, though the binding interaction with CIAO1 (CIA1) was not affected (van Wietmarschen et al. 2012). Evidence from these aforementioned papers suggests that the C-terminal HEAT repeats in MMS19 is necessary for binding to downstream DNA repair enzymes, thus ubiquitination may also disrupt MMS19-

apoprotein interaction in addition to destabilization, leading to overall decreased Fe-S cluster incorporation.

Other possible roles for MAGE-F1 in the cell

MAGE-F1 likely has other, additional roles outside regulation of Fe-S cluster incorporation into DNA repair enzymes because knockdown of MAGE-F1 causes acute decrease in viability in multiple cell lines, suggesting that MAGE-F1 may play an essential role in cell viability. Although a viable MAGE-F1 knockout cell line was generated, it should be noted that it was the only verified MAGE-F1 knockout cell line out of 150 clones, also suggesting that MAGE-F1 may play a role in cell viability that may only be compensated for in rare circumstances.

MAGE-F1 was previously found to bind to the SUMO ligase PIAS1, along with fellow type II MAGEs NECDIN, MAGE-D1, and MAGE-L2, although this interaction was not further elaborated upon for MAGE-F1 (Gur et al. 2014). Necdin was found to promote the degradation of PIAS1 in a proteasome-dependent manner and also suppress PIAS1 SUMOylation of its targets, STAT1 and PML (Gur et al. 2014). Intriguingly, knockdown of PIAS1 has been shown to decrease rates of both homologous recombination and non-homologous end joining, suggesting that PIAS1 plays an important role in repair of double-stranded breaks (Galanty et al. 2009). If MAGE-F1 degrades PIAS1 in a manner similar to Necdin, then it may be an additional mechanism by which MAGE-F1 attenuates homologous recombination in a dose-dependent fashion.

Possible explanations for the evolution of the MAGE-F1 gene

Throughout the course of evolution, the MAGE-F1 gene appears to have undergone multiple insertions and deletions events to convert it from a coding gene to pseudogene and back (Figure 1-3). What is the cause for this rapid gain and loss across species? One plausible theory is that since many immune response-related genes evolve quickly due to the nature of host-pathogen competition (Barreiro and Quintana-Murci 2010), MAGE-F1 may harbor roles in pathogen defense. As mentioned earlier, MAGE-F1 may mediate host defense via downregulation of MMS19, leading to upregulation of the transferrin receptor and sequestering iron away from extracellular pathogens as a trade-off for the less crucial assembly of DNA repair enzymes in this context. Conversely, promoting iron uptake is detrimental in the context of intracellular viral infections (Drakesmith and Prentice 2008). With these considerations, MAGE-F1 may be required in species that are exposed to certain extracellular bacterial infections. Alternatively, MAGE-F1 may have been actively selected against to protect against heavy exposure to intracellular viruses or to preserve a more efficient DNA repair process in species with high or long-term exposure to DNA damage over time. An interesting observation is that species with MAGE-F1 pseudogenes include those that have been noted to have relatively long lifespans with low observed cancer-associated mortality, such as elephants (lifespan: 60-80+ years, mortality from cancer: 5%) (Lahdenpera, Mar, and Lummaa 2014) (Abegglen et al. 2015), whales (Bowhead lifespan: ~200 years, mortality from cancer: unknown, but is presumed to be low due to their incredible lifespan) (Keane et al. 2015), and naked mole rats (lifespan: ~32 years, mortality from cancer: only 2 natural cases ever recorded) (Rodriguez et al. 2012), whereas animals such as cats and dogs that possess the full-length coding MAGE-F1 appear to have

incidences of cancers similar to humans (maximum lifespan recorded: 122 years, mortality from cancer: 11-25%) (Abegglen et al. 2015; Dong, Milholland, and Vijg 2016). In statistics collected from hospitals and veterinarians in Alameda County, it was shown that excluding skin cancers, humans had a rate of 272 cancers per 100,000 in three years, whereas dogs had 381 and cats had 155 per 100,000 over the same time period (Dorn 1967). Although some of the differences in cancer incidence could be attributed to differences in the number of animals studied, it is an interesting observation that has been followed up for some species. Part of the underlying reason for elephant resistance to cancer is thought to lie in the 20 copies of TP53 they possess (Abegglen et al. 2015), and naked mole rats have been shown to produce a much larger version of hyaluronan than humans that appears to dampen the ability of cancers to form (Tian et al. 2013). It will be interesting to see if the loss MAGE-F1, and thus the loss of its inhibitory effect on DNA repair, also contributes to this lower incidence of cancer in these animals.

Conclusions

Through this study, MAGE-F1 has been functionally annotated as a protein that binds to the E3 RING ligase NSE1 to confer a new role outside of the SMC5/6 complex and is involved in regulating cytosolic iron sulfur cluster assembly via ubiquitination and degradation of the assembly protein MMS19. This is the first example of specific post-translational regulation of the cytosolic iron sulfur cluster assembly machinery and may have implications for both modulation of DNA repair and iron homeostasis in the organism.

BIBLIOGRAPHY

Abegglen, L. M., A. F. Caulin, A. Chan, K. Lee, R. Robinson, M. S. Campbell, W. K. Kiso, D. L. Schmitt, P. J. Waddell, S. Bhaskara, S. T. Jensen, C. C. Maley, and J. D. Schiffman. 2015. 'Potential Mechanisms for Cancer Resistance in Elephants and Comparative Cellular Response to DNA Damage in Humans', *JAMA*, 314: 1850-60.

Aisen, P. 2004. 'Transferrin receptor 1', *Int J Biochem Cell Biol*, 36: 2137-43.

Alexander, C., and E. T. Rietschel. 2001. 'Bacterial lipopolysaccharides and innate immunity', *J Endotoxin Res*, 7: 167-202.

Alexandrov, L. B., S. Nik-Zainal, D. C. Wedge, S. A. Aparicio, S. Behjati, A. V. Biankin, G. R. Bignell, N. Bolli, A. Borg, A. L. Borresen-Dale, S. Boyault, B. Burkhardt, A. P. Butler, C. Caldas, H. R. Davies, C. Desmedt, R. Eils, J. E. Eyfjord, J. A. Foekens, M. Greaves, F. Hosoda, B. Hutter, T. Ilicic, S. Imbeaud, M. Imielinski, N. Jager, D. T. Jones, D. Jones, S. Knappskog, M. Kool, S. R. Lakhani, C. Lopez-Otin, S. Martin, N. C. Munshi, H. Nakamura, P. A. Northcott, M. Pajic, E. Papaemmanuil, A. Paradiso, J. V. Pearson, X. S. Puente, K. Raine, M. Ramakrishna, A. L. Richardson, J. Richter, P. Rosenstiel, M. Schlesner, T. N. Schumacher, P. N. Span, J. W. Teague, Y. Totoki, A. N. Tutt, R. Valdes-Mas, M. M. van Buuren, L. van 't Veer, A. Vincent-Salomon, N. Waddell, L. R. Yates, Initiative Australian Pancreatic Cancer Genome, Icgc Breast Cancer Consortium, Icgc Mmml- Seq Consortium, Icgc PedBrain, J. Zucman-Rossi, P. A. Futreal, U. McDermott, P. Lichter, M. Meyerson, S. M. Grimmond, R. Siebert, E. Campo, T. Shibata, S. M. Pfister, P. J. Campbell, and M. R. Stratton. 2013. 'Signatures of mutational processes in human cancer', *Nature*, 500: 415-21.

Andrade, V. C., A. L. Vettore, R. S. Felix, M. S. Almeida, F. Carvalho, J. S. Oliveira, M. L. Chauffaille, A. Andriolo, O. L. Caballero, M. A. Zago, and G. W. Colleoni. 2008. 'Prognostic impact of cancer/testis antigen expression in advanced stage multiple myeloma patients', *Cancer Immun*, 8: 2.

Andrew, A. J., J. Y. Song, B. Schilke, and E. A. Craig. 2008. 'Posttranslational regulation of the scaffold for Fe-S cluster biogenesis, Isu', *Mol Biol Cell*, 19: 5259-66.

Aprelikova, O., S. Pandolfi, S. Tackett, M. Ferreira, K. Salnikow, Y. Ward, J. I. Risinger, J. C. Barrett, and J. Niederhuber. 2009. 'Melanoma antigen-11 inhibits the hypoxia-inducible factor prolyl hydroxylase 2 and activates hypoxic response', *Cancer Res*, 69: 616-24.

Atanackovic, D., Y. Hildebrandt, A. Jadczak, Y. Cao, T. Luetkens, S. Meyer, S. Kobold, K. Bartels, C. Pabst, N. Lajmi, M. Gordic, T. Stahl, A. R. Zander, C. Bokemeyer, and N. Kroger. 2010. 'Cancer-testis antigens MAGE-C1/CT7 and MAGE-A3 promote the survival of multiple myeloma cells', *Haematologica*, 95: 785-93.

Atanackovic, D., T. Luetkens, Y. Hildebrandt, J. Arfsten, K. Bartels, C. Horn, T. Stahl, Y. Cao, A. R. Zander, C. Bokemeyer, and N. Kroger. 2009. 'Longitudinal analysis and prognostic effect of cancer-testis antigen expression in multiple myeloma', *Clin Cancer Res*, 15: 1343-52.

Ayyoub, M., C. M. Scarlata, A. Hamai, P. Pignon, and D. Valmori. 2014. 'Expression of MAGE-A3/6 in primary breast cancer is associated with hormone receptor negative status, high histologic grade, and poor survival', *J Immunother*, 37: 73-6.

Bai, S., B. He, and E. M. Wilson. 2005. 'Melanoma antigen gene protein MAGE-11 regulates androgen receptor function by modulating the interdomain interaction', *Mol Cell Biol*, 25: 1238-57.

Bai, S., and E. M. Wilson. 2008. 'Epidermal-growth-factor-dependent phosphorylation and ubiquitinylation of MAGE-11 regulates its interaction with the androgen receptor', *Mol Cell Biol*, 28: 1947-63.

Barker, P. A., and A. Salehi. 2002. 'The MAGE proteins: emerging roles in cell cycle progression, apoptosis, and neurogenetic disease', *J Neurosci Res*, 67: 705-12.

Barreiro, L. B., and L. Quintana-Murci. 2010. 'From evolutionary genetics to human immunology: how selection shapes host defence genes', *Nat Rev Genet*, 11: 17-30.

Barrow, C., J. Browning, D. MacGregor, I. D. Davis, S. Sturrock, A. A. Jungbluth, and J. Cebon. 2006. 'Tumor antigen expression in melanoma varies according to antigen and stage', *Clin Cancer Res*, 12: 764-71.

Baselga, J., M. Campone, M. Piccart, H. A. Burris, 3rd, H. S. Rugo, T. Sahmoud, S. Noguchi, M. Gnant, K. I. Pritchard, F. Lebrun, J. T. Beck, Y. Ito, D. Yardley, I. Deleu, A. Perez, T. Bachelot, L. Vittori, Z. Xu, P. Mukhopadhyay, D. Lebwohl, and G. N. Hortobagyi. 2012. 'Everolimus in postmenopausal hormone-receptor-positive advanced breast cancer', *N Engl J Med*, 366: 520-9.

Beinert, H. 2000. 'Iron-sulfur proteins: ancient structures, still full of surprises', *J Biol Inorg Chem*, 5: 2-15.

Beinert, H., R. H. Holm, and E. Munck. 1997. 'Iron-sulfur clusters: nature's modular, multipurpose structures', *Science*, 277: 653-9.

Bencze, K. Z., K. C. Kondapalli, J. D. Cook, S. McMahon, C. Millan-Pacheco, N. Pastor, and T. L. Stemmler. 2006. 'The structure and function of frataxin', *Crit Rev Biochem Mol Biol*, 41: 269-91.

Bhatia, N., T. Z. Xiao, K. A. Rosenthal, I. A. Siddiqui, S. Thiyagarajan, B. Smart, Q. Meng, C. L. Zuleger, H. Mukhtar, S. C. Kenney, M. R. Albertini, and B. Jack Longley. 2013.

'MAGE-C2 promotes growth and tumorigenicity of melanoma cells, phosphorylation of KAP1, and DNA damage repair', *J Invest Dermatol*, 133: 759-67.

Brasseur, F., D. Rimoldi, D. Lienard, B. Lethe, S. Carrel, F. Arienti, L. Suter, R. Vanwijck, A. Bourlond, Y. Humblet, and et al. 1995. 'Expression of MAGE genes in primary and metastatic cutaneous melanoma', *Int J Cancer*, 63: 375-80.

Bridwell-Rabb, J., N. G. Fox, C. L. Tsai, A. M. Winn, and D. P. Barondeau. 2014. 'Human frataxin activates Fe-S cluster biosynthesis by facilitating sulfur transfer chemistry', *Biochemistry*, 53: 4904-13.

Brosh, R. M., Jr., and S. B. Cantor. 2014. 'Molecular and cellular functions of the FANCJ DNA helicase defective in cancer and in Fanconi anemia', *Front Genet*, 5: 372.

Camaschella, C., A. Campanella, L. De Falco, L. Boschetto, R. Merlini, L. Silvestri, S. Levi, and A. Iolascon. 2007. 'The human counterpart of zebrafish shiraz shows sideroblastic-like microcytic anemia and iron overload', *Blood*, 110: 1353-8.

Campuzano, V., L. Montermini, M. D. Molto, L. Pianese, M. Cossee, F. Cavalcanti, E. Monros, F. Rodius, F. Duclos, A. Monticelli, F. Zara, J. Canizares, H. Koutnikova, S. I. Bidichandani, C. Gellera, A. Brice, P. Trouillas, G. De Michele, A. Filla, R. De Frutos, F. Palau, P. I. Patel, S. Di Donato, J. L. Mandel, S. Cocozza, M. Koenig, and M. Pandolfo. 1996. 'Friedreich's ataxia: autosomal recessive disease caused by an intronic GAA triplet repeat expansion', *Science*, 271: 1423-7.

Cantor, S. B., D. W. Bell, S. Ganesan, E. M. Kass, R. Drapkin, S. Grossman, D. C. Wahrer, D. C. Sgroi, W. S. Lane, D. A. Haber, and D. M. Livingston. 2001. 'BACH1, a novel helicase-like protein, interacts directly with BRCA1 and contributes to its DNA repair function', *Cell*, 105: 149-60.

Chen, Y. T., D. S. Ross, R. Chiu, X. K. Zhou, Y. Y. Chen, P. Lee, S. A. Hoda, A. J. Simpson, L. J. Old, O. Caballero, and A. M. Neville. 2011. 'Multiple cancer/testis antigens are preferentially expressed in hormone-receptor negative and high-grade breast cancers', *PLoS One*, 6: e17876.

Choi, A. M., S. W. Ryter, and B. Levine. 2013. 'Autophagy in human health and disease', *N Engl J Med*, 368: 651-62.

Ciesielski, S. J., B. A. Schilke, J. Osipiuk, L. Bigelow, R. Mulligan, J. Majewska, A. Joachimiak, J. Marszalek, E. A. Craig, and R. Dutkiewicz. 2012. 'Interaction of J-protein co-chaperone Jac1 with Fe-S scaffold Isu is indispensable in vivo and conserved in evolution', *J Mol Biol*, 417: 1-12.

Ciesielski, S. J., B. Schilke, J. Marszalek, and E. A. Craig. 2016. 'Protection of scaffold protein Isu from degradation by the Lon protease Pim1 as a component of Fe-S cluster biogenesis regulation', *Mol Biol Cell*, 27: 1060-8.

Cook, J. D., K. C. Kondapalli, S. Rawat, W. C. Childs, Y. Murugesan, A. Dancis, and T. L. Stemmler. 2010. 'Molecular details of the yeast frataxin-Isu1 interaction during mitochondrial Fe-S cluster assembly', *Biochemistry*, 49: 8756-65.

Curioni-Fontecedro, A., N. Nuber, D. Mihic-Probst, B. Seifert, D. Soldini, R. Dummer, A. Knuth, M. van den Broek, and H. Moch. 2011. 'Expression of MAGE-C1/CT7 and MAGE-C2/CT10 predicts lymph node metastasis in melanoma patients', *PLoS One*, 6: e21418.

Daudi, S., K. H. Eng, P. Mhawech-Fauceglia, C. Morrison, A. Miliotto, A. Beck, J. Matsuzaki, T. Tsuji, A. Groman, S. Gnjatic, G. Spagnoli, S. Lele, and K. Odunsi. 2014. 'Expression and immune responses to MAGE antigens predict survival in epithelial ovarian cancer', *PLoS One*, 9: e104099.

De Piccoli, G., F. Cortes-Ledesma, G. Ira, J. Torres-Rosell, S. Uhle, S. Farmer, J. Y. Hwang, F. Machin, A. Ceschia, A. McAleenan, V. Cordon-Preciado, A. Clemente-Blanco, F. Vilella-Mitjana, P. Ullal, A. Jarmuz, B. Leitao, D. Bressan, F. Dotiwala, A. Papusha, X. Zhao, K. Myung, J. E. Haber, A. Aguilera, and L. Aragon. 2006. 'Smc5-Smc6 mediate DNA double-strand-break repair by promoting sister-chromatid recombination', *Nat Cell Biol*, 8: 1032-4.

De Smet, C., S. J. Courtois, I. Faraoni, C. Lurquin, J. P. Szikora, O. De Backer, and T. Boon. 1995. 'Involvement of two Ets binding sites in the transcriptional activation of the MAGE1 gene', *Immunogenetics*, 42: 282-90.

De Smet, C., C. Lurquin, B. Lethe, V. Martelange, and T. Boon. 1999. 'DNA methylation is the primary silencing mechanism for a set of germ line- and tumor-specific genes with a CpG-rich promoter', *Mol Cell Biol*, 19: 7327-35.

Dong, X., B. Milholland, and J. Vijg. 2016. 'Evidence for a limit to human lifespan', *Nature*, 538: 257-59.

Dorn, C. R. 1967. 'The epidemiology of cancer in animals', *Calif Med*, 107: 481-9.

Doyle, J. M., J. Gao, J. Wang, M. Yang, and P. R. Potts. 2010. 'MAGE-RING protein complexes comprise a family of E3 ubiquitin ligases', *Mol Cell*, 39: 963-74.

Drakesmith, H., and A. Prentice. 2008. 'Viral infection and iron metabolism', *Nat Rev Microbiol*, 6: 541-52.

Fairman-Williams, M. E., U. P. Guenther, and E. Jankowsky. 2010. 'SF1 and SF2 helicases: family matters', *Curr Opin Struct Biol*, 20: 313-24.

Fan, L., J. O. Fuss, Q. J. Cheng, A. S. Arvai, M. Hammel, V. A. Roberts, P. K. Cooper, and J. A. Tainer. 2008. 'XPD helicase structures and activities: insights into the cancer and aging phenotypes from XPD mutations', *Cell*, 133: 789-800.

Floyd, R. A., and J. M. Carney. 1992. 'Free radical damage to protein and DNA: mechanisms involved and relevant observations on brain undergoing oxidative stress', *Ann Neurol*, 32 Suppl: S22-7.

Fuss, J. O., C. L. Tsai, J. P. Ishida, and J. A. Tainer. 2015. 'Emerging critical roles of Fe-S clusters in DNA replication and repair', *Biochim Biophys Acta*, 1853: 1253-71.

Galanty, Y., R. Belotserkovskaya, J. Coates, S. Polo, K. M. Miller, and S. P. Jackson. 2009. 'Mammalian SUMO E3-ligases PIAS1 and PIAS4 promote responses to DNA double-strand breaks', *Nature*, 462: 935-9.

Ganz, T., and E. Nemeth. 2015. 'Iron homeostasis in host defence and inflammation', *Nat Rev Immunol*, 15: 500-10.

Gari, K., A. M. Leon Ortiz, V. Borel, H. Flynn, J. M. Skehel, and S. J. Boulton. 2012. 'MMS19 links cytoplasmic iron-sulfur cluster assembly to DNA metabolism', *Science*, 337: 243-5.

Gu, X., M. Fu, Z. Ge, F. Zhan, Y. Ding, H. Ni, W. Zhang, Y. Zhu, X. Tang, L. Xiong, J. Li, L. Qiu, Y. Mao, and J. Zhu. 2014. 'High expression of MAGE-A9 correlates with unfavorable survival in hepatocellular carcinoma', *Sci Rep*, 4: 6625.

Gur, I., K. Fujiwara, K. Hasegawa, and K. Yoshikawa. 2014. 'Necdin promotes ubiquitin-dependent degradation of PIAS1 SUMO E3 ligase', *PLoS One*, 9: e99503.

Gure, A. O., R. Chua, B. Williamson, M. Gonen, C. A. Ferrera, S. Gnjatic, G. Ritter, A. J. Simpson, Y. T. Chen, L. J. Old, and N. K. Altorki. 2005. 'Cancer-testis genes are coordinately expressed and are markers of poor outcome in non-small cell lung cancer', *Clin Cancer Res*, 11: 8055-62.

Hadari, Y. R., N. Gotoh, H. Kouhara, I. Lax, and J. Schlessinger. 2001. 'Critical role for the docking-protein FRS2 alpha in FGF receptor-mediated signal transduction pathways', *Proc Natl Acad Sci U S A*, 98: 8578-83.

Haller, R. G., K. G. Henriksson, L. Jorfeldt, E. Hultman, R. Wibom, K. Sahlin, N. H. Areskog, M. Gunder, K. Ayyad, C. G. Blomqvist, and et al. 1991. 'Deficiency of skeletal muscle succinate dehydrogenase and aconitase. Pathophysiology of exercise in a novel human muscle oxidative defect', *J Clin Invest*, 88: 1197-206.

Hao, Y. H., J. M. Doyle, S. Ramanathan, T. S. Gomez, D. Jia, M. Xu, Z. J. Chen, D. D. Billadeau, M. K. Rosen, and P. R. Potts. 2013. 'Regulation of WASH-dependent actin polymerization and protein trafficking by ubiquitination', *Cell*, 152: 1051-64.

Hardie, D. G. 2015. 'Molecular Pathways: Is AMPK a Friend or a Foe in Cancer?', *Clin Cancer Res*.

Hardie, D. G., F. A. Ross, and S. A. Hawley. 2012. 'AMPK: a nutrient and energy sensor that maintains energy homeostasis', *Nat Rev Mol Cell Biol*, 13: 251-62.

Hatfield, M. D., A. M. Reis, D. Obeso, J. R. Cook, D. M. Thompson, M. Rao, E. C. Friedberg, and L. Queimado. 2006. 'Identification of MMS19 domains with distinct functions in NER and transcription', *DNA Repair (Amst)*, 5: 914-24.

Hocke, S., Y. Guo, A. Job, M. Orth, A. Ziesch, K. Lauber, E. N. De Toni, T. M. Gress, A. Herbst, B. Goke, and E. Gallmeier. 2016. 'A synthetic lethal screen identifies ATR-inhibition as a novel therapeutic approach for POLD1-deficient cancers', *Oncotarget*, 7: 7080-95.

Hou, S. Y., M. X. Sang, C. Z. Geng, W. H. Liu, W. H. Lu, Y. Y. Xu, and B. E. Shan. 2014. 'Expressions of MAGE-A9 and MAGE-A11 in breast cancer and their expression mechanism', *Arch Med Res*, 45: 44-51.

Imlay, J. A. 2006. 'Iron-sulphur clusters and the problem with oxygen', *Mol Microbiol*, 59: 1073-82.

Irmisch, A., E. Ampatzidou, K. Mizuno, M. J. O'Connell, and J. M. Murray. 2009. 'Smc5/6 maintains stalled replication forks in a recombination-competent conformation', *EMBO J*, 28: 144-55.

Ito, S., L. J. Tan, D. Andoh, T. Narita, M. Seki, Y. Hirano, K. Narita, I. Kuraoka, Y. Hiraoka, and K. Tanaka. 2010. 'MMXD, a TFIIH-independent XPD-MMS19 protein complex involved in chromosome segregation', *Mol Cell*, 39: 632-40.

Jeon, C. H., I. H. Kim, and H. D. Chae. 2014. 'Prognostic value of genetic detection using CEA and MAGE in peritoneal washes with gastric carcinoma after curative resection: result of a 3-year follow-up', *Medicine (Baltimore)*, 93: e83.

Johnson, D. C., D. R. Dean, A. D. Smith, and M. K. Johnson. 2005. 'Structure, function, and formation of biological iron-sulfur clusters', *Annu Rev Biochem*, 74: 247-81.

Johnson, E. E., and M. Wessling-Resnick. 2012. 'Iron metabolism and the innate immune response to infection', *Microbes Infect*, 14: 207-16.

Jordan, B. W., D. Dinev, V. LeMellay, J. Troppmair, R. Gotz, L. Wixler, M. Sendtner, S. Ludwig, and U. R. Rapp. 2001. 'Neurotrophin receptor-interacting mage homologue is an inducible inhibitor of apoptosis protein-interacting protein that augments cell death', *J Biol Chem*, 276: 39985-9.

Jungbluth, A. A., Y. T. Chen, K. J. Busam, K. Coplan, D. Kolb, K. Iversen, B. Williamson, F. K. Van Landeghem, E. Stockert, and L. J. Old. 2002. 'CT7 (MAGE-C1) antigen expression in normal and neoplastic tissues', *Int J Cancer*, 99: 839-45.

Kanno, T., D. G. Berta, and C. Sjogren. 2015. 'The Smc5/6 Complex Is an ATP-Dependent Intermolecular DNA Linker', *Cell Rep*, 12: 1471-82.

Karpf, A. R., S. Bai, S. R. James, J. L. Mohler, and E. M. Wilson. 2009. 'Increased expression of androgen receptor coregulator MAGE-11 in prostate cancer by DNA hypomethylation and cyclic AMP', *Mol Cancer Res*, 7: 523-35.

Kasznicki, J., A. Sliwinska, and J. Drzewoski. 2014. 'Metformin in cancer prevention and therapy', *Ann Transl Med*, 2: 57.

Keane, M., J. Semeiks, A. E. Webb, Y. I. Li, V. Quesada, T. Craig, L. B. Madsen, S. van Dam, D. Brawand, P. I. Marques, P. Michalak, L. Kang, J. Bhak, H. S. Yim, N. V. Grishin, N. H. Nielsen, M. P. Heide-Jorgensen, E. M. Oziolor, C. W. Matson, G. M. Church, G. W. Stuart, J. C. Patton, J. C. George, R. Suydam, K. Larsen, C. Lopez-Otin, M. J. O'Connell, J. W. Bickham, B. Thomsen, and J. P. de Magalhaes. 2015. 'Insights into the evolution of longevity from the bowhead whale genome', *Cell Rep*, 10: 112-22.

Kendall, S. E., C. Battelli, S. Irwin, J. G. Mitchell, C. A. Glackin, and J. M. Verdi. 2005. 'NRAGE mediates p38 activation and neural progenitor apoptosis via the bone morphogenetic protein signaling cascade', *Mol Cell Biol*, 25: 7711-24.

Kennedy, M. C., L. Mende-Mueller, G. A. Blondin, and H. Beinert. 1992. 'Purification and characterization of cytosolic aconitase from beef liver and its relationship to the iron-responsive element binding protein', *Proc Natl Acad Sci U S A*, 89: 11730-4.

Khwaja, A., P. Rodriguez-Viciana, S. Wennstrom, P. H. Warne, and J. Downward. 1997. 'Matrix adhesion and Ras transformation both activate a phosphoinositide 3-OH kinase and protein kinase B/Akt cellular survival pathway', *EMBO J*, 16: 2783-93.

Kim, Y. D., H. R. Park, M. H. Song, D. H. Shin, C. H. Lee, M. K. Lee, and S. Y. Lee. 2012. 'Pattern of cancer/testis antigen expression in lung cancer patients', *Int J Mol Med*, 29: 656-62.

Kondo, T., X. Zhu, S. L. Asa, and S. Ezzat. 2007. 'The cancer/testis antigen melanoma-associated antigen-A3/A6 is a novel target of fibroblast growth factor receptor 2-IIIb through histone H3 modifications in thyroid cancer', *Clin Cancer Res*, 13: 4713-20.

Kouhara, H., Y. R. Hadari, T. Spivak-Kroizman, J. Schilling, D. Bar-Sagi, I. Lax, and J. Schlessinger. 1997. 'A lipid-anchored Grb2-binding protein that links FGF-receptor activation to the Ras/MAPK signaling pathway', *Cell*, 89: 693-702.

Kozakova, L., L. Vondrova, K. Stejskal, P. Charalabous, P. Kolesar, A. R. Lehmann, S. Uldrijan, C. M. Sanderson, Z. Zdrahal, and J. J. Palecek. 2015. 'The melanoma-associated antigen 1 (MAGEA1) protein stimulates the E3 ubiquitin-ligase activity of TRIM31 within a TRIM31-MAGEA1-NSE4 complex', *Cell Cycle*, 14: 920-30.

Kraemer, K. H., N. J. Patronas, R. Schiffmann, B. P. Brooks, D. Tamura, and J. J. DiGiovanna. 2007. 'Xeroderma pigmentosum, trichothiodystrophy and Cockayne syndrome: a complex genotype-phenotype relationship', *Neuroscience*, 145: 1388-96.

Lahdenpera, M., K. U. Mar, and V. Lummaa. 2014. 'Reproductive cessation and post-reproductive lifespan in Asian elephants and pre-industrial humans', *Front Zool*, 11: 54.

Lauder, S., M. Bankmann, S. N. Guzder, P. Sung, L. Prakash, and S. Prakash. 1996. 'Dual requirement for the yeast MMS19 gene in DNA repair and RNA polymerase II transcription', *Mol Cell Biol*, 16: 6783-93.

Le Guen, T., L. Jullien, F. Touzot, M. Schertzer, L. Gaillard, M. Perderiset, W. Carpentier, P. Nitschke, C. Picard, G. Couillault, J. Soulier, A. Fischer, I. Callebaut, N. Jabado, A. Londono-Vallejo, J. P. de Villartay, and P. Revy. 2013. 'Human RTEL1 deficiency causes Hoyeraal-Hreidarsson syndrome with short telomeres and genome instability', *Hum Mol Genet*, 22: 3239-49.

Lemire, J. A., J. J. Harrison, and R. J. Turner. 2013. 'Antimicrobial activity of metals: mechanisms, molecular targets and applications', *Nat Rev Microbiol*, 11: 371-84.

Lev, I., M. Volpe, L. Goor, N. Levinton, L. Emuna, and S. Ben-Aroya. 2013. 'Reverse PCA, a systematic approach for identifying genes important for the physical interaction between protein pairs', *PLoS Genet*, 9: e1003838.

Li, M., Y. H. Yuan, Y. Han, Y. X. Liu, L. Yan, Y. Wang, and J. Gu. 2005. 'Expression profile of cancer-testis genes in 121 human colorectal cancer tissue and adjacent normal tissue', *Clin Cancer Res*, 11: 1809-14.

Lill, R. 2009. 'Function and biogenesis of iron-sulphur proteins', *Nature*, 460: 831-8.

Lill, R., R. Dutkiewicz, S. A. Freibert, T. Heidenreich, J. Mascarenhas, D. J. Netz, V. D. Paul, A. J. Pierik, N. Richter, M. Stumpfig, V. Srinivasan, O. Stehling, and U. Muhlenhoff. 2015. 'The role of mitochondria and the CIA machinery in the maturation of cytosolic and nuclear iron-sulfur proteins', *Eur J Cell Biol*, 94: 280-91.

Lill, R., and U. Muhlenhoff. 2005. 'Iron-sulfur-protein biogenesis in eukaryotes', *Trends Biochem Sci*, 30: 133-41.

Linette, G. P., E. A. Stadtmauer, M. V. Maus, A. P. Rapoport, B. L. Levine, L. Emery, L. Litzky, A. Bagg, B. M. Carreno, P. J. Cimino, G. K. Binder-Scholl, D. P. Smethurst, A. B. Gerry, N. J. Pumphrey, A. D. Bennett, J. E. Brewer, J. Dukes, J. Harper, H. K. Tayton-Martin, B. K. Jakobsen, N. J. Hassan, M. Kalos, and C. H. June. 2013. 'Cardiovascular toxicity and titin cross-reactivity of affinity-enhanced T cells in myeloma and melanoma', *Blood*, 122: 863-71.

Linnekin, D. 1999. 'Early signaling pathways activated by c-Kit in hematopoietic cells', *Int J Biochem Cell Biol*, 31: 1053-74.

Litman, R., M. Peng, Z. Jin, F. Zhang, J. Zhang, S. Powell, P. R. Andreassen, and S. B. Cantor. 2005. 'BACH1 is critical for homologous recombination and appears to be the Fanconi anemia gene product FANCJ', *Cancer Cell*, 8: 255-65.

Liu, W., S. Cheng, S. L. Asa, and S. Ezzat. 2008. 'The melanoma-associated antigen A3 mediates fibronectin-controlled cancer progression and metastasis', *Cancer Res*, 68: 8104-12.

Lloyd, S. J., H. Lauble, G. S. Prasad, and C. D. Stout. 1999. 'The mechanism of aconitase: 1.8 A resolution crystal structure of the S642a:citrate complex', *Protein Sci*, 8: 2655-62.

Maffettone, C., G. Chen, I. Drozdov, C. Ouzounis, and K. Pantopoulos. 2010. 'Tumorigenic properties of iron regulatory protein 2 (IRP2) mediated by its specific 73-amino acids insert', *PLoS One*, 5: e10163.

Malkin, R., and J. C. Rabinowitz. 1966. 'The reconstitution of clostridial ferredoxin', *Biochem Biophys Res Commun*, 23: 822-7.

Maloisel, L., F. Fabre, and S. Gangloff. 2008. 'DNA polymerase delta is preferentially recruited during homologous recombination to promote heteroduplex DNA extension', *Mol Cell Biol*, 28: 1373-82.

Marcar, L., B. Ihrig, J. Hourihan, S. E. Bray, P. R. Quinlan, L. B. Jordan, A. M. Thompson, T. R. Hupp, and D. W. Meek. 2015. 'MAGE-A Cancer/Testis Antigens Inhibit MDM2 Ubiquitylation Function and Promote Increased Levels of MDM4', *PLoS One*, 10: e0127713.

Marcar, L., N. J. Maclaine, T. R. Hupp, and D. W. Meek. 2010. 'Mage-A cancer/testis antigens inhibit p53 function by blocking its interaction with chromatin', *Cancer Res*, 70: 10362-70.

Martincorena, I., and P. J. Campbell. 2015. 'Somatic mutation in cancer and normal cells', *Science*, 349: 1483-9.

Mashberg, A., P. Boffetta, R. Winkelman, and L. Garfinkel. 1993. 'Tobacco smoking, alcohol drinking, and cancer of the oral cavity and oropharynx among U.S. veterans', *Cancer*, 72: 1369-75.

Mochel, F., M. A. Knight, W. H. Tong, D. Hernandez, K. Ayyad, T. Taivassalo, P. M. Andersen, A. Singleton, T. A. Rouault, K. H. Fischbeck, and R. G. Haller. 2008. 'Splice mutation in the iron-sulfur cluster scaffold protein ISCU causes myopathy with exercise intolerance', *Am J Hum Genet*, 82: 652-60.

Moiseeva, T. N., A. M. Gamper, B. L. Hood, T. P. Conrads, and C. J. Bakkenist. 2016. 'Human DNA polymerase epsilon is phosphorylated at serine-1940 after DNA damage and interacts with the iron-sulfur complex chaperones CIAO1 and MMS19', *DNA Repair (Amst)*, 43: 9-17.

Monte, M., M. Simonatto, L. Y. Peche, D. R. Bublik, S. Gobessi, M. A. Pierotti, M. Rodolfo, and C. Schneider. 2006. 'MAGE-A tumor antigens target p53 transactivation function through histone deacetylase recruitment and confer resistance to chemotherapeutic agents', *Proc Natl Acad Sci U S A*, 103: 11160-5.

Morgan, R. A., N. Chinnasamy, D. Abate-Daga, A. Gros, P. F. Robbins, Z. Zheng, M. E. Dudley, S. A. Feldman, J. C. Yang, R. M. Sherry, G. Q. Phan, M. S. Hughes, U. S. Kammula, A. D. Miller, C. J. Hessman, A. A. Stewart, N. P. Restifo, M. M. Quezado, M. Alimchandani, A. Z. Rosenberg, A. Nath, T. Wang, B. Bielekova, S. C. Wuest, N. Akula, F. J. McMahon, S. Wilde, B. Mosetter, D. J. Schendel, C. M. Laurencot, and S. A. Rosenberg. 2013. 'Cancer regression and neurological toxicity following anti-MAGE-A3 TCR gene therapy', *J Immunother*, 36: 133-51.

Mori, M., H. Inoue, K. Mimori, K. Shibuta, K. Baba, H. Nakashima, M. Haraguchi, K. Tsuji, H. Ueo, G. F. Barnard, and T. Akiyoshi. 1996. 'Expression of MAGE genes in human colorectal carcinoma', *Ann Surg*, 224: 183-8.

Mouri, A., A. Sasaki, K. Watanabe, C. Sogawa, S. Kitayama, T. Mamiya, Y. Miyamoto, K. Yamada, Y. Noda, and T. Nabeshima. 2012. 'MAGE-D1 regulates expression of depression-like behavior through serotonin transporter ubiquitylation', *J Neurosci*, 32: 4562-80.

Murray, J. M., and A. M. Carr. 2008. 'Smc5/6: a link between DNA repair and unidirectional replication?', *Nat Rev Mol Cell Biol*, 9: 177-82.

Nakad, R., and B. Schumacher. 2016. 'DNA Damage Response and Immune Defense: Links and Mechanisms', *Front Genet*, 7: 147.

Nardiello, T., A. A. Jungbluth, A. Mei, M. Diliberto, X. Huang, A. Dabrowski, V. C. Andrade, R. Wasserstrum, S. Ely, R. Niesvizky, R. Pearse, M. Coleman, D. S. Jayabalan, N. Bhardwaj, L. J. Old, S. Chen-Kiang, and H. J. Cho. 2011. 'MAGE-A inhibits apoptosis in proliferating myeloma cells through repression of Bax and maintenance of survivin', *Clin Cancer Res*, 17: 4309-19.

Netz, D. J., J. Mascarenhas, O. Stehling, A. J. Pierik, and R. Lill. 2014. 'Maturation of cytosolic and nuclear iron-sulfur proteins', *Trends Cell Biol*, 24: 303-12.

Odermatt, D. C., and K. Gari. 2017. 'The CIA Targeting Complex Is Highly Regulated and Provides Two Distinct Binding Sites for Client Iron-Sulfur Proteins', *Cell Rep*, 18: 1434-43.

Olsson, A., L. Lind, L. E. Thornell, and M. Holmberg. 2008. 'Myopathy with lactic acidosis is linked to chromosome 12q23.3-24.11 and caused by an intron mutation in the ISCU gene resulting in a splicing defect', *Hum Mol Genet*, 17: 1666-72.

Otte, M., M. Zafrakas, L. Riethdorf, U. Pichlmeier, T. Loning, F. Janicke, and K. Pantel. 2001. 'MAGE-A gene expression pattern in primary breast cancer', *Cancer Res*, 61: 6682-7.

Palecek, J., S. Vidot, M. Feng, A. J. Doherty, and A. R. Lehmann. 2006. 'The Smc5-Smc6 DNA repair complex. bridging of the Smc5-Smc6 heads by the KLEISIN, Nse4, and non-Kleisin subunits', *J Biol Chem*, 281: 36952-9.

Paradkar, P. N., K. B. Zumbrennen, B. H. Paw, D. M. Ward, and J. Kaplan. 2009. 'Regulation of mitochondrial iron import through differential turnover of mitoferrin 1 and mitoferrin 2', *Mol Cell Biol*, 29: 1007-16.

Parent, A., X. Elduque, D. Cornu, L. Belot, J. P. Le Caer, A. Grandas, M. B. Toledano, and B. D'Autreaux. 2015. 'Mammalian frataxin directly enhances sulfur transfer of NFS1 persulfide to both ISCU and free thiols', *Nat Commun*, 6: 5686.

Paul, V. D., and R. Lill. 2015. 'Biogenesis of cytosolic and nuclear iron-sulfur proteins and their role in genome stability', *Biochim Biophys Acta*, 1853: 1528-39.

Paul, V. D., U. Muhlenhoff, M. Stumpfig, J. Seebacher, K. G. Kugler, C. Renicke, C. Taxis, A. C. Gavin, A. J. Pierik, and R. Lill. 2015. 'The deca-GX3 proteins Yae1-Lto1 function as adaptors recruiting the ABC protein Rli1 for iron-sulfur cluster insertion', *Elife*, 4: e08231.

Pebernard, S., J. J. Perry, J. A. Tainer, and M. N. Boddy. 2008. 'Nse1 RING-like domain supports functions of the Smc5-Smc6 holocomplex in genome stability', *Mol Biol Cell*, 19: 4099-109.

Peche, L. Y., M. Scolz, M. F. Ladelfa, M. Monte, and C. Schneider. 2012. 'MageA2 restrains cellular senescence by targeting the function of PMLIV/p53 axis at the PML-NBs', *Cell Death Differ*, 19: 926-36.

Pineda, C. T., S. Ramanathan, K. Fon Tacer, J. L. Weon, M. B. Potts, Y. H. Ou, M. A. White, and P. R. Potts. 2015. 'Degradation of AMPK by a cancer-specific ubiquitin ligase', *Cell*, 160: 715-28.

Pleasance, E. D., R. K. Cheetham, P. J. Stephens, D. J. McBride, S. J. Humphray, C. D. Greenman, I. Varela, M. L. Lin, G. R. Ordonez, G. R. Bignell, K. Ye, J. Alipaz, M. J. Bauer, D. Beare, A. Butler, R. J. Carter, L. Chen, A. J. Cox, S. Edkins, P. I. Kokko-Gonzales, N. A. Gormley, R. J. Grocock, C. D. Haudenschild, M. M. Hims, T. James, M. Jia, Z. Kingsbury, C. Leroy, J. Marshall, A. Menzies, L. J. Mudie, Z. Ning, T. Royce, O. B. Schulz-Trieglaff, A. Spiridou, L. A. Stebbings, L. Szajkowski, J. Teague, D. Williamson, L. Chin, M. T. Ross, P. J. Campbell, D. R. Bentley, P. A. Futreal, and M. R.

Stratton. 2010. 'A comprehensive catalogue of somatic mutations from a human cancer genome', *Nature*, 463: 191-6.

Pleasance, E. D., P. J. Stephens, S. O'Meara, D. J. McBride, A. Meynert, D. Jones, M. L. Lin, D. Beare, K. W. Lau, C. Greenman, I. Varela, S. Nik-Zainal, H. R. Davies, G. R. Ordonez, L. J. Mudie, C. Latimer, S. Edkins, L. Stebbings, L. Chen, M. Jia, C. Leroy, J. Marshall, A. Menzies, A. Butler, J. W. Teague, J. Mangion, Y. A. Sun, S. F. McLaughlin, H. E. Peckham, E. F. Tsung, G. L. Costa, C. C. Lee, J. D. Minna, A. Gazdar, E. Birney, M. D. Rhodes, K. J. McKernan, M. R. Stratton, P. A. Futreal, and P. J. Campbell. 2010. 'A small-cell lung cancer genome with complex signatures of tobacco exposure', *Nature*, 463: 184-90.

Plechanovova, A., E. G. Jaffray, M. H. Tatham, J. H. Naismith, and R. T. Hay. 2012. 'Structure of a RING E3 ligase and ubiquitin-loaded E2 primed for catalysis', *Nature*, 489: 115-20.

Porteus, M. H., and D. Baltimore. 2003. 'Chimeric nucleases stimulate gene targeting in human cells', *Science*, 300: 763.

Potts, P. R. 2009. 'The Yin and Yang of the MMS21-SMC5/6 SUMO ligase complex in homologous recombination', *DNA Repair (Amst)*, 8: 499-506.

Potts, P. R., M. H. Porteus, and H. Yu. 2006. 'Human SMC5/6 complex promotes sister chromatid homologous recombination by recruiting the SMC1/3 cohesin complex to double-strand breaks', *EMBO J*, 25: 3377-88.

Prakash, L., and S. Prakash. 1977. 'Isolation and characterization of MMS-sensitive mutants of Saccharomyces cerevisiae', *Genetics*, 86: 33-55.

Rizvi, N. A., M. D. Hellmann, A. Snyder, P. Kvistborg, V. Makarov, J. J. Havel, W. Lee, J. Yuan, P. Wong, T. S. Ho, M. L. Miller, N. Rekhtman, A. L. Moreira, F. Ibrahim, C. Bruggeman, B. Gasmi, R. Zappasodi, Y. Maeda, C. Sander, E. B. Garon, T. Merghoub, J. D. Wolchok, T. N. Schumacher, and T. A. Chan. 2015. 'Cancer immunology. Mutational landscape determines sensitivity to PD-1 blockade in non-small cell lung cancer', *Science*, 348: 124-8.

Rodriguez, K. A., Y. H. Edrey, P. Osmulski, M. Gaczynska, and R. Buffenstein. 2012. 'Altered composition of liver proteasome assemblies contributes to enhanced proteasome activity in the exceptionally long-lived naked mole-rat', *PLoS One*, 7: e35890.

Rotig, A., P. de Lonlay, D. Chretien, F. Foury, M. Koenig, D. Sidi, A. Munnich, and P. Rustin. 1997. 'Aconitase and mitochondrial iron-sulphur protein deficiency in Friedreich ataxia', *Nat Genet*, 17: 215-7.

Rouault, T. A. 2006. 'The role of iron regulatory proteins in mammalian iron homeostasis and disease', *Nat Chem Biol*, 2: 406-14.

———. 2015. 'Mammalian iron-sulphur proteins: novel insights into biogenesis and function', *Nat Rev Mol Cell Biol*, 16: 45-55.

Rouault, T. A., and W. H. Tong. 2008. 'Iron-sulfur cluster biogenesis and human disease', *Trends Genet*, 24: 398-407.

Rual, J. F., K. Venkatesan, T. Hao, T. Hirozane-Kishikawa, A. Dricot, N. Li, G. F. Berriz, F. D. Gibbons, M. Dreze, N. Ayivi-Guedehoussou, N. Klitgord, C. Simon, M. Boxem, S. Milstein, J. Rosenberg, D. S. Goldberg, L. V. Zhang, S. L. Wong, G. Franklin, S. Li, J. S. Albala, J. Lim, C. Fraughton, E. Llamosas, S. Cevik, C. Bex, P. Lamesch, R. S. Sikorski, J. Vandenhaute, H. Y. Zoghbi, A. Smolyar, S. Bosak, R. Sequerra, L. Doucette-Stamm, M. E. Cusick, D. E. Hill, F. P. Roth, and M. Vidal. 2005. 'Towards a proteome-scale map of the human protein-protein interaction network', *Nature*, 437: 1173-8.

Ruiz, R., B. Hunis, and L. E. Raez. 2014. 'Immunotherapeutic agents in non-small-cell lung cancer finally coming to the front lines', *Curr Oncol Rep*, 16: 400.

Sasaki, A., Y. Masuda, K. Iwai, K. Ikeda, and K. Watanabe. 2002. 'A RING finger protein Praja1 regulates Dlx5-dependent transcription through its ubiquitin ligase activity for the Dlx/Msx-interacting MAGE/Necdin family protein, Dlxin-1', *J Biol Chem*, 277: 22541-6.

Scarcella, D. L., C. W. Chow, M. F. Gonzales, C. Economou, F. Brasseur, and D. M. Ashley. 1999. 'Expression of MAGE and GAGE in high-grade brain tumors: a potential target for specific immunotherapy and diagnostic markers', *Clin Cancer Res*, 5: 335-41.

Schaeffer, L., V. Moncollin, R. Roy, A. Staub, M. Mezzina, A. Sarasin, G. Weeda, J. H. Hoeijmakers, and J. M. Egly. 1994. 'The ERCC2/DNA repair protein is associated with the class II BTF2/TFIIH transcription factor', *EMBO J*, 13: 2388-92.

Schertzer, M., K. Jouravleva, M. Perderiset, F. Dingli, D. Loew, T. Le Guen, B. Bardoni, J. P. de Villartay, P. Revy, and A. Londono-Vallejo. 2015. 'Human regulator of telomere elongation helicase 1 (RTEL1) is required for the nuclear and cytoplasmic trafficking of pre-U2 RNA', *Nucleic Acids Res*, 43: 1834-47.

Schlaepfer, D. D., S. K. Hanks, T. Hunter, and P. van der Geer. 1994. 'Integrin-mediated signal transduction linked to Ras pathway by GRB2 binding to focal adhesion kinase', *Nature*, 372: 786-91.

Schwarzenbach, H., C. Eichelser, B. Steinbach, J. Tadewaldt, K. Pantel, V. Lobanenkov, and D. Loukinov. 2014. 'Differential regulation of MAGE-A1 promoter activity by BORIS and Sp1, both interacting with the TATA binding protein', *BMC Cancer*, 14: 796.

Seki, M., Y. Takeda, K. Iwai, and K. Tanaka. 2013. 'IOP1 protein is an external component of the human cytosolic iron-sulfur cluster assembly (CIA) machinery and functions in the MMS19 protein-dependent CIA pathway', *J Biol Chem*, 288: 16680-9.

Sheftel, A. D., O. Stehling, A. J. Pierik, D. J. Netz, S. Kerscher, H. P. Elsasser, I. Wittig, J. Balk, U. Brandt, and R. Lill. 2009. 'Human ind1, an iron-sulfur cluster assembly factor for respiratory complex I', *Mol Cell Biol*, 29: 6059-73.

Simpson, A. J., O. L. Caballero, A. Jungbluth, Y. T. Chen, and L. J. Old. 2005. 'Cancer/testis antigens, gametogenesis and cancer', *Nat Rev Cancer*, 5: 615-25.

Soares, M. P., and G. Weiss. 2015. 'The Iron age of host-microbe interactions', *EMBO Rep*, 16: 1482-500.

Stehling, O., H. P. Elsasser, B. Bruckel, U. Muhlenhoff, and R. Lill. 2004. 'Iron-sulfur protein maturation in human cells: evidence for a function of frataxin', *Hum Mol Genet*, 13: 3007-15.

Stehling, O., and R. Lill. 2013. 'The role of mitochondria in cellular iron-sulfur protein biogenesis: mechanisms, connected processes, and diseases', *Cold Spring Harb Perspect Biol*, 5: a011312.

Stehling, O., J. Mascarenhas, A. A. Vashisht, A. D. Sheftel, B. Niggemeyer, R. Rosser, A. J. Pierik, J. A. Wohlschlegel, and R. Lill. 2013. 'Human CIA2A-FAM96A and CIA2B-FAM96B integrate iron homeostasis and maturation of different subsets of cytosolic-nuclear iron-sulfur proteins', *Cell Metab*, 18: 187-98.

Stehling, O., D. J. Netz, B. Niggemeyer, R. Rosser, R. S. Eisenstein, H. Puccio, A. J. Pierik, and R. Lill. 2008. 'Human Nbp35 is essential for both cytosolic iron-sulfur protein assembly and iron homeostasis', *Mol Cell Biol*, 28: 5517-28.

Stehling, O., A. D. Sheftel, and R. Lill. 2009. 'Chapter 12 Controlled expression of iron-sulfur cluster assembly components for respiratory chain complexes in mammalian cells', *Methods Enzymol*, 456: 209-31.

Stehling, O., A. A. Vashisht, J. Mascarenhas, Z. O. Jonsson, T. Sharma, D. J. Netz, A. J. Pierik, J. A. Wohlschlegel, and R. Lill. 2012. 'MMS19 assembles iron-sulfur proteins required for DNA metabolism and genomic integrity', *Science*, 337: 195-9.

Stemmler, T. L., E. Lesuisse, D. Pain, and A. Dancis. 2010. 'Frataxin and mitochondrial FeS cluster biogenesis', *J Biol Chem*, 285: 26737-43.

Stone, B., M. Schummer, P. J. Paley, M. Crawford, M. Ford, N. Urban, and B. H. Nelson. 2001. 'MAGE-F1, a novel ubiquitously expressed member of the MAGE superfamily', *Gene*, 267: 173-82.

Svejstrup, J. Q. 2002. 'Mechanisms of transcription-coupled DNA repair', *Nat Rev Mol Cell Biol*, 3: 21-9.

Tajima, K., Y. Obata, H. Tamaki, M. Yoshida, Y. T. Chen, M. J. Scanlan, L. J. Old, H. Kuwano, T. Takahashi, T. Takahashi, and T. Mitsudomi. 2003. 'Expression of cancer/testis (CT) antigens in lung cancer', *Lung Cancer*, 42: 23-33.

Taylor, E. M., A. C. Copsey, J. J. Hudson, S. Vidot, and A. R. Lehmann. 2008. 'Identification of the proteins, including MAGEG1, that make up the human SMC5-6 protein complex', *Mol Cell Biol*, 28: 1197-206.

Teichmann, R., and W. Stremmel. 1990. 'Iron uptake by human upper small intestine microvillous membrane vesicles. Indication for a facilitated transport mechanism mediated by a membrane iron-binding protein', *J Clin Invest*, 86: 2145-53.

Teuber, J., B. Mueller, R. Fukabori, D. Lang, A. Albrecht, and O. Stork. 2013. 'The ubiquitin ligase Praja1 reduces NRAGE expression and inhibits neuronal differentiation of PC12 cells', *PLoS One*, 8: e63067.

Tian, L., J. Chen, M. Chen, C. Gui, C. Q. Zhong, L. Hong, C. Xie, X. Wu, L. Yang, V. Ahmad, and J. Han. 2014. 'The p38 pathway regulates oxidative stress tolerance by phosphorylation of mitochondrial protein IscU', *J Biol Chem*, 289: 31856-65.

Tian, X., J. Azpurua, C. Hine, A. Vaidya, M. Myakishev-Rempel, J. Ablaeva, Z. Mao, E. Nevo, V. Gorbunova, and A. Seluanov. 2013. 'High-molecular-mass hyaluronan mediates the cancer resistance of the naked mole rat', *Nature*, 499: 346-9.

Torti, S. V., and F. M. Torti. 2013. 'Iron and cancer: more ore to be mined', *Nat Rev Cancer*, 13: 342-55.

Tyagi, P., and B. Mirakhur. 2009. 'MAGRIT: the largest-ever phase III lung cancer trial aims to establish a novel tumor-specific approach to therapy', *Clin Lung Cancer*, 10: 371-4.

Uhlmann, F. 2016. 'SMC complexes: from DNA to chromosomes', *Nat Rev Mol Cell Biol*, 17: 399-412.

Upton, R. L., Y. Chen, S. Mumby, J. M. Gutteridge, P. B. Anning, A. G. Nicholson, T. W. Evans, and G. J. Quinlan. 2003. 'Variable tissue expression of transferrin receptors: relevance to acute respiratory distress syndrome', *Eur Respir J*, 22: 335-41.

Uringa, E. J., J. L. Youds, K. Lisaingo, P. M. Lansdorp, and S. J. Boulton. 2011. 'RTEL1: an essential helicase for telomere maintenance and the regulation of homologous recombination', *Nucleic Acids Res*, 39: 1647-55.

Uzarska, M. A., R. Dutkiewicz, S. A. Freibert, R. Lill, and U. Muhlenhoff. 2013. 'The mitochondrial Hsp70 chaperone Ssq1 facilitates Fe/S cluster transfer from Isu1 to Grx5 by complex formation', *Mol Biol Cell*, 24: 1830-41.

Van Allen, E. M., D. Miao, B. Schilling, S. A. Shukla, C. Blank, L. Zimmer, A. Sucker, U. Hillen, M. H. Geukes Foppen, S. M. Goldinger, J. Utikal, J. C. Hassel, B. Weide, K. C. Kaehler, C. Loquai, P. Mohr, R. Gutzmer, R. Dummer, S. Gabriel, C. J. Wu, D. Schadendorf, and L. A. Garraway. 2015. 'Genomic correlates of response to CTLA-4 blockade in metastatic melanoma', *Science*, 350: 207-11.

van Wietmarschen, N., A. Moradian, G. B. Morin, P. M. Lansdorp, and E. J. Uringa. 2012. 'The mammalian proteins MMS19, MIP18, and ANT2 are involved in cytoplasmic iron-sulfur cluster protein assembly', *J Biol Chem*, 287: 43351-8.

Vashisht, A. A., C. C. Yu, T. Sharma, K. Ro, and J. A. Wohlschlegel. 2015. 'The Association of the Xeroderma Pigmentosum Group D DNA Helicase (XPD) with Transcription Factor IIH Is Regulated by the Cytosolic Iron-Sulfur Cluster Assembly Pathway', *J Biol Chem*, 290: 14218-25.

Vatolin, S., Z. Abdullaev, S. D. Pack, P. T. Flanagan, M. Custer, D. I. Loukinov, E. Pugacheva, J. A. Hong, H. Morse, 3rd, D. S. Schrump, J. I. Risinger, J. C. Barrett, and V. V. Lobanenkov. 2005. 'Conditional expression of the CTCF-paralogous transcriptional factor BORIS in normal cells results in demethylation and derepression of MAGE-A1 and reactivation of other cancer-testis genes', *Cancer Res*, 65: 7751-62.

Weber, J., M. Salgaller, D. Samid, B. Johnson, M. Herlyn, N. Lassam, J. Treisman, and S. A. Rosenberg. 1994. 'Expression of the MAGE-1 tumor antigen is up-regulated by the demethylating agent 5-aza-2'-deoxycytidine', *Cancer Res*, 54: 1766-71.

Wei, Y., Z. Zou, N. Becker, M. Anderson, R. Sumpter, G. Xiao, L. Kinch, P. Koduru, C. S. Christudass, R. W. Veltri, N. V. Grishin, M. Peyton, J. Minna, G. Bhagat, and B. Levine. 2013. 'EGFR-mediated Beclin 1 phosphorylation in autophagy suppression, tumor progression, and tumor chemoresistance', *Cell*, 154: 1269-84.

White, E. 2012. 'Deconvoluting the context-dependent role for autophagy in cancer', *Nat Rev Cancer*, 12: 401-10.

Wienand, K., and K. Shires. 2015. 'The use of MAGE C1 and flow cytometry to determine the malignant cell type in multiple myeloma', *PLoS One*, 10: e0120734.

Wischnewski, F., O. Friese, K. Pantel, and H. Schwarzenbach. 2007. 'Methyl-CpG binding domain proteins and their involvement in the regulation of the MAGE-A1, MAGE-A2, MAGE-A3, and MAGE-A12 gene promoters', *Mol Cancer Res*, 5: 749-59.

Wischnewski, F., K. Pantel, and H. Schwarzenbach. 2006. 'Promoter demethylation and histone acetylation mediate gene expression of MAGE-A1, -A2, -A3, and -A12 in human cancer cells', *Mol Cancer Res*, 4: 339-49.

Wu, Y., and R. M. Brosh, Jr. 2012. 'DNA helicase and helicase-nuclease enzymes with a conserved iron-sulfur cluster', *Nucleic Acids Res*, 40: 4247-60.

Wu, Y., J. A. Sommers, A. N. Suhasini, T. Leonard, J. S. Deakyne, A. V. Mazin, K. Shin-Ya, H. Kitao, and R. M. Brosh, Jr. 2010. 'Fanconi anemia group J mutation abolishes its DNA repair function by uncoupling DNA translocation from helicase activity or disruption of protein-DNA complexes', *Blood*, 116: 3780-91.

Xiao, T. Z., Y. Suh, and B. J. Longley. 2014. 'MAGE proteins regulate KRAB zinc finger transcription factors and KAP1 E3 ligase activity', *Arch Biochem Biophys*, 563: 136-44.

Xu, Y., C. Wang, Y. Zhang, L. Jia, and J. Huang. 2015. 'Overexpression of MAGE-A9 Is Predictive of Poor Prognosis in Epithelial Ovarian Cancer', *Sci Rep*, 5: 12104.

Yamada, R., A. Takahashi, T. Torigoe, R. Morita, Y. Tamura, T. Tsukahara, T. Kanaseki, T. Kubo, K. Watarai, T. Kondo, Y. Hirohashi, and N. Sato. 2013. 'Preferential expression of cancer/testis genes in cancer stem-like cells: proposal of a novel sub-category, cancer/testis/stem gene', *Tissue Antigens*, 81: 428-34.

Yang, B., S. M. O'Herrin, J. Wu, S. Reagan-Shaw, Y. Ma, K. M. Bhat, C. Gravekamp, V. Setaluri, N. Peters, F. M. Hoffmann, H. Peng, A. V. Ivanov, A. J. Simpson, and B. J. Longley. 2007. 'MAGE-A, mMage-b, and MAGE-C proteins form complexes with KAP1 and suppress p53-dependent apoptosis in MAGE-positive cell lines', *Cancer Res*, 67: 9954-62.

Yang, B., S. O'Herrin, J. Wu, S. Reagan-Shaw, Y. Ma, M. Nihal, and B. J. Longley. 2007. 'Select cancer testes antigens of the MAGE-A, -B, and -C families are expressed in mast cell lines and promote cell viability in vitro and in vivo', *J Invest Dermatol*, 127: 267-75.

Yang, B., J. Wu, N. Maddodi, Y. Ma, V. Setaluri, and B. J. Longley. 2007. 'Epigenetic control of MAGE gene expression by the KIT tyrosine kinase', *J Invest Dermatol*, 127: 2123-8.

Yang, F., X. Zhou, X. Miao, T. Zhang, X. Hang, R. Tie, N. Liu, F. Tian, F. Wang, and J. Yuan. 2014. 'MAGEC2, an epithelial-mesenchymal transition inducer, is associated with breast cancer metastasis', *Breast Cancer Res Treat*, 145: 23-32.

Ye, H., and T. A. Rouault. 2010. 'Human iron-sulfur cluster assembly, cellular iron homeostasis, and disease', *Biochemistry*, 49: 4945-56.

Yin, B., Y. Zeng, G. Liu, X. Wang, P. Wang, and Y. Song. 2014. 'MAGE-A3 is highly expressed in a cancer stem cell-like side population of bladder cancer cells', *Int J Clin Exp Pathol*, 7: 2934-41.

Zhang, S., X. Zhai, G. Wang, J. Feng, H. Zhu, L. Xu, G. Mao, and J. Huang. 2015. 'High expression of MAGE-A9 in tumor and stromal cells of non-small cell lung cancer was correlated with patient poor survival', *Int J Clin Exp Pathol*, 8: 541-50.

Zhang, S., X. Zhou, H. Yu, and Y. Yu. 2010. 'Expression of tumor-specific antigen MAGE, GAGE and BAGE in ovarian cancer tissues and cell lines', *BMC Cancer*, 10: 163.

Zou, J., F. Tian, J. Li, W. Pickner, M. Long, K. Rezvani, H. Wang, and D. Zhang. 2013. 'FancJ regulates interstrand crosslinker induced centrosome amplification through the activation of polo-like kinase 1', *Biol Open*, 2: 1022-31.